Aus dem Institut für Pathologie
der Medizinischen Fakultät Charité – Universitätsmedizin Berlin

DISSERTATION

Evaluierung der Potenz von glykosylierten Impfstoffen am Beispiel des RSV-F Proteins

zur Erlangung des akademischen Grades
Doctor rerum medicinalium (Dr. rer. medic.)

vorgelegt der Medizinischen Fakultät
Charité – Universitätsmedizin Berlin

von

Lars Radke

geboren in Schwedt/Oder

Datum der Promotion: 23. Juni 2019

Wir Menschen sind merkwürdige Wesen.
Von einer mysteriösen Unruhe erfasst;
der Verstand immer in Bewegung.
Staunend zwar, aber auch immer fragend.
Und vor allem zweifelnd.
Die Kenntnis einer Grenze - für uns nur Verlockung.

Nach Prof. Harald Lesch

Inhaltsverzeichnis

Verzeichnis der in der Dissertation verwendete Publikationen

Es folgt eine Auflistung der in der vorliegenden Dissertation verwendeten Publikationen. Bei den Publikationen 1 bis 3 besteht Erstautorenschaft und in Publikation 5 geteilte Erstautorenschaft.

Publikation 1

Induced cytokine response of human PMBC-cultures: Correlation of gene expression and secretion profiling and the effect of cryopreservation

Radke L, López Hemmerling DA, Lubitz A, Giese C, Frohme M

Cellular Immunology 2011, 272: 144-153

http://www.sciencedirect.com/science/article/pii/S0008874911002796

Publikation 2

Reference gene stability in peripheral blood mononuclear cells determined by qPCR and NanoString

Radke L, Giese C, Lubitz A, Hinderlich S, Sandig G, Hummel M, Frohme M

Microchimica Acta 2014, 181: 1733-42

http://link.springer.com/article/10.1007/s00604-014-1221-x

Publikation 3

In-vitro evaluation of glycoengineered RSV-F in the Human artifical Lymph Node Reactor

Radke L, Sandig G, Lubitz A, Schließer U, von Horsten HH, Blanchard V, Keil K, Sandig V, Giese C, Hummel M, Hinderlich S, Frohme M

Bioengineering 2017, 4(3), 70; doi:10.3390/bioengineering4030070

http://www.mdpi.com/2306-5354/4/3/70

Publikation 4

Engineering of CHO Cells for the Production of Recombinant Glycoprotein Vaccines with Xylosylated N-glycans

Sandig G, von Horsten HH, Radke L, Blanchard V, Frohme M, Giese C, Sandig V, Hinderlich S

Bioengineering 2017, *4*(2), 38; doi:10.3390/bioengineering4020038

http://www.mdpi.com/2306-5354/4/2/38

Publikation 5

Miniaturized Flow-Through Bioreactor for Processing and Testing in Pharmacology

Böhme A, Radke L, Schütze F, Schneider S, Liebscher T, Sauer S, Santo L, Quadrini F, Hummel M, Giese C, Frohme M, Foitzik A

Materials Science Forum 2017, 879: 236-243

https://www.scientific.net/MSF.879.236

Abkürzungsverzeichnis

µl	Mikroliter
3D	Dreidimensional
AG	Aktiengesellschaft
AICDA	aktivierungsinduzierte Cytidin-Desaminase, engl. activation induced cytidine deaminase
ANOVA	Varianzanalyse, engl. analysis of variance
APC	Antigenpräsentierende Zelle, engl. Antigen presenting cell
AS03	Adjuvant System 03
AS04	Adjuvant System 04
BCR	B-Zellrezeptor, engl. B cell receptor
CAMP	Cathelicidine Antimikrobielles Peptid
CCL5	CC-Chemokine-Ligand 5, engl. Chemokine (C-C motif) ligand 5
CD4	CD4-Rezeptor, engl. Cluster of Differentiation 4
CD8	CD8-Rezeptor, engl. Cluster of Differentiation 8
cDNA	komplementäre Desoxyribonukleinsäure, engl. complementary deoxyribonucleic acid
CHO	Ovarienzellen des Chinesischen Hamsters, engl. Chinese Hamster Ovary
ConA	Concanavalin A
Cq	engl. quantification cycle
DC	Dendritische Zellen, engl. Dendritic Cells
ELISA	Enzym-gebundener Immunassay, engl. Enzyme linked Immuno sorbent assay
FACS	Durchflusszytometer, engl. fluorescence-activated cell sorting
GlcNAc	N-Acetylglucosamin
GmbH	Gesellschaft mit begrenzter Haftung
GM-CSF	Granulozyten-Monozyten-Kolonie-stimulierende Faktor, engl. granulocyte macrophage colony-stimulating factor
H1N1	Influenza-A-Virus Subtyp H1N1
huALN®	Humaner Artifizieller Lymphknotenreaktor, engl. human Artificial Lymph Node Reactor
iDC	Unreife Dendritische Zelle, engl. immature Dendritic Cell
IFNA	Gen des Interferon Alpha
IFNB	Gen des Interferon beta
IFN-γ	Interferon-γ
Ig	Immunglobuline
IgA	Immunglobulin A
IgE	Immunglobulin E

IgG	Immunglobulin G
IgM	Immunglobulin M
IHP Frankfurt	Institut für High Performances, Frankfurt
IKB	Gen des Proteins IkB, engl. nuclear factor of kappa light polypeptide gene enhancer in B-cells inhibitor
IL-10	Interleukin-10
IL-12	Interleukin-12
IL12b	Gen des Interleukin-12b
IL-13	Interleukin-13
IL-17	Interleukin-17
IL-2	Interleukin-2
IL21	Interleukin-21
IL28	Interleukin-28
IL-4	Interleukin-4
IL-5	Interleukin-5
IPoGly	BMBF gefördertes Projekt „Potenzierung von Impfstoffen durch gezieltes Design der Glykosylierung“
JAK-STAT	Januskinase Signalübertragungsmechanismus zur Aktivierung der Transkription, engl. Janus Kinase-Signal Transducers and Activators of Transcription
LPS	Lipopolysaccharid
MALDI-TOF MS	Matrix-unterstützte Laser-Desorption/Ionisation Flugzeitanalyse Massenspektrometrie, engl. matrix-assisted laser desorption/ionization time-of-flight mass spectrometry
mDC	Gereifte dendritische Zell, engl. mature Dendritic Cell
MHCII	Haupthistokompatibilitätskomplex der Klasse 2, engl. Major Histocompatibility Complex
MOSFET	Metall-Oxid-Halbleiter-Feldeffekttransistor, engl. metal oxide semiconductor field-effect transistor
mRNAs	Boten-Ribonukleinsäure, engl. messenger ribonucleic acid
MTP	Multititerplatten
MYD88	Gen des Proteins MYD88, engl. Myeloid differentiation primary response 88
NF-kB	Nuklearfaktor, engl. nuclear factor 'kappa-light-chain-enhancer' of activated B-cells
Ni-NTA	Nickel-Nitrilotriessigsäure, engl. Nickel-Nitrilotriacetic acid
NOS2	Gen der Stickstoffmonoxid Synthase, engl. Nitric oxide synthase 2
OKT3®	Muromonab-CD3 (Handelsname Orthoclone OKT3): ein muriner therapeutischer monoklonaler Antikörper gegen den CD3-Rezeptor

PAMPs	Pathogen-assoziierte molekulare Muster, engl. Pathogen-associated molecular patterns
PBMCs	mononukleäre Zellen des peripheren Bluts, engl. Peripheral Blood Mononuclear Cells
PI	Propidiumiodid
PPIA	Gen der Peptidylprolyl isomerase A
p-Wert	Signifkanzwert, engl. p-value von probability, engl. Wahrscheinlichkeit
PWM	Mitogen der Kermesbeerengewächse, engl. Pokeweed mitogen
qPCR	quantitative Polymerase Kettenreaktion, engl. quantitative polymerase chain reaction
RAG1	Rekombination aktivierendes Gen 1, engl. Recombination Activation Gene 1
RAG2	Rekombination aktivierendes Gen 2, engl. Recombination Activation Gene 2
RELA	Gen des Transkritptionsfaktors RelA
RELB	Gen des Transkritptionsfaktors RelB
RMD	GDP-6-deoxy-D-lyxo-4-Hexulosereduktase
RSV	Respiratorisches Synzytial-Virus
SDHA	Gen der Succinat-Dehydrogenase
SEB	Staphylococcus Enterotoxin B
TBP	Gen des TATA-bindendes Protein, engl. TATA-binding protein
TCR	T-Zell-Rezeptoren, engl. T cell receptor
T_H1	T-Helferzellen vom Typ 1
T_H17	T-Helferzellen vom Typ 17
T_H2	T-Helferzellen vom Typ 2
TLR	Toll-ähnlicher Rezeptor, engl. toll-like receptor
TLR3	Toll-like-Rezeptor 3
TLR4	Toll-like-Rezeptor 3
TNF-α	Tumornekrosefaktor-α
UDP	Uridin-Di-Phosphat
XylT	Xylose-Transferase

1. Abstract

Despite intense research and immense demand there is no RSV vaccine available today. Modern subunit vaccines require adjuvants to generate a sufficiently strong immune response. By editing the glycosylation pattern of the RSV-F Protein covalently coupled adjuvants are produced, which generate comprehensive immune responses via the activation of the innate immune system. In this work recombinantly produced variants of the RSV-F protein with defucosylated or xylosylated N-glycans were tested for their potential to activate the immune system. For that, cytokines from cell culture supernatants were quantified and methods for gene expression analysis of stimulated cells were established.

In preliminary PBMC stimulation experiments the influence of cryopreservation on cells was examined and the expression of cytokines on gene and protein level was correlated.

Within the scope of stimulation experiments with complex cell mixtures (PBMC and DC) the reference genes SDHA, TBP and PPIA were identified as stably expressed in order to establish a valid gene expression analysis. A mathematical conversion of quantitative transcript numbers from a probe-based direct RNA detection assay (NanoString®) and the relative quantification via qPCR was developed.

The cytokine pattern in cell culture supernatants from long-term experiments performed with PBMC, mDC and each vaccine candidate in a highly complex perfusion reactor system (HuALN®) were quantified by automated bead-based multiplex analytics. In connection with the analysis of broad gene panels increased immune responses could be detected caused by the glycosidically altered RSV-F proteins. Defucosylation leads to a comprehensive activation of the immune system. Xylosylated RSV-F additionally activates components of the innate immune system. Furthermore, there is evidence that the ratio of the Th1 and Th2 based immune response can be modified by the grade of the defucosylation. The applied and established methods are suited to distinguish the potency of vaccine candidates with minor structural differences.

In order to perform stimulation experiments in a higher throughput, this work contributed to the establishment of a miniaturized bioreactor. Leakage testing of the reactor via fluorescence microscopy and the examination of the biocompatibility of all single components directly influenced the reactor design, its assembly and connection techniques as well as the choice of materials. The reactors functionality was confirmed in different 2D and 3D cultivation approaches by means of a long-lasting high cell viability.

The stronger modulated immune response evoked by modified glycosidic structures provides a promising method that can be applied to other pathogens, too. By its potential for higher throughput (more time points, more replicas) the miniaturized perfusion reactor could be able to provide a more precise insight into the immunological processes.

2. Zusammenfassung

Trotz intensiver Forschung und immensen Bedarfs steht heutzutage kein RSV-Impfstoff zur Verfügung. Moderne Subunit-Vakzine bedürfen einer Adjuvantierung, um eine ausreichend starke Immunantwort zu generieren. Mit der Veränderung von Glykoslierungsmustern des RSV-F Proteins wird eine kovalent gekoppelte Adjuvantierung hergestellt, die über die Aktivierung des angeborenen Immunsystems eine umfassende Immunantwort generiert. In dieser Arbeit wurden rekombinant hergestellte Varianten des RSV-F Proteins mit defukosylierten oder xylosylierten N-Glykanen auf ihr Potential, das Immunsystem zu aktivieren, untersucht. Dazu wurden Zytokine aus Zellkulturüberständen quantifiziert und Methoden zur Genexpressionsanalyse stimulierter Zellen etabliert.

In Vorbereitung auf Stimulationsexperimente mit PBMCs wurde der Einfluss der Kryokonservierung auf Zellen untersucht und die Zytokinexpression auf Gen- und Proteinebene korreliert.

Im Rahmen der Stimulationsexperimente mit komplexen Zellgemischen (PBMC und mDC) wurden die stabil exprimierten Referenzgene SDHA, TBP und PPIA für die Etablierung einer validen Genexpressionsanalyse identifiziert. Dabei wurde eine mathematische Konvertierung quantitativer Transkriptzahlen aus dem Sonden-basierten direkten RNA-Nachweis (NanoString®) und der relativen Quantifizierung mittels qPCR entwickelt.

Die Zytokinmuster in Zellkulturüberständen aus Langzeitstimulationsexperimenten, welche mit PBMC, mDC und den beiden Impfstoffvarianten in einem komplexen Perfusionsreaktorsystem (HuALN®) durchgeführt worden waren, wurden mittels automatisierter Bead-basierter Multiplexanalytik quantifiziert. Im Zusammenhang mit der Untersuchung umfangreicher Genpanels konnten verstärkte Immunreaktionen durch die glykosidisch veränderten RSV-F Proteine nachgewiesen werden. Die Defukosylierung führt zu einer breiten Aktivierung des zellulären und humoralen adaptiven Immunsystems. Das xylosylierte RSV-F aktiviert zusätzlich Komponenten des angeborenen Immunsystems. Zudem gibt es Hinweise darauf, dass durch den Grad der Defukosylierung das Verhältnis zwischen Th1 und Th2 basierter Antwort modifiziert werden kann. Mit den verwendeten und etablierten Methoden ist es möglich, die Potenz von Impfstoffkandidaten mit geringen strukturellen Veränderungen zu unterscheiden.

Um die komplexen Stimulationsexperimente in einem höheren Durchsatz durchführen zu können, wurde an der Entwicklung eines miniaturisierten Bioreaktors mitgewirkt. Die Untersuchungen der Dichtheit des Reaktors mittels Fluoreszenzmikroskopie und der Biokompatibilität der einzelnen Komponenten hatten direkten Einfluss auf das Design des Reaktors, dessen Aufbau- und Verbindungstechnik sowie die Wahl der Materialien. Die Funktionalität konnte in verschiedenen 2D und 3D Kultivierungsansätzen über eine langanhaltende Zellviabilität bestätigt werden.

Die verstärkte Modulierung der Immunantwort, hervorgerufen durch modifizierte Glykanstrukturen, zeugt von einer aussichtsreichen Methode, die auf andere Pathogene angewandt werden kann. Das höhere Durchsatzpotential des miniaturisierten Perfusionsreaktors (mehr Zeitpunkte, mehr Replikate) kann zukünftig einen präziseren Einblick in die immunologischen Vorgänge gewähren.

3. Einführung

Mit der Entwicklung der Vakzination vor etwa 250 Jahren wurden erstmals nicht nur die Symptome von Krankheiten behandelt, sondern bereits ihr möglicher Ausbruch verhindert. Das Prinzip bei der Pockenimpfung abgeschwächte oder abgetötete Erreger zu injizieren, wurde später u.a. durch Louis Pasteur auf andere Krankheiten übertragen. Seitdem ist es gelungen - einhergehend mit dem zunehmenden Wissen über die Erreger und die Funktionsweise des Immunsystems – eine Vielzahl von Impfstoffen zu entwickeln. Attenuierte Impfstoffe sind äußerst wirkungsvoll, da die spezifischen Antigene vorhanden sind, sich die lebenden Erreger replizieren können und in das Zielgewebe eindringen. So wird ein der natürlichen Infektion ähnlicher Krankheitsverlauf hervorgerufen, was zu einer starken Aktivierung des angeborenen Immunsystems führt. Durch die lange Verweildauer und die durch die Replikation generierte hohe Antigenkonzentration, wird eine effektive und langanhaltende Immunität hervorgerufen [1].
Der Ansatz mit vollständigen inaktivierten Pathogen ist nicht immer anwendbar (z.B. wenn ein komplexes Pathogen-Wirts-Verhältnis vorliegt) und kann ungewollte Immuneffekte hervorrufen: In den 1960er Jahren entwickelten Personen, die mit einem Formalin-inaktivierten Respiratorischen Synzytial-Virus (RSV) Vakzin geimpfte wurden, bei einer nachfolgenden natürlichen Infektion eine schwerwiegende Lungenpathologie, welche in mehreren Fällen tödlich endete. Bisher nahm man an, dass die Ursache hierfür eine Veränderung der protektiven Antigene im Zuge der Formalin-Behandlung gewesen sei, welche anschließend zur Generierung nicht neutralisierender Antikörper geführt hat [2]. Delgado et al hingegen zeigen in einer Studie, dass ein Ausbleiben der Antikörperreifung, hervorgerufen durch eine zu geringe Stimulierung der Toll-like Rezeptoren (TLR), zum unzureichenden Schutz geführt hat [3].
In dieser Arbeit wird die Effektivität eines rekombinanten RSV-Proteins untersucht, welcher mit atypischer Glykosierung adjuvantiert, eine stärkere Aktivierung des angeborenen Immunsystems über die Toll-Like Rezeptoren erzielen soll. In den folgenden Abschnitten wird daher näher auf die Wechselwirkung moderner Vakzinen mit dem Immunsystem sowie auf Methoden zum Bestimmen von deren Aktivierungseffizienz eingegangen.

3.1. Immunsystem und Vakzinierung

Das Immunsystem dient dem Schutz vor Pathogenen sowie der Deaktivierung von körperfremden Molekülen und veränderten körpereigenen Zellen. Die Immunantwort umfasst dabei zwei Systeme: das angeborene und das erworbene Immunsystem. Ersteres besteht neben der Haut als einfachste Schutzbarriere aus einem zellulären und einem humoralen Abwehrsystem (dem Komplementsystem). Das erworbene Immunsystem beruht auf der Fähigkeit der Lymphozyten hochspezifische Rezeptormoleküle zu bilden. Dabei sind die im Thymus gebildeten T-Lymphozyten für die zelluläre Immunantwort und die im Knochenmark gebildeten B-Lymphozyten für die humorale Antikörper-Antwort verantwortlich.

Beide Teile sind eng miteinander verknüpft und arbeiten sequentiell. Dabei dient das angeborene Immunsystem als frühe Abwehr und überbrückt die Phase bis eine adaptive Immunantwort zur Verfügung steht. Insbesondere unreife dendritische Zellen (iDC) sind darauf spezialisiert, anhand von PAMPs (engl. Pathogen-associated molecular patterns), eindringende Pathogene über Oberflächenrezeptoren wie Toll-like Rezeptoren (TLRs) zu erkennen. Nach ihrer Aktivierung durchgehen Dendritische Zellen (DCs) einen Reifungsprozess und wandern als Antigenpräsentierende Zelle (engl. Antigen presenting cell, APC) zu den sekundären lymphatischen Organen. Durch die Aktivierung der dort ansässigen T- und B-Zellen verknüpfen sie beide Immunsysteme [4]. Die naïven T-Zellen exprimieren auf ihrer Oberfläche einzigartige antigenspezifische T-Zell-Rezeptoren (engl. T cell receptor, TCR). Bei einer Aktivierung durch APC können sie zu Zellen mit unterschiedlichen Funktionen differenzieren. $CD4^+$ T-Helferzellen vom Typ 1 (T_H1) sekretieren vor allem proinflammatorische Zytokine und Zytokine zur Aktivierung der zellulären Immunantwort - beschleunigen also die Proliferation und Differenzierung von T-Zellen und Makrophagen und hemmen gleichzeitig die Aktivität von T_H2. Letztere sekretieren als wichtigste Zytokine IL-4 und anti-inflammatorisches IL-10. IL-4 führt zur Aktivierung, Proliferation und Differenzierung von B-Zellen und hemmt die Aktivierung von Makrophagen. So wird eine überschießende inflammatorische Reaktion verhindert und eine ausgewogene Immunantwort erzeugt [4]. $CD8^+$ T-Lymphozyten, sogenannte zytotoxische T-Zellen, erkennen und töten mit intrazellulären Pathogenen (z.B. Viren) infizierte Körperzellen und verhindern die Produktion weiterer Viruspartikel [5].
Die aus aktivierten B-Zellen gereiften Plasmazellen produzieren Immunglobuline (Ig) in großer Menge, welche bereits freigesetzte Virenpartikel und andere Pathogene binden. Ähnlich wie die T-Zellen exprimieren auch die B-Zellen unikale antigenspezifische Rezeptoren (engl. B cell receptor, BCR). Bei ihrer Reifung spielt die durch das Gen AICDA (engl. activation induced cytidine deaminase) kodierte Cytidin-Desaminase eine zentrale Rolle. Sie steuert die Antikörperreifung durch somatische Hypermutation, welche die Affinität der produzierten Antikörper einiger Plasmazellen erhöht. Außerdem ist sie am Klassenwechsel der sezernierten Ig beteiligt, so dass anstelle von IgM die Effektorantikörper IgA, IgG und IgE gebildet werden [4, 5].
Bei einer RSV Infektion ist insbesondere die Ig-vermittelte Inhibierung von Rezeptor-Liganden-Interaktionen zwischen Pathogen und Wirtszelle von Bedeutung, da sie die Zellfusion, über die sich RSV verbreitet, unterbindet. IgA – aufgrund des Vorkommens in mukösen Geweben – und IgG, welche ebenfalls durch Epithelzellen in den Respirationstrakt einwandern können, bilden einen guten Marker für die Güte eines Impfstoffes, da der Titer an neutralisierenden Antikörpern meist mit dem Schutz vor einer RSV-Infektion korreliert [6].
Impfstoffe, welche die Antigene des Zielpathogens erfolgreich abbilden, rufen B-Zellen, T-Zellen und cytotoxische T-Lymphozyten als Effektorzellen hervor und nutzen damit die gesamte Leistung des Immunsystems. Durch die Proliferation und Differenzierung aktivierter T- und B-Zellen zu Gedächtniszellen, wird das zelluläre Verhältnis und das TCR- bzw. BCR-Repertoire nachhaltig verändert. Dies führt bei einer erneuten Infektion mit dem gleichen oder einem ähnlichen Pathogen

sehr schnell zur Expansion neuer Effektorzellen. Die Ausbildung dieser Gedächtniszellen ist per Definition das Ziel eines Impfstoffes, da dadurch ein lang anhaltender Schutz erreicht wird. Die Voraussetzung für die Entwicklung eines erfolgreichen Vakzins besteht daher in der Wahl des potenten Antigens, welches eine Antwort des angeborenen Immunsystems induziert. Die inflammatorische Reaktion muss – evtl. durch geeignete Adjuvanz – stark genug sein, um T-Helferzellen zu aktivieren, welche die adaptive Immunantwort qualitativ und quantitativ modulieren. Durch das Wissen über Infektionsmechanismen können anhand des Impfstoffdesigns die richtigen Effektorzellpopulationen aktiviert werden [4, 5].

3.2. Moderne Vakzine und Adjuvanzien

Für eine definierte Immunantwort werden heutzutage häufig nur noch einzelne immunogene Teile von Erregern für die Herstellung so genannter Subunit-Vakzine genutzt. Die verwendeten antigenen Determinanten werden synthetisch oder rekombinant hergestellt. Allgemein sind die Immunogenität und die Reaktogenität von Subunit-Vakzinen häufig herabgesetzt, da nicht mehr der gesamte Umfang an Antigenen zur Verfügung steht und häufig das angeborene Immunsystem nicht ausreichend stimuliert wird [7].

Verschiedene Molekülklassen können als wirkungsverstärkende Adjuvanzien verwendet werden, um diesen Effekt auszugleichen und die Immunogenität des Vakzins zu modulieren. Ihre unspezifische Wirkung beruht häufig auf einer verstärkten Stimulierung des angeborenen Immunsystems, u.a. durch eine verstärkte Rekrutierung von Phagozyten (Granulozyten und Monozyten) am Injektionsort. Dadurch wird die Anzahl aktivierter APC erhöht, welche in die Lymphknoten einwandern, so dass es zur verstärkten Stimulation des adaptiven Immunsystems kommt. Aluminiumsalze aktivieren bspw. Zellen des angeborenen Immunsystems, um eine ausgeprägte Antikörperantwort zu generieren [8].

Adjuvanzien mit einer Reservoirfunktion setzen den Impfstoff über einen längeren Zeitraum frei und ermöglichen so eine fortlaufende Stimulation, was zu einer stärkeren Immunantwort und zur Ausbildung einer langanhaltenden Gedächtnisfunktion führt. Freunds Adjuvanz ist eine einfache Wasser-in-Öl-Emulsion. Artifizielle Vesikel, können neben den Vakzin-spezifischen Antigenen auch noch virale Glykoproteine (z.B. Hämagglutinin oder Neuraminidase des Influenza Virus) enthalten, um so die Aufnahme durch APC zu erhöhen [8]. Noch komplexer sind Mischungen aus verschiedenen Adjuvanzien, wie AS04, welches neben Aluminiumsalz auch Bestandteile von Lipopolysaccharid (LPS) enthält und so eine komplementäre zelluläre und humorale Immunantwort hervorruft [9].

Adjuvanzien stehen immer wieder in der Diskussion, Auslöser für verschiedene Nebenreaktionen zu sein. So wurden das Golfkriegs-Syndrom und weitere Autoimmunerkrankungen in Verbindung mit Squalen-adjuvantierten Impfstoffen gebracht [10, 11] und von anderer Seite widerlegt [12]. Verunreinigungen im Mineralöl von Freunds Adjuvanz führten früher häufig zu einer überhöhten Reaktogenität [8]. Die Neurotoxizität von Aluminium ist bekannt, aber wenig verstanden. Selten

kommt es an der Injektionsstelle zu lokalen Unverträglichkeiten, z.B. Granulombildung (Fremdkörperreaktion) aufgrund fehlerhafter intradermaler Applikation [13]. Als jüngstes Beispiel konnte anhand von *in vitro* Experimenten gezeigt werden, dass α-Tocopherol im Squalen-basierten Adjuvanz AS03 das Risiko von Narkolepsie nach H1N1 Vakzinierung erhöhte [14].

3.3. RSV

Das humane Respiratorische Synzytien Virus stammt aus der Familie der *Paramyxoviridae*. Es infiziert die oberen und unteren Atemwege und verursacht dabei meist grippeähnliche Symptome. Die Prävalenz ist hoch (die Durchseuchung beträgt 82,6 % innerhalb der ersten 24 Lebensmonate) [15] und Reinfektionen innerhalb einer Grippesaison sind möglich. Das Virus selbst besteht aus einer Lipoprotein-Hülle, welche eine einzelsträngige lineare RNA mit negativer Polarität umhüllt. Die Virenhülle besteht hauptsächlich aus den Glykoproteinen RSV-G und RSV-F, welche für die Anlagerung an und die Fusionierung mit den Wirtszellen verantwortlich sind.
Eine RSV-Infektion ist insbesondere für Immungeschwächte, Frühgeborene und Menschen mit altersbedingter Immundefizienz risikoreich. Nach Schätzungen sterben jährlich bis zu 600.000 Menschen direkt oder indirekt an den Folgen einer RSV-Infektion [16]. Die höchste Hospitalisierungsrate mit 25,9 pro 1000 Kindern haben dabei Säuglinge im 1. Lebensmonat [17].
Zurzeit gibt es keinen Impfstoff gegen eine RSV-Infektion. 2016 konnte die Wirkung des von Novavax entwickelten Impfstoffkandidaten in einer klinischen Phase III Studie an älteren Patienten nicht bestätigt werden. Eine präventive Behandlung mit dem therapeutischen Antikörper Palivizumab ist aufgrund enormer Kosten auf Hochrisikogruppen beschränkt.
Die Entwicklung eines Impfstoffes ist aufgrund der ungewöhnlichen Immunreaktion schwierig. Das Virus löst beim Eindringen in die Zelle eine einseitige T_H2 basierte Immunreaktion hervor und verhindert die Bildung einer spezifischen adaptiven T-Zellantwort, wodurch die für die Reduktion der Lungenpathologie benötigten zytotoxischen T-Zellen in zu geringer Menge in die Lunge einwandern. Des Weiteren besitzt das RSV-G zwar die größte Immunogenität, jedoch besitzt es auch die größte Variabilität zwischen den humanen RSV-Genotypen (53 % Aminosäurehomologie) [18]. Dementsprechend ist bereits die natürlich erworbene Immunität weder vollständig noch langanhaltend [15].
Eine detaillierte Übersicht bisher entwickelter RSV-Vakzine und ihrer Wirksamkeit gibt der Review von J. L. Hurwitz [5]. Sie sieht die größten Probleme vieler Ansätze in der unzureichenden Aktivierung des angeborenen Immunsystems und damit einhergehend einem unausgewogenem T_H1/T_H2 Verhältnis. Des Weiteren scheitern zahlreiche Studien daran, das Immunsystem von Neugeborenen und Älteren gleichermaßen zu adressieren. Viele RSV-Impfstoffkandidaten werden vorwiegend an älteren Menschen getestet, welche jedoch häufig seropositiv für RSV sind, was die Interpretation der Studienresultate verkompliziert.

3.4. Glykosylierung als Adjuvanz

Moderne Adjuvanzien modulieren die Immunantwort durch eine gezielte Interaktion mit Bestandteilen des angeborenen Immunsystems; so können bspw. Oligosaccharidstrukturen durch TLR erkannt werden. 60 % der Masse des RSV-G Proteins sind auf Glykosylierung zurückzuführen und auch das RSV-F Protein besitzt drei N-Glykane, welche eine große Rolle bei der Zellfusion spielen [19]. Die Modifikation von Glykanen stellt ein wichtiges Mittel zur Generierung von Adjuvanzien dar, mit denen gezielt eine komplementäre Immunantwort eingeleitet werden kann. Grundlage ist das Säugerglykom – das komplexeste Gebilde, welches es in der Natur gibt [20]. Über 250 verschiedene Glykosyltransferasen sind am posttranslationalen Aufbau der Glykane beteiligt. Von zentraler Bedeutung sind dabei N-Glykane, mit ihrer konservierten Grundstruktur aus β-1,4-verknüpften N-Acetylglucosaminen (GlcNAc) und drei Mannosen, an die weitere Zucker wie Galaktose, Sialinsäure oder Fukose angelagert werden. O-Glykane sind im Aufbau wesentlich unregelmäßiger und werden in der Biotechnologie seltener genutzt.

Glykosylierungen spielen bei für die Funktionalität des Immunsystems eine große Rolle. Einerseits werden die Sensitivität der TCR-, BCR- und Zytokin-Signalwege sowie die Antikörperbindung beeinflusst [21, 22] und sogar die Leukozytenbewegung basiert auf Glykanen und L-Selektinen [23]. Andererseits wird das Immunsystem von bestimmten Glykosylierungsmustern aktiviert (z.B. bindet TLR4 LPS) und bestimmte prozessierte Kohlenhydrate werden den T-Zellen über MHCII Rezeptoren präsentiert [24].

Künstlich veränderte Glykosylierungsstrukturen werden zunehmend bei der Entwicklung von Impfstoffen und Medikamenten eingesetzt. Oligosaccharidstrukturen werden bereits chemisch synthetisiert und dann als immunogenes Kohlenhydrat-Protein-Konjugat genutzt [25]. Andere Ansätze modifizieren die Glykosylierungsmuster über selektive Fütterungsstrategien bei der Produktion rekombinanter Proteine in Zellkulturen oder nutzen direkt gentechnische Ansätze und passen den Metabolismus von Expressionssystemen an.

Im Rahmen dieser Arbeit wurde zur Expression von defukosylierten RSV-F Protein die Glymaxx-Technologie [26] genutzt, welche eine veränderte CHO (engl. Chinese Hamster Ovary)-Zellinie verwendet. Hier wird durch die heterologe Expression des prokaryotischen Enzyms GDP-6-deoxy-D-lyxo-4-Hexulosereduktase (RMD) die *de novo* Synthese von Fukose minimiert, da die Vorstufe GDP-4-keto-6-deoxy-Mannose abgeführt wird. Nachfolgend könnten Fukoseanaloga als Supplement über Nährmedien zugeführt, über den Salvage Pathway an der Core-Struktur der Glykane eingebaut und zum Provozieren einer verstärkten Immunantwort genutzt werden.

In einem anderen Ansatz wurden die N-Glykane am RSV-F Protein xylosyliert. Dazu wurde in den gleichen CHO-Zellen β1,2-Xylosyltransferase exprimiert, welche die Xylose an N-Glykanen des RSV-F Proteins anlagerte. Die Potenz beider Modifikationen, eine immunologische Reaktion hervorzurufen, wurde im Projekt IPoGly untersucht.

3.5. Das Projekt IPoGly

Ziel des Projektes „Potenzierung von Impfstoffen durch gezieltes Design der Glykosylierung“ (IpoGly; BMBF; FörderKZ 17025B10) ist die Entwicklung einer Plattformtechnologie für die Herstellung hochpotenter rekombinanter Impfstoffe, bei denen Antigen und Adjuvanz in einem Molekül vereint sind. Die Strategie über eine atypische Glykosylierung bifunktionelle Proteine zu erzeugen, wurde auf das RSV-F Protein angewandt. Im Verbund mit akademischen (Beuth Hochschule für Technik Berlin) und industriellen Partnern (ProBioGen AG Berlin, RiNA GmbH Berlin) wird an der rekombinanten Expression von RSV-F in verschiedenen Zelllinien und der gezielten Veränderung des Glykosylierungsmusters gearbeitet. Die Evaluierung der Wirksamkeitstestung der entwickelten RSV-F Proteine ist die zentrale Grundlage der vorliegenden Arbeit und erfolgt anhand der Quantifizierung von Zytokinmustern und der Analyse umfangreicher Genexpressionstudien *in vitro* stimulierter Lymphozyten. Zusätzlich wurde im Projekt an der Miniaturisierung eines Perfusionsreaktors gearbeitet, um - alternativ zum Tiermodell – parallelisierte Stimulationsexperimente durchführen zu können.

3.6. Nachweis der Effizienz der Impfstoffkandidaten

Die Bestimmung der Wirksamkeit eines Impfstoffes, also der Immunogenität und der Reaktogenität, geht heutzutage weit über die Messung von hervorgerufenen Antikörpertitern hinaus [1.4]. Die Kostimulation von mononukleären Blutzellen (PBMCs, engl. Peripheral Blood Mononuclear Cells) mit Impfstoffvarianten und gereiften DCs (mDCs, engl. mature) gibt bereits im *in vitro* Experiment anhand der Veränderung der zellulären Zusammensetzung (T_H1 / T_H2 Verhältnis) Aufschluss über Ausgewogenheit der Aktivierung des Immunsystems. Die Stimulation von PBMCs und mDCs erfolgte im Projekt im humanen Lymphknotenreaktor (huALN, engl. human Artificial Lymph Node Reactor) [27, 28] des Kooperationspartners ProBioGen AG. Dabei handelt es sich um einen Perfusionsreaktor, in welchem die Zellen in einer 3D Matrix (z.B. Agarose und Kollagen) kultiviert werden. Dies ermöglicht die Sammlung von Zellkulturüberständen aus Langzeitkultivierungen mit mehrfachen Restimulationen. Die Zellen können jedoch nur am Ende eines Experiments aus der Matrix geerntet werden, so dass für die Bestimmung zellulärer Parameter auf zusätzliche Experimente in Multititerplatten zurückgegriffen werden muss.

Die Messung von Zytokinen in den Zellkulturüberständen erlaubt die Beobachtung von zellulären Aktivierungsprozessen. Aufgrund der geringen Mengen an Zellkulturüberständen, die zur Verfügung stehen, müssen multiplexe Methoden zur Analyse genutzt werden. Suspensionsarrays, wie die Luminex®-Technologie, sind in der Lage, dutzende Analyten gleichzeitig in einer Probe zu detektieren. Auf der Oberfläche fluoreszenzkodierter Beads werden mittels Sandwich-Immuno-Assay spezifisch Proteine gebunden und mithilfe von Durchflusszytometrie selektiv analysiert. Anhand erzeugter Standardkurven werden die Analyten mit hoher Sensitivität und einem großen dynamischen Messbereich (10^5) quantifiziert. Da Beads und Antikörper als mischbare Reagenzien ohne Kreuzreaktivität kommerziell erworben werden können, ist im Gegensatz zu Microarrays eine Anpassung des Analytenumfangs unproblematisch. Im Gegensatz zu ELISAs (engl. Enzyme

linked Immuno sorbent assay) ist die Bead-basierte Multiplexanalytik weniger arbeits- und kostenintensiv [29], insbesondere, da zur Steigerung der Präzision im Rahmen dieser Arbeit nahezu alle Arbeitsschritte automatisiert wurden [30]. Nach anfänglichen Etablierungsarbeiten mit umfangreichen Zytokinspektren, wurde für die spätere Analyse der Aktivierungseffizienz der Umfang auf die sechs Schlüssel-Zytokine IL-2, IL-4, IL-10, GM-CSF, IFN-γ und TNF-α verringert.
Mithilfe der Genexpressionsanalyse kann die Aktivierung des Immunsystems in einem noch breiteren Spektrum analysiert werden. Für die Analyse einer begrenzten Anzahl an Transkipten wurde die quantitative Polymerase Kettenreaktion (qPCR) verwendet, bei welcher in cDNA revers transkribierte mRNAs zyklisch amplifiziert werden. Die Quantifizierung erfolgt zumeist relativ zwischen Referenzgen-normierten behandelten und unbehandelten Kontrollen und wird mithilfe der Effizienzkorrigierten ΔΔct Methode berechnet. Die Validierung von Referenzgenen ist komplex und muss für jeden Zelltyp und jedes experimentelle Setup durchgeführt werden, da es bedeutend für eine korrekte Normierung der Daten ist (s. Publ. 2).
Bei einer größeren Targetgenzahl ist die qPCR im Vergleich zu arraybasierten Methoden sehr zeitintensiv, da der Grad des Multiplexings stark begrenzt ist und viel Etablierungsarbeit geleistet werden muss. Eine in dieser Arbeit gewählte Methode zur Quantifizierung umfangreicher Gensets, ist die direkte mRNA Quantifizierung mittels NanoString®. Diese Chip-basierte Technologie benutzt Sonden mit einem „Fluoreszenz-Strichcode“ und automatisierte fluoreszenzmikroskopische Bildgebung, um einige hundert Transkripte innerhalb einer Hybridisierungsreaktion zu detektieren. Da keine enzymatischen Reaktionen erforderlich sind, ist die Technik effizienter und präziser als qPCR bei geringem Signal-Rausch-Verhältnis. Im Gegensatz zur häufig nichtspezifischen Bindung bei Microarrays, benutzt NanoString ein duales Probensystem, so dass die Spezifität erhöht wird, obwohl Fänger- und Reportermoleküle eine vergleichbare Länge haben [31].
Auch bei NanoString Assays sind Referenzgene notwendig, um Mengenunterschiede des Probenmaterials auszugleichen. Eine detaillierte Beschreibung der Methode und wie sie zur Evaluation von Referenzgenen genutzt werden kann, ist in Publ. 2 dargelegt.
In einer studentischen Abschlussarbeit, wurde die Verschiebung des TCR-Repertoires nach Stimulation mit LPS mittels Pyrosequenzierung analysiert. Die Ergebnisse waren jedoch nicht aufschlussreich genug, um die Methode auf Vakzinkandidaten anzuwenden [32].

3.7. Miniaturisierte Bioreaktoren

Physiologie und Anatomie von Labortier und Mensch unterscheiden sich teilweise beträchtlich weswegen die Übertragbarkeit von Ergebnissen aus Tierversuchen häufig nur begrenzt möglich ist [33]. Die Stimulationsexperimente wurden daher im hochentwickelten Perfusionsreaktor HuALN® durchgeführt, welcher als humanes *in vitro*-Testsystem eine Vorhersage von Immunreaktionen ermöglicht. Die Herstellung des Reaktors und der Betrieb in Langzeitstimulationsexperimenten sind allerdings aufwändig und kostenintensiv. Daher war ein Teilziel des Projektes I-PoGly die Entwicklung von miniaturisierten Einweg-Bioreaktoren mit geringen Herstellungskos-

ten. Diese bestehen aus einer Kultivierungskammer, welche durch poröse Membranen mit Nährmedien und über eine gaspermable Membran mit Sauerstoff versorgt werden können. Die Kultivierung von adhärenten Zellen oder Suspensionszellen kann im Batch, Fed-Batch oder Perfusionsmodus erfolgen. Außerdem können Zellen in Flüssigmedium oder in einer 3D Matrix kultiviert werden. Der detaillierte Aufbau der Prototypen und deren Herstellungsmethoden (Spritzguss, Mikrofräsen, Aufbau und Verbindungstechnik) sind in der Doktorarbeit von Andrea Böhme beschrieben [34].
Im Rahmen der vorliegenden wissenschaftlichen Arbeit wurden die Dichtheit und die Biokompatibilität der entwickelten Mikroreaktoren untersucht. Dazu wurde einerseits eine Methode entwickelt, mithilfe der Autofluoreszenz von Cyanobakterien und Fluoreszenzmikroskopie die Dichtheit von Prototypen zu kontrollieren. Die Biokompatibilität wurde anhand von Vitalitätsuntersuchungen in verschiedenen Zellkulturexperimenten überprüft.

3.8. Zielstellung

Im Rahmen von IPoGly wurden von den Partnern Fusionsproteine des RSV in defukosylierter und xylosylierter Form produziert und in dieser Arbeit in Stimulationsversuchen mit humanen Immunzellen verwendet, um den Einfluss der atypischen Glykosylierung auf die Aktivierung des Immunsystems zu untersuchen. Dazu sollen geeignete Parameter auf Zytokinebene und Genexpressionsebene identifiziert und bestehende Methoden des analytischen Nachweises, wie die Bead-basierte Multiplexanalytik oder qPCR, optimiert werden. Weitere Methoden beispielsweise für umfangreiche Genexpressionsanalysen sollen etabliert und Auswertungsmethoden angewandt werden.
Zusätzlich soll in einem Teilprojekt die Entwicklung eines miniaturisierten Perfusionsreaktors zur parallelisierten Durchführung von Stimulationsversuchen erfolgen. Bei der Entwicklung des Reaktors sollen die Dichtheit des Reaktors und die Biokompatibilität der verwendeten Materialien überprüft werden und die Funktionalität des Reaktors in verschiedenen Kultivierungsmodi anhand der Zellviabilität evaluiert werden.

4. Methodik

Aufgrund der zahlreichen eingesetzten Methoden wird auf eine umfassende Erläuterung verzichtet. Die nachfolgende Auflistung enthält die in den einzelnen Publikationen (vgl. S. II) verwendeten und beschriebenen Techniken.

	Methoden und Materialien	Publikation				
		1	2	3	4	5
RSV-F Protein	Präparation von RSV-F Proteinen, auch defukosyliert oder xylosyliert		*	*	*	
	Aufreinigung von Proteinen mittels Ni-NTA Säule			*	*	
	Glykananalyse mittels MALDI-TOF MS			*	*	
	Monosaccharidanalyse			*	*	
Zellpräparation	Präparation von PBMC mittels Dichtegradientenzentrifugation	*				
	Generierung von mDC		*	*	*	
	Kryokonservierung von PBMC	*				
	Stimulation von PBMC mit Standardstimulanzien (PWM/SEB, OKT3®, ConA)	*				
	Stimulationsexperimente mit RSV-F Protein im HuALN® o. in MTP		*	*	*	
Nukleinsäureaufreinigung	mRNA-Extraktion mit RNeasy® Plus Mini Kit (Qiagen) oder High Pure RNA Isolation Kit (Roche)	*	*			
	mRNA Qualitätskontrolle mittels 2100 Bioanalyzer RNA 6000 Pico Assay (Agilent) oder Nanodrop 1000 (Nanodrop Instruments) oder DNF-472 High Sensitivity RNA Analysis Kit auf Fragment Analyzer™ (Advanced Analytical Technologies)	*	*	*	*	
	mRNA Quantifizierung mittels Nanodrop 1000 (Nanodrop Instruments) oder mit Qubit® RNA HS AssayKit (Molecular Probes)		*	*	*	
	Reverse Transkription mit Transcriptor High Fidelity cDNA Synthesis Kit (Roche) o. Maxima Reverse Transcriptase (Fermentas)	*	*			
Analysen	qPCR (SYBR Green I), Roche LightCycler®480, ΔΔct-Methode	*	*			
	Zytokinquantifizierung mittels Bead-basierte Multiplexanalytik (auch automatisiert auf Tecan Freedom Evo® 200) mit Bio-Plex® 200, Bio-Plex Pro™ Human Cytokine Assay, 8-Plex und Bio-Plex Human Cytokine Th1/Th2 Panel oder Bio-Plex Express assay, (Bio-Rad®)	*		*	*	
	NanoString® nCounter Gene Expression Assay mit GX Immunology Panel oder Human Immunology v2 Panel		*	*	*	
Auswertung	Transformation von NanoString counts in Cq Equivalente		*			
	Referenzgenanalyse (Normfinder, Bestkeeper, GeNorm)		*			
	Statistische Bewertung mittels Bland-Altman Plot		*			
	Hierarchische Clusteranalyse mit RStudio			*		
	Differentielle Genexpressionsanalyse, nSolver				*	
	Differentielle Genexpressionsanalyse, NanoStringDiff (R package)			*		
Bioreaktor	Design und Herstellung des miniaturisierten Bioreaktors					*
	Dichtheitstest mit Cyanobakterien Synechocystis sp. PCC 6803 und Keyence BZ-9000					*
	Zytotoxizitätstest und Viabilitätstests mit PI und SYTO®9 aus LIVE/DEAD® BacLight Bacterial Viability Kit (Invitrogen)					*
	Kultivierung von L929 Mausfibroblasten im miniaturisierten Bioreaktor					*
	Kultivierung humaner PBMC in 3D-Kollagenmatrizen im miniaturisierten Bioreaktor					*

5. Ergebnisse

Es folgen die Ergebnisse aus den in diese Arbeit eingeflossenen Publikationen (vgl. S. II).

5.1. Einfluss der Kryokonservierung auf die Stimulierbarkeit von PBMC

Radke L, López Hemmerling DA, Lubitz A, Giese C, Frohme M. Induced cytokine response of human PMBC-cultures: Correlation of gene expression and secretion profiling and the effect of cryopreservation. Cell Immunol 2011, 272: 144-153.

Die Analyse der Genexpression stimulierter PBMC und den von ihnen sekretierten Zytokinen zur Beurteilung der Aktivierung des Immunsystems stellt einen zentralen Bestandteil in der Arbeit dar. Entsprechend intensive Vorarbeiten nutzen qPCR und Bead-basierter Immunoassays, um die Stärke und das zeitliche Einsetzen von Stimulationsreaktionen miteinander zu vergleichen. Die Untersuchung von PBMC zweier Spender deutet das Ausmaß Donor-spezifischer Einflüsse an.
Um später umfangreiche und vergleichbare Studien zu ermöglichen, wurde der Einfluss der Kryokonservierung untersucht. Dafür wurden frische und kryokonservierte PBMCs mit ConA und OKT3® für 4 bzw. 24 h stimuliert und anschließend analysiert. Die Quantifizierung von neun Zytokinen (IL-2, IL-4, IL-5, IL-10, IL-12, IL-13, GM-CSF, IFN-γ und TNF-α) nach 24 stündiger Inkubation zeigte dabei vernachlässigbare Konzentrationsunterschiede (Publikation 1, Bild 2). Die mRNA der vier Zytokine IL-2, IL-4, IFN-γ und TNF-α zeigen Unterschiede beim Einsetzen der Genexpression. Kryokonservierte PBMC sind nach vierstündiger Inkubation mit ConA stärker aktiviert, als frische PBMC, während es bei der Stimulation mit OKT3® umgekehrt ist. Nach 24 stündiger Inkubation ist jedoch für beide Stimulanzien ein Angleichen der Expressionslevel zu beobachten (Publ. 1, Bild 1). Aufgrund der geringen Unterschiede bei der Aktivierung kryokonservierter Zellen, ist es möglich, sowohl frische als auch kryokonservierte PBMC für Stimulationsversuche zu nutzen – bspw., bei der Untersuchung der Korrelation der Zytokinproduktion auf mRNA und Proteinebene. Sowohl die Transkription (Publ. 1, Bild 3) als auch die Sekretion (Publ. 1, Bild 4) sind im zeitlichen Verlauf sehr dynamisch und setzen je nach Stimulus unterschiedlich schnell ein. Dabei stimmt das zeitliche Einsetzen in Abhängigkeit des jeweiligen Stimulus überein: eine frühere Genexpression führt zu einer früheren Zytokinsekretion; und auch die Intensität von Expression und Sekretion korreliert (Publ. 1, Bild 5). Allerdings fällt diese Korrelation unterschiedlich stark aus, wenn PBMC von unterschiedlichen Spendern stammen, auch wenn Genregulation und Zytokinsekretion zeitlich kongruent verlaufen.

5.2. Optimierung der Genexpressionsanalyse

Radke L, Giese C, Lubitz A, Hinderlich S, Sandig G, Hummel M, Frohme M. Reference gene stability in peripheral blood mononuclear cells determined by qPCR and NanoString. Microchimica Acta 2014, 181: 1733-42.

Die Genexpressionsanalyse mittels qPCR bedarf umfangreicher Etablierungsarbeiten, bspw. bei der Extraktion von mRNA und der reversen Transkription. Ergebnisse dieser Optimierungsarbeit

wurden 2012 unter Ko-Autorenschaft in der Fachzeitschrift BioSpektrum mit dem Titel *„Qualitätsmanagement in der RT-qPCR“* publiziert. Diese Veröffentlichung geht jedoch nicht in die vorliegende Arbeit ein.

Weitere Parameter wie das Temperaturprofil und die Effizienz der Amplifikationsreaktion müssen für eine exakte Quantifizierung in der qPCR optimiert und bestimmt werden. Die Analyse der differentiellen Genexpression erfordert den Bezug zu einem Fixpunkt, um den Einfluss variierender PCR-Performance oder Mengen an Ausgangsmaterial sowie Ungenauigkeiten bei der Durchführung auszugleichen. Diesen Zweck erfüllen Referenzgene, welche bezogen auf das jeweilige Experiment, stabil exprimiert und daher ebenfalls evaluiert werden müssen. In der Publikation wurden Referenzgene für PBMC-Stimulationsexperimenten mit und ohne Zugabe von mDC analysiert. Um beide Probenarten einheitlich zu normieren, wurde ein umfangreiches Set an Referenzgenen untersucht. Da sich vorhandene Softwaretools für die Bestimmung von Referenzgenen in qPCR-Experimenten in den Ergebnissen stark unterscheiden, wurde als zusätzliche „Enzym-freie“ Methode NanoString® eingeführt. Im Gegensatz zur relativen Quantifizierung der qPCR werden mit NanoString® mRNAs absolut quantifiziert. Für die Vergleichbarkeit der Methoden wurden zunächst die absoluten Counts der NanoString Methode mit der selbst entwickelten Formel in sogenannte Cq-Equivalente umgerechnet, welche die Effizienz der Amplifikationsreaktion und die Menge an Ausgangsmaterial berücksichtigt (Herleitung siehe Anlage von Publ. 2):

$$CqEquivalent = log_E\left(\frac{2^{34}}{nrc}\right) - log_E\left(\frac{m_{qPCR}}{m_{NanoString}}\right), \text{ mit}$$

E: Effizienz der Amplifikationsreaktion des jeweiligen Gens in der qPCR

nrc: Anzahl mit der Positivkontrolle normalisierter raw counts im Nanostring

m: jeweils eingesetzte Menge mRNA

Bei der anschließenden Überprüfung der Vergleichbarkeit beider Methoden mittels Bland-Altman Plot (Publ. 2, Abb. 2), wurde eine hohe Übereinstimmung der Ergebnisse festgestellt.

Bei der Analyse mittels qPCR zeigte sich für fast alle getesteten Referenzgene eine Verschiebung der Expression (gemessen in Cq) zwischen den verschieden stimulierten reinen PBMC und PBMC-mDC Gemischen. Diese Verschiebung konnte im NanoString Versuch nur für einige Gene nachgewiesen werden. Gleichzeitig war die Varianz der Referenzgene im NanoString Experiment geringer (Publ. 2, Abb. 1). Die Stabilität der Referenzgene wurde für beide Methoden (für NanoString in Cq-Equivalenten) mit den Programmen Bestkeeper, GeNorm und Normfinder überprüft. Die Reihenfolge der nach Stabilität sortierten Referenzgene unterscheidet sich dabei stark (z.T. exakt umgekehrt, siehe Publ. 2, Tab. 3). Ursache sind die ungleichen Ansätze, welche die einzelnen Algorithmen nutzen. Dabei berücksichtigt Bestkeeper stärker die Streuung des einzelnen Gens, Normfinder und GeNorm jedoch beruhen auf paarweisen Vergleichen der Gene untereinander. Dementsprechend konnten Referenzgene ausgewählt werden, die in NanoString und qPCR die geringste Streuung aufwiesen und durch Bestkeeper in beiden Methoden als am stabilsten bewertet wurden. Die Normalisierung von drei Zielgenen (CCL5, IL12b und TLR3) zeigte nahezu

kongruente Expressionswerte zwischen qPCR und NanoString Messung, wenn die stabilen Referenzgene SDHA, PPIA und TBP verwendet wurden, jedoch keinerlei Korrelation, wenn die von Normfinder oder GeNorm vorgeschlagenen Referenzgene verwendet wurden.
Mit der Validierung von Referenzgenen konnte für die exakte Genexpressionsanalyse von RSV-Vakzinen eine wichtige Grundlage gelegt werden. Zudem wurden erstmals umfangreiche Expressionsdaten von RSV-F Protein-stimulierten PBMC analysiert, was jedoch nicht in den Fokus dieser Veröffentlichung gerückt wurde.

5.3. Analyse von defukosyliertem RSV-F Protein

Radke L, Sandig G, Lubitz A, Schließer U, von Horsten HH, Blanchard V, Keil K, Sandig V, Giese C, Hummel M, Hinderlich S, Frohme M. In-vitro evaluation of glycoengineered RSV-F in the Human artifical Lymph Node Reactor. Bioengineering 2017, 4(3), 70.

Mithilfe der der GlymaxX®-Technologie [26], bei welcher das Enzym GDP-6-deoxy-D-lyxo-4-hexulose Reduktase (RMD) die *de novo* Synthese von Fukose in CHO-DG44 Zellen blockiert, wurde eine defukosylierte Variante des RSV-F Proteins hergestellt. Die korrekte Spaltung des Enzyms in seine natürliche Form wurde mittels Western Blot überprüft und die Glykosylierungsmuster massenspektrometrisch analysiert (Pub. 3, Abb. 1). Mit diesen defukosylierten und mit wildtyp RSV-F Proteinen wurden PBMC und zuvor erzeugte mDCs im huALN® in einem Langzeitexperiment über 28 Tage und parallel in Multiterplatten mehrfach stimuliert.
Zur Überprüfung, welchen Einfluss die veränderte Glykosylierung auf die Immunreaktion hat, wurden die Zytokinkonzentrationen der Zellkulturüberstände dieser und parallel kultivierter Kontrollen mittels automatisierter Bead-basierter Multiplex-Analyse untersucht. Eine vergleichende Übersicht befindet sich in Publikation 3 (Abb. 2). Zellen, die mit defukosyliertem RSV-F Protein stimuliert wurden, zeigen eine prominente IL-4 Ausschüttung, welche stark mit den Restimulationszeitpunkten korreliert. Die Induktion einer derartigen T_H2-Antwort erfolgt in der Wildtyp Kontrolle nicht. Trotz einer geringen Konzentration an T_H1-aktivierenden IL-2, wurde mit der Ausschüttung von IFN-γ eine pro-inflammatorische Antwort erzeugt. Im Gegensatz dazu zeigt die Wildtyp-Kontrolle stärkere IL-2 Antworten nach jeder Restimulation sowie erhöhte IL-10 Konzentrationen, welche einer zu starken IFN-γ Sekretion entgegenwirken. TNF-α und GM-CSF sind weitere Zytokine, deren Sekretion deutlich stimulationsabhängig erfolgt und für beide RSV-F Varianten auftritt. Auf Basis der gemessenen Zytokine ist die Reaktion des Wildtyps eher T_H1 basiert, während die defukosylierte Variante ebenso T_H2 Zellen zu aktivieren scheint.
Für eine umfangreiche Analyse der Genexpression mittels Human Immunology v2 nCounter® Gene Expression Assay (NanoString®) wurden PBMCs sieben Tage im Fed-batch Modus kultiviert und stimuliert. Als zusätzliche Positivkontrolle wurden Zellen ebenfalls mit LPS stimuliert. Eine Übersicht über die Unterschiede zwischen den Proben wurde anhand einer hierarchischen Clusteranalyse erstellt (Publ. 3, Abb. 3). Diese zeigt mit Ausnahme von LPS primär eine zeitliche

und sekundär eine stimulationsabhängige Gruppierung der Proben. Allerdings zeigt das Genexpressionsmuster nach 48 stündiger Stimulation für den Wildtyp eine höhere Ähnlichkeit zur Negativkontrolle, was auf eine schnellere oder stärkere Aktivierung der Immunreaktion durch das defukosylierte Vakzin hinweist. Mithilfe des R-Tools NanoStringDiff [35] wurde die Signifikanz der Expressionsunterschiede zwischen beiden Vakzinvarianten für diesen Zeitpunkt untersucht und verschiedene Gencluster identifiziert (Publ. 3, Abb. 4). Diese umfassten die Aktivierung von T-Zellen im Allgemeinen und T_H17 im Besonderen sowie DC und B-Zellen, aber auch generellen antimikrobiellen und antiviralen Immunantworten und umfassender Signalketten (z.B. JAK-STAT oder NF-kB Pfad).
Obwohl Glykane mit und ohne Fukose im menschlichen Körper vorkommen, und somit eine direkte adjuvante Wirkung unwahrscheinlich ist, weisen die Analysen der Zytokine und Genexpression auf eine umfangreiche Aktivierung des Immunsystems hin. Die Zytokinmuster deuten eine unterschiedlich starke Aktivierung von T_H1 und T_H2 Zellen an. Daher könnte es möglich sein, über eine stufenweise Anpassung des Fukosylierungsgrades das T_H1/T_H2 Verhältnis zu modulieren. Ebenso von Bedeutung ist, dass der HuALN®-Reaktor und die Downstream-Analyse-Methoden in der Lage sind, Effekte zu unterscheiden, die durch kleine Modifikationen der Glykan-Struktur verursacht werden.

5.4. Analyse von xylosylierten RSV-F Protein

Sandig G, von Horsten HH, Radke L, Blanchard V, Frohme M, Giese C, Sandig V, Hinderlich S. Engineering of CHO Cells for the Production of Recombinant Glycoprotein Vaccines with Xylosylated N-glycans. Bioengineering *2017,* 4*(2), 38.*

Xylosylierte N-Glykane finden sich nur in Pflanzen und Würmern und sind somit für Säugerzellen fremdartige Strukturen. Die Herstellung des RSV-F Proteins mit xylosylierten N-Glykanen in Säugerzellen ist ein Novum im Bereich des Glycoengineerings. Durch Koexpression von β1,2-xylosyltransferase (XylT) aus *Nicotiana tabacum* kann die in Säugerzellen auf natürliche Weise vorkommende UDP-Xylose in CHO-DG44 Zellen auf N-Glykane übertragen werden. Western Blots, Hochleistungs-Ionenaustauschchromatographie und Massenspektrometrie (Publ. 4, Abb. 1-4) zeigen, dass xylosyliertes RSV-F Protein erfolgreich produziert wurde. Wie zuvor beim defukosylierten RSV-F Protein wurden Langzeitstimulationsexperimente im huALN-Reaktor durchgeführt. Die mit xylosylierten RSV-F Protein und mDC stimulierten PBMC erzeugten dabei höhere und stärker akzentuierte Zytokinausschüttungen als nicht xylosyliertes RSV-F. Die pro-inflammatorische Antwort ist durch anhaltend hohe IFN-γ Konzentrationen und Sekretion von TNF-α nach den Stimulationen stark ausgeprägt. Neben diesen Effektorzytokinen der T_H1 Zellen werden mit IL-4 und IL-10 aber auch T_H2-assoziierte Zytokine ausgeschüttet, was auf eine umfassende Aktivierung durch das xylosylierte RSV-F hinweist.
Zusätzlich wurden Genexpressionsstudien durchgeführt, um die immunologische Antwort auf die erste Stimulation (nach 48 h) im Detail zu untersuchen. Mithilfe eines Human Immunology v2

nCounter® Gene Expression assay (NanoString) wurden die Genexpression analysiert und Veränderungsraten (engl. fold change) der Expression zwischen den Proben berechnet. Dabei zeigte sich, dass die Schlüsselzytokine der einzelnen T-Zellpopulationen, also IL-2 der T_H1 Zellen, IL-4 und IL-5 der T_H2 Zellen und IL-17 der T_H17 Zellen durch xylosyliertes RSV-F deutlich stärker exprimiert wurden. Die Expression der Gene für pro-inflammatorische IFN-γ und TNF-α hingegen war relativ gering. Dies spricht einerseits für eine bereits ausreichende Aktivierung, andererseits hat das hoch exprimierte IL-17 eine synergistische Wirkung [36]. Neben den zellulären Aktivierungsmarkern, sind auch einige Gene mit humoraler Funktion aktiviert, wie bspw. RAG1 Recombination Activation Gene 1) und RAG2, welche bei der Reifung von Antikörper eine wichtige Rolle spielen. Weitere Gencluster umfassen ganze Teile des angeborenen Immunsystems, wie das Komplementsystem, antimikrobielle Defensine, Kohlenhyrat-bindende Lektine und antivirale Zytokine, wie IFNA, IFNB oder IL28. Die Aktivierung weiterer Gene wie RELA und RELB, welche Teile des NF-κB Komplexes sind, sowie proinflammatorische Faktoren wie NOS2 (Stickstoffmonooxid Synthase), CAMP (Cathelicidine Antimikrobielles Peptid) oder IL21 unterstreichen die umfassende Aktivierung des Immunsystems durch xylosyliertes RSV-F.

5.5. Validierung eines miniaturisierten Bioreaktors

Böhme A, Radke L, Schütze F, Schneider S, Liebscher T, Sauer S, Santo L, Quadrini F, Hummel M, Giese C, Frohme M, Foitzik. Miniaturized Flow-Through Bioreactor for Processing and Testing in Pharmacology. Materials Science Forum 2017, 879: 236-243.

Der HuALN® erlaubt durch seine Nachahmung der physiologischen Umgebung die Kultivierung und Stimulation von T-Zellen über einen langen Zeitraum. Allerdings ist die Kultivierung aufwändig und nur in geringer Anzahl parallel durchführbar. Ein miniaturisierter Bioreaktors für die Parallelisierung von Stimulationsexperimenten wurde mittels Mikrofrästechnik sowie Aufbau- und Verbindungstechnik aus Polycarbonat mit einem Kulturvolumen von 200 µl hergestellt, welcher über eine gaspermeable Folie und über Hohlfasern mit Gasen und Medium versorgt werden kann. Alle schließlich verwendeten Materialien wie Klebstoffe, Folien und Schläuche wurden auf ihre Bioverträglichkeit untersucht und zeigten gute Ergebnisse bei Lebend/Totfärbung (Publ. 5, Abb. 2). Die Dichtheit der Reaktoren wurde fluoreszenzmikroskopisch überprüft. Dabei wurde die Autofluoreszenz von Cyanobakterien (*Synechocystis sp. PCC 6803*) genutzt, um undichte Verbindungsstellen zwischen den verschiedenen Materialien zu finden. Eine LabView gesteuerte Temperierung der Reaktoren konnte etabliert werden, bei welcher die Wärme durch einen Wärmespreizer von einem Leistungs-MOSFET übertragen wird. Des Weiteren wurde ein am IHP Frankfurt/O. entwickelter viskosimetrischer Glukosesensor [37] integriert. Die Funktionalität des Reaktors im autonomen Betrieb wurde in verschiedenen Experimenten überprüft. Bei der Untersuchung des Einflusses der Versorgung mit Nährmedium an L929 Mausfibroblasten zeigte sich unter periodischer Mediumperfusion eine höhere Zelldichte bei gleicher Viabilität der Zellen (Publ. 5, Abb. 4). Die Kultivierungen von PBMC in verschiedenen Kollagen-basierten 3D Matrizes zeigten eine anhaltend hohe Viabilität für die gesamte Kulturdauer von 7 Tagen (Publ. 5, Abb. 5).

6. Diskussion

Im Projekt IPoGly konnten erfolgreich RSV-F Proteine mit veränderter Glyoksylierung hergestellt werden. In der vorliegenden Arbeit wurde deren immunologische Wirksamkeit untersucht.
In einer zunächst durchgeführten Voruntersuchung (Publ. 1) wurden die einsetzenden Immunreaktionen für verschiedene Stimulanzien anhand eines zur damaligen Zeitpunkt äußerst umfangreichen Zytokinsprektrums und einer sehr hohen Dichte an Messpunkten auf Protein- und Genexpressionsebene untersucht. Beim Vergleich frisch isolierter und kryokonservierter PBMC zeigten sich nur in den ersten Stunden nach einer Stimulation Unterschiede auf Genexpressionsebene, welche aber im Verlauf nur geringen Einfluss auf die Menge sekretierter Zytokine hatte. Dadurch ist die Nutzung kryokonservierter PBMC eines Spenders zu unterschiedlichen Zeitpunkten möglich, um z.B. die veränderte Wirksamkeit abgewandelter Impfstoffvarianten zu untersuchen und mit früheren Ergebnissen zu vergleichen. Die Analyse der Genexpression zum frühen Zeitpunkt ist interessant, da die mRNA-Menge mit der späteren Sekretionsstärke einzelner Zytokine korreliert und so abgeschätzt werden kann. Jedoch variieren die Expressionsmuster in Abhängigkeit von Stimulanz, Donor und Zytokin, so dass die Detektion der maximalen Expressionsrate oder der Dauer erhöhter Genexpression aufwändig ist.
In allen Studien wurden die PBMC aus Vollblutspenden gewonnen, welche vor der Nutzung nach transfusionsmedizinischen Vorschriften untersucht wurden. Zwischen den PBMC der beiden Spender aus Publ. 1 fallen Donor-spezifische Unterschiede der immunologischen Antwort bei den verwendeten Standardstimulanzien gering aus. Ein vorheriger Kontakt mit diesen Stimulanzien ist eher unwahrscheinlich, so dass von vergleichbaren Mechanismen der Immunreaktion ausgegangen werden kann. Bei der späteren Untersuchung von RSV-F Proteinen erfolgte keine Bestimmung des Serostatus für RSV Antikörper. Aufgrund der hohen Prävalenz von RSV-Infektionen ist es jedoch wahrscheinlich, dass der Spender bereits eine RSV-Infektion erlebt hat, was wiederum Einfluss auf die Immunantwort haben kann.
Eine Vielzahl von Faktoren erschwert die Genauigkeit der Analysen. Um die Immunantwort so naturnah und komplex wie möglich abzubilden, müssen verschiedene Immunzellen zusammenarbeiten können. Dabei kann die zelluläre Zusammensetzung variieren und in der Folge das Ergebnis beeinflussen. Bspw. könnten sich die Unterschiede der TNF-α Konzentrationen der Spender in Publ. 1 auf ungleiche Lymphozyten und Monozyten Verhältnisse zurückführen lassen [38].
Da im Zusammenspiel der Immunreaktion die Erkennung von Antigenen über zelluläre Rezeptoren (TCR, BCR) erfolgt, muss bei Stimulationsexperimenten gewährleistet sein, dass eine ausreichende Anzahl Zellen zur Verfügung steht, um die Diversität zu erhalten. Zum einen sind dadurch der Miniaturisierung von Reaktorräumen Grenzen gesetzt, zum anderen müssen Spender frei von Infektionen oder Entzündungen sein, da diese das Rezeptorrepertoire stark verschieben können.
Die Nutzung von Mischpopulationen erschwert die Analyse der differentiellen Genexpression, da selbst eine starke Aktivierung einer kleinen Zellfraktion verdeckt sein kann und nicht mehr als

signifikant erkannt wird. Für eine genauere Analyse müssten Zellen z.B. mittels FACS in die typischen Klassen T_H1, T_H2, T_H17 und DC separiert werden. Der dadurch erhöhte experimentelle und analytische Aufwand könnte durch kleinere spezifischere Analytensets ausgeglichen werden. Eine besondere Herausforderung stellt bei der Genexpressionsanalyse von gemischten Zellpopulationen auch die Wahl geeigneter Referenzgene dar, deren Stabilität in allen Zellsubpopulationen gewährleistet sein muss. Die in Publ. 2 durchgeführten umfangreichen Untersuchungen führten zur Validierung von Referenzgenen für PBMC und PBMC-DC Gemische in Stimulationsexperimenten mit RSV-F Proteinen, wodurch eine hohe Genauigkeit für speziell diese Analyse ermöglicht wird. Die dabei genutzten Methoden qPCR und NanoString unterscheiden sich grundlegend in der Art des Gennachweises. In der qPCR wird cDNA durch zyklische Amplifikation unter Nutzung eines hybridisierenden Farbstoffs nachgewiesen. Bei diesem enzymatischen Verfahren ist die Bestimmung der Amplifikationseffizienz, die von vielerlei Faktoren beeinflusst wird, von hoher Bedeutung. Die NanoString Technologie hingegen bindet die mRNA bestimmter Gene direkt und nutzt Fluoreszenzlabel zum optischen Nachweis. Hier begrenzt die Bindungseffizienz der Sonde die Genauigkeit der Quantifizierung. Mit Hilfe einer selbstentwickelten Formel konnten die Counts (Anzahl quantifizierter mRNA Fragmente eines Gens) der NanoString Analyse in Cq-Equivalente (Cq ist die Maßeinheit der Quantifizierung von Amplifikationsprodukten in der qPCR) umgerechnet werden und mittels Bland-Altman-Plot die Vergleichbarkeit beider Methoden erfolgreich gezeigt werden. Anhand mehrerer Target-Gene konnte demonstriert werden, dass die Wahl instabiler Referenzgene zu starken Abweichungen der Expressionswerten zwischen beiden Methoden führt.

6.1. Immunaktivierungspotenz der hergestellten RSV-F Proteinvarianten

Bei der Bewertung der Aktivierung des Immunsystems durch die modifizierten RSV-F Proteine liefern die Zytokinmuster und die Genexpressionsmuster ein zusammenhängendes Bild. Sowohl die vom defukosylierten als auch vom xylosylierten RSV-F hervorgerufenen Zytokinsekretionen (Publ. 3, Abb. 5 und Publ. 4, Abb. 2) korrelieren deutlich mit den Zeitpunkten der Stimulationen. Im Vergleich zum Wildtyp RSV-F Protein führen die modifizierten Varianten zu höheren Ausschüttungen von TNF-α und IFN-γ (beides Effektorzytokine aktivierter TH1 Zellen), so dass die Immunantworten stärker pro-inflammatorisch ausgeprägt sind. Einhergehend mit einer geringeren Sekretion von anti-inflammatorischen IL-10 modulieren beide RSV-F Proteinvarianten zudem das TH2 assoziierte IL-4 sehr präzise. Zusätzlich zeigen die Genexpressionsanalysen zum Zeitpunkt 24 Stunden nach den ersten Stimulationen (Publ. 3, Abb. 6 und Publ. 4, Abb. 4) für beide modifizierten RSV-F Proteine eine starke Aktivierung von T_H17 Zellen. Somit sind beide RSV-F Proteine in der Lage, das Immunsystem umfassend zu aktivieren. Das defukosylierte F-Protein reguliert außerdem DC und B-Zell-Marker nach oben und zeigt erhöhte Transkriptionsraten für große Teile immunrelevanter Signalketten (z.B. JAK-STAT, IKB, NFKB und MYD88) und den dazugehörigen Transkriptionsfaktoren. Bei der xylosylierten Variante sind stattdessen ganze Gencluster des

angeborenen Immunsystems hochreguliert, wie z.B. des Komplementsystems oder mehrere Defensine. Beide modifizierten viralen Proteine aktivieren antivirale Gene (z.B. IFNA o. IL28) und zuckerbindende Lektine. Auch hier zeigt sich eine ganzheitliche Aktivierung der Immunantwort.
Die Generierung neutralisierender Antikörper wird als wichtiges Merkmal für die Wirksamkeit eines RSV-Vakzins angesehen [6]. Anhand der stimulationsinduzierten IL-4 Sekretion ist eine deutliche Aktivierung der humoralen Immunantwort bei beiden Impfstoffvarianten erkennbar. Die defukosylierte RSV-F Variante zeigt neben den erhöhten B-Zell- Aktivierungs- und Reifungsmarkern auch erhöhte Expressionswerte von Antikörperrezeptoren. Gene des Reifungsmechanismus von Antikörpern (somatische Hypermutation) waren zum untersuchten Zeitpunkt jedoch nur teilweise aktiviert (RAG2, z.T. RAG1, jedoch nicht AICDA). Der Nachweis von spezifischen Antikörpern wäre in nachfolgenden Untersuchungen daher der naheliegende Schritt. Kürzlich konnte die Physiologie des verwendeten HuALN Reaktors verbessert werden, indem die Co-Kultivierung von Stromazellen erfolgreich implementiert wurde [39]. Hierdurch wird erwartet, dass die strukturelle Verbesserung der zellulären Organisation zur verbesserten humoralen Immunantwort führt.

6.2. Statistische Bewertung

Die Durchführung von Langzeitexperimenten im HuALN ist arbeits- und kostenintensiv. Die Versuche konnten aus diesen Gründen nicht mit unterschiedlichem Spendermaterial wiederholt werden und die Zytokinanalyse wurde nur in Duplikaten durchgeführt. Daher beschränkt sich die statistische Bewertung der Messergebnisse der Bioplex-Analyse auf die Wiederfindungsrate der Spike-in Kontrollen. Zwar ist mathematisch die Berechnung von Mittel- und Streuungswerten bei Duplikaten möglich, aber statistisch nicht aussagekräftig und zeigt in diesem Falle auch nur die technische Messgenauigkeit.
Bei der Genexpressionsanalyse ist die statistische Bewertung von Natur aus komplizierter. Der häufig genutzte Schwellenwert von zwei ist sowohl biologisch als auch statistisch willkürlich und lässt sich in Messungen mit geringer Anzahl an Wiederholungen durch einzelne Ausreißer leicht hervorrufen. Heute übliche statistische Tests (ANOVA oder andere Tools) ziehen neben dem Schwellenwert noch die Varianz in die Berechnung ein, und können zusätzlich die Wahrscheinlichkeit des beobachteten Ergebnisses in Form eines p-Werts angeben. Dabei kann sich die Varianz auf das einzelne Gen, alle Gene oder alle Behandlungen beziehen. Allerdings ergibt sich das Problem, dass bei umfangreichen Gensets eine hohe Anzahl falschpositiver Ergebnisse in Kauf genommen wird (z.B. 5% bei einem p-value von 0,05). Andererseits kann durch stringentere Korrekturmechanismen die Zahl der als signifikant unterschiedlich exprimiert identifizierten Gene gegen Null gehen. Mittelwege führen zu einer Vielzahl von verschiedenen Tools, die zu unterschiedlichen Ergebnissen kommen [40]. Unabhängig von der gewählten Methode und deren Grundannahmen gilt jedoch, dass die Ergebnisse ähnlicher werden, je mehr Messwiederholungen zur Verfügung stehen. Bei der Bestimmung der Signifikanz der Genexpression der modifizierten RSV-F Proteine wurde das R Programm NanoStringDiff verwendet, welches speziell für nCounter Assays entwickelt wurde, da das Problem geringer Messwiederholungen bekannt ist. Dabei werden die

Messwerte in ein generalisiertes lineares Model überführt, die Streuungsparameter des Models mittels Bayes shrinkage geschätzt und mittels Likelihood-ratio-Test differentiell exprimierte Gene identifiziert. Aufgrund der Messung in Duplikaten wurde eine höhere Varianz zugelassen und somit das Risiko falschpositiver Ergebnisse erhöht. Durch die Beobachtung umfangreicher funktioneller Gencluster, deren Expression häufig kollektiv erhöht war, verringert sich die Gefahr einer Fehlinterpretation. Jedoch könnte die statistische Sicherheit mit einer größeren Zahl an Messungen und der Wahl anderer statistischer Verfahren erhöht werden.
Der im Projekt entwickelte miniaturisierte Perfusionsreaktor (Publ. 5) würde sich als kostengünstiges aber hochentwickeltes Kultivierungssystem für Stimulationsexperimente in höherem Durchsatz eignen. Dichtheit und Biokompatibilität konnten nachgewiesen werden und PBMC wurden erfolgreich über mehrere Tage in verschiedenen 3D-Kollagenmatrizen kultiviert (Publ. 5, Abb. 5). Durch den kleineren Kulturraum (ca. 230 µl) ist die Anzahl an kultivierbaren Zellen verringert (max. 10^6 Zellen). Wie stark sich das im Vergleich zum huALN eingeschränkte Repertoire an T-Zellen auf die immunologische Antwort auswirkt, ist allerdings noch nicht im Detail untersucht.

6.3. Ausblick

Es konnte erfolgreich gezeigt werden, dass die hergestellten RSV-F Proteine mit veränderten Glykanstrukturen das Immunsystem stärker und früher aktivieren als Wildtyp RSV-F. Die rekombinante Herstellung β-1,2-xylosylierter n-Glykane stellt dabei ein Novum dar.
Mit der Verwendung der CHO-Zelllinie DG44 konnte erfolgreich die defukosylierte RSV-F Variante hergestellt werden, da die Fukosesynthese enzymatisch blockiert wurde. Als nächster Schritt könnte durch die Bereitstellung modifizierter Fukoseanaloga über den sogenannten *salvage pathway* weitere modifizierte Glykane entstehen [41], die allein eine verstärkte immunogene Wirkung aufweisen oder Startpunkt weiterer chemischer Modifikationen sein können.
Mit der Untersuchung aufgetrennter Zellfraktionen und umfangreicherer Messungen könnte zunächst ein genaueres Bild der Zellaktivierung auf Ebene der Genexpression erfolgen. Im Weiteren sollte die Generierung neutralisierender Antikörper untersucht werden. Bei erfolgreichen Bindungsassays mit RSV-F Proteinen könnte im Anschluss die Untersuchung der protektiven Wirkung der Impfstoffkandidaten im Tiermodell erfolgen.
Durch den Einsatz des HuALN® konnte auf Tierversuche in dieser frühen Phase der Vakzinentwicklung verzichtet werden. Zudem stehen mit der Stimulation menschlicher Immunzellen direkt Ergebnisse aus dem humanen System zur Verfügung, so dass bei der Weiterentwicklung der bestehenden Impfstoffvarianten gezielte Verbesserung durchgeführt können, die auf die Wirksamkeit im menschlichen Immunsystem abgestimmt sind. Dadurch wird das Risiko verringert, dass ein in Versuchstieren entwickelter Impfstoff seine Wirksamkeit beim Wechsel ins humane System verliert und trägt so zu einem beschleunigten Entwicklungsprozess bei.

7. Literaturverzeichnis

[1] Leroux-Roels G, Bonanni P, Tantawichien T, Zepp F. Vaccine development. Perspectives in Vaccinology 2011;1(1):115-150.

[2] Openshaw PJ, Culley FJ, Olszewska W. Immunopathogenesis of vaccine-enhanced RSV disease. Vaccine 2001;20 Suppl 1:27-31.

[3] Delgado MF, Coviello S, Monsalvo AC, Melendi GA, Hernandez JZ, Batalle JP, Diaz L, Trento A, Chang HY, Mitzner W, Ravetch J, Melero JA, Irusta PM, Polack FP. Lack of antibody affinity maturation due to poor Toll-like receptor stimulation leads to enhanced respiratory syncytial virus disease. Nat Med 2009;15:34-41.

[4] Leo O, Cunningham A, Stern PL. Vaccine Immunology. Perspectives in Vaccinology 2011;1(1): 25-59.

[5] Hurwitz JL, Respiratory syncytial virus vaccine development. Expert Rev Vaccines 2014 10(10): 1415–33.

[6] Walsh EE, Falsey AR. Humoral and mucosal immunity in protection from natural respiratory syncytial virus infection in adults. J Infect Dis 2004;190:373–8.

[7] Strugnell R, Zepp F, Cunningham A, Tantawichien T. Vaccine Antigens. Perspectives in Vaccinology 2011;1(1):61-88.

[8] Garçon N, Leroux-Roels G, Cheng WF. Vaccine Adjuvants. Perspectives in Vaccinology 2011;1(1):89-113.

[9] Paavonen J, Naud P, Salmerón J, Wheeler CM, Chow SN, Apter D, Kitchener H, Castellsague X, Teixeira JC, Skinner SR, Hedrick J, Jaisamrarn U, Limson G, Garland S, Szarewski A, Romanowski B, Aoki FY, Schwarz TF, Poppe WA, Bosch FX, Jenkins D, Hardt K, Zahaf T, Descamps D, Struyf F, Lehtinen M, Dubin G, HPV PATRICIA Study Group. Efficacy of human papillomavirus (HPV)-16/18 AS04-adjuvanted vaccine against cervical infection and precancer caused by oncogenic HPV types (PATRICIA): final analysis of a double-blind, randomised study in young women. Lancet 2009;374(9686):301-14.

[10] Asa PB, Wilson RB, Garry RF. Antibodies to Squalene in Recipients of Anthrax Vaccine. Exp Mol Pathol 2002;73(1):19–27.

[11] Carlson BC, Jansson AM, Larsson A, Bucht A, Lorentzen JC. The Endogenous Adjuvant Squalene Can Induce a Chronic T-Cell-Mediated Arthritis in Rats. American J Pathol 2000;156(6):2057–65.

[12] Phillips CJ, Matyas GR, Hansen CJ, Alving CR, Smith TC, Ryan MA. Antibodies to squalene in US Navy Persian Gulf War veterans with chronic multisymptom illness. Vaccine 2009;27(29):3921–6.

[13] Vogelbruch M, Nuss B, Körner M, Kapp A, Kiehl P, Bohm W. Aluminium-induced granulomas after inaccurate intradermal hyposensitization injections of aluminium-adsorbed depot preparations. Allergy 2000;55:883-7.

[14] Masoudi S, Ploen D, Kunz K, Hildt E. The adjuvant component α-tocopherol triggers via modulation of Nrf2 the expression and turnover of hypocretin in vitro and its implication to the development of narcolepsy. Vaccine 2014;32(25):2980-8.

[15] Glezen WP, Taber LH, Frank AK, Kasel JA. Risk of primary infection and reinfection with respiratory syncytial virus. Am J Dis Child 1986;140(6): 543-6.

[16] Thorburn, K. Pre-existing disease is associated with a significantly higher risk of death in severe respiratory syncytial virus infection. Arch Dis Child 2009;94(2):99-103.

[17] Hall CB, Weinberg, GA, Blumkin AK, Edwards KM, Staat MA, Schultz AF, Poehling KA, Szilagyi PG, Griffin MR, Williams JV, Zhu Y, Grijalva CG, Prill MM, Iwane MK. Respiratory syncytial virus-associated hospitalizations among children less than 24 months of age. Pediatrics 2013;132(2):e341-8.

[18] Johnson PR, Spriggs MK, Olmsted RA, Collins PL. The G glycoprotein of human respiratory syncytial viruses of subgroups A and B: extensive sequence divergence between antigenically related proteins. Proc Natl Acad Sci U S A 1987;84(16):5625-9.

[19] Zimmer G, Budz L, Herrler G. Proteolytic activation of respiratory syncytial virus fusion protein. Cleavage at two furin consensus sequences. J Biol Chem 2001;276(34):31642-50.

[20] Cummings RD. The repertoire of glycans determinants in the human glycome. Mol BioSyst 2009;5:1087-104.

[21] Marth JD, Grewal PK. Mammalian glycosylation in immunity. Nat Rev Immunol 2009;8(11):874-87.

[22] Wolfert MA, Boons GJ. Adaptive immune activation: glycosylation does matter. Nat Chem Biol 2013;9(12):776-84.

[23] Rosen SD. Ligands for L-Selctin: Homing, Inflammation, and Beyond. Annu Rev Immunol 2004;22:129-156.

[24] Cobb BA, Kasper DL. Coming of age: carbohydrates and immunity. Eur J Immunol 2005;35:352-6.

[25] Oberli MA, Hecht ML, Bindschädler P, Adibekian A, Adam T, Seeberger PH. A Possible Oligosaccharide-Conjugate Vaccine Candidate for Clostridium difficile Is Antigenic and Immunogenic. Chem Biol 2011;18(5):580-8.

[26] Von Horsten HH, Ogorek C, Blanchard V, Demmler C, Giese C, Winkler K, Kaup M, Berger M, Jordan I, Sandig V. Production of non-fucosylated antibodies by co-expression of heterologous GDP-6-deoxy-D-lyxo-4-hexulose reductase. Glycobiology 2010;20:1607–18.

[27] Giese C, Demmler CD, Ammer R, Hartmann S, Lubitz A, Miller L, Müller R, Marx U. A human lymph node in vitro – challenges and progress. Artif Organs 2006;30:803-8.

[28] Giese C, Lubitz A, Demmler CD, Reuschel J, Bergner K, Marx U. Immunological substance testing on human lymphatic micro-organoids in vitro. J Biotechnol 2010;148(1):38-45.

[29] Radke L. Etablierung verschiedener Bead-basierter Multiplexmethoden mit einem Suspensions-Array-System. Masterarbeit, TFH Wildau (2009).

[30] Keil K. Automatisierung des Bio-Plex Pro™ Analyseverfahrens. Bachelorarbeit, TH Wildau (2014).

[31] Prokopec SD, Watson JD, Waggott DM, Smith AB, Wu AH, Okey AB, Pohjanvirta R, Boutros PC. Systematic evaluation of medium-throughput mRNA abundance platforms. RNA 2013;19:51–62.

[32] Paul U. Analyse des T-Zell-Rezeptor-Repertoires mittels Hochdurchsatz-Sequenzierung. Masterarbeit, TH Wildau (2012).

[33] Leist M, Hartung T. Inflammatory findings on species extrapolations: humans are definitely no 70-kg mice. Arch Toxicol 2013;87:563–7.

[34] Böhme A. Artificial Lymph Node for Processing and Testing in Pharmacology. Doktorarbeit, Università Degli Studi da Roma „Tor Vergata“ (2016).

[35] Wang H, Horbinski C, Wu H, Liu Y, Stromberg AJ, Wang C. A Negative Binomial Model-Based Method for Differential Expression Analysis Based on NanoString nCounter Data. Nucleic Acids Res 2016;44(20):e151.

[36] Gabr MA, Jung L, Helbling AR, Sinclair SM, Allen KD, Shamji MF, Richardson WJ, Fitch RD, Setton LA, Chen L. Interleukin-17 synergizes with IFN or TNF to promote inflammatory mediator release and intercellular adhesion molecule-1 (ICAM-1) expression in human intervertebral disc cells. J Orthop Res 2011;29:1–7.

[37] Birkholz M, Ehwald KE, Basmer T, Kulse P, Reich C, Drews J, Genschow D, Haak U, Marschmeyer S, Matthus E, Schulz K, Wolansky D, Winkler W, Guschauski T, Ehwald R. Sensing glucose concentrations at GHz frequencies with a fully embedded Biomicroelectromechanical system (BioMEMS), J Appl Phys 2013;113(24):244904.

[38] Yan Z, Yang DCH, Neill R, Jett M. Production of tumor necrosis factor alpha in human T lymphocytes by Staphylococcal Enterotxin B correlates with toxininduced proliferation and is regulated through protein kinase C, Infect Immun 1999;67:6611–8.

[39] Sardi M, Lubitz A, Giese C. Modeling Human Immunity In Vitro: Improving Artificial Lymph Node Physiology by Stromal Cells. Appl In Vitro Toxicol 2016;3:143–50.

[40] Yauk CL, Berndt ML. Review of the literature examining the correlation among DNA microarray technologies. Environ Mol Mutagen 2007;48(5):380–94.

[41] Rosenlöcher J, Böhrsch V, Sacharjat M, Blanchard V, Giese C, Sandig V, Hackenberger CPR, Hinderlich S. Applying Acylated Fucose Analogues to Metabolic Glycoengineering. Bioengineering 2015;2:213-34.

8. Eidesstattliche Versicherung

„Ich, Lars Radke, versichere an Eides statt durch meine eigenhändige Unterschrift, dass ich die vorgelegte Dissertation mit dem Thema: „Evaluierung der Potenz von glykosylierten Impfstoffen am Beispiel des RSV-F Proteins“ selbstständig und ohne nicht offengelegte Hilfe Dritter verfasst und keine anderen als die angegebenen Quellen und Hilfsmittel genutzt habe.
Alle Stellen, die wörtlich oder dem Sinne nach auf Publikationen oder Vorträgen anderer Autoren beruhen, sind als solche in korrekter Zitierung (siehe „Uniform Requirements for Manuscripts (URM)“ des ICMJE -*www.**icmje**.org*) kenntlich gemacht. Die Abschnitte zu Methodik (insbesondere praktische Arbeiten, Laborbestimmungen, statistische Aufarbeitung) und Resultaten (insbesondere Abbildungen, Graphiken und Tabellen) entsprechen den URM (s.o) und werden von mir verantwortet.
Meine Anteile an den ausgewählten Publikationen entsprechen denen, die in der untenstehenden gemeinsamen Erklärung mit dem/der Betreuer/in, angegeben sind. Sämtliche Publikationen, die aus dieser Dissertation hervorgegangen sind und bei denen ich Autor bin, entsprechen den URM (s.o) und werden von mir verantwortet.
Die Bedeutung dieser eidesstattlichen Versicherung und die strafrechtlichen Folgen einer unwahren eidesstattlichen Versicherung (§156,161 des Strafgesetzbuches) sind mir bekannt und bewusst.“

Datum _____ Unterschrift

<u>Anteilserklärung an den erfolgten Publikationen</u>

Lars Radke hatte folgenden Anteil an den folgenden Publikationen:

Publikation 1: *Radke L, López Hemmerling DA, Lubitz A, Giese C, Frohme M*, Induced cytokine response of human PMBC-cultures: Correlation of gene expression and secretion profiling and the effect of cryopreservation, Cellular Immunology, 2011
Beitrag im Einzelnen:
Durchführung der experimentellen Arbeiten zur Extraktion, reversen Transkription und Quantifizierung von Nukleinsäuren aus stimulierten kryokonservierten PBMC-Kulturen mittels qPCR sowie Quantifizierung der Zytokine aus Zellkulturüberständen stimulierter PBMC-Kulturen; Datenanalyse sowie das Schreiben der Veröffentlichung.

Publikation 2: Radke L, Giese C, Lubitz A, Hinderlich S, Sandig G, Hummel M, Frohme M, Reference gene stability in peripheral blood mononuclear cells determined by qPCR and NanoString, Microchimica Acta, 2014
Beitrag im Einzelnen:
Durchführung der experimentellen Arbeiten zur Extraktion, reversen Transkription und Quantifizierung von Nukleinsäuren aus stimulierten PBMC-Kulturen mittels qPCR; Analyse von qPCR und NanoString Assay Daten mittels Referenzgensoftware und statistischer Korrelation sowie das Schreiben der Veröffentlichung.

Publikation 3: Radke L, Sandig G, Lubitz A, Schließer U, von Horsten HH, Blanchard V, Keil K, Sandig V, Giese C, Hummel M, Hinderlich S, Frohme M, In-vitro evaluation of glycoengineered RSV-F in the Human artifical Lymph Node Reactor, Bioengineering, 2017
Beitrag im Einzelnen:

Durchführung der experimentellen Arbeiten zur Extraktion, reversen Transkription und Quantifizierung von Nukleinsäuren aus stimulierten PBMC-Kulturen mittels NanoString Assay; Mitarbeit an der automatisierten Quantifizierung der Zytokine aus Zellkulturüberständen stimulierter PBMC-Kulturen; Analyse von NanoString Daten und statistischer Bewertung; sowie das Schreiben der Veröffentlichung mit Ausnahme von Abschnitten der Methoden- und Diskussionsteile.

Publikation 4: Sandig G, von Horsten HH, Radke L, Blanchard V, Frohme M, Giese C, Sandig V, Hinderlich S, Engineering of CHO Cells for the Production of Recombinant Glycoprotein Vaccines with Xylosylated N-glycans, Bioengineering, 2017
Beitrag im Einzelnen:
Durchführung der experimentellen Arbeiten zur Extraktion, reversen Transkription und Quantifizierung von Nukleinsäuren aus stimulierten PBMC-Kulturen mittels NanoString Assay; Mitarbeit an der automatisierten Quantifizierung der Zytokine aus Zellkulturüberständen stimulierter PBMC-Kulturen; Analyse von NanoString Daten und statistischer Bewertung; sowie das Schreiben von Teilen der Ergebnisse und Diskussion der ersten Fassung der Veröffentlichung.

Publikation 5: Böhme A, Radke L, Schütze F, Schneider S, Liebscher T, Sauer S, Santo L, Quadrini F, Hummel M, Giese C, Frohme M, Foitzik A, Miniaturized Flow-Through Bioreactor for Processing and Testing in Pharmacology, Materials Science Forum, 2017
Beitrag im Einzelnen:
Experimentelle Arbeiten zur Überprüfung der Toxizität einzelner Bauteile und Klebstoffe des Bio-reaktors, zur Dichtheit der Reaktoren, Etablierung verschiedener 2D und 3D-Kultivierungmethoden; sowie Mitarbeit beim Verfassen der Veröffentlichung.

Unterschrift, Datum und Stempel des betreuenden Hochschullehrers/der betreuenden Hochschullehrerin

_____

Unterschrift des Doktoranden/der Doktorandin

_____

9. Druckexemplare der ausgewählten Publikationen

Publikation 1

Induced cytokine response of human PMBC-cultures: Correlation of gene expression and secretion profiling and the effect of cryopreservation

Radke L, López Hemmerling DA, Lubitz A, Giese C, Frohme M

Cellular Immunology 2011, 272: 144-153, Impact Factor: 3.172 (2016)

http://www.sciencedirect.com/science/article/pii/S0008874911002796

Publikation 2

Reference gene stability in peripheral blood mononuclear cells determined by qPCR and NanoString

Radke L, Giese C, Lubitz A, Hinderlich S, Sandig G, Hummel M, Frohme M

Microchimica Acta 2014, 181: 1733-42; Impact Factor: 4.580 (2016)

http://link.springer.com/article/10.1007/s00604-014-1221-x

Publikation 3

In-vitro evaluation of glycoengineered RSV-F in the Human artifical Lymph Node Reactor

Radke L, Sandig G, Lubitz A, Schließer U, von Horsten H, Blanchard V, Keil K, Sandig V, Giese C, Hummel M, Hinderlich S, Frohme M

Bioengineering 2017, 4(3), 70; Impact Factor: n/a

http://www.mdpi.com/2306-5354/4/3/70 doi:10.3390/bioengineering4030070

Publikation 4

Engineering of CHO Cells for the Production of Recombinant Glycoprotein Vaccines with Xylosylated N-glycans

Sandig G, von Horsten H, Radke L, Blanchard V, Frohme M, Giese C, Sandig V, Hinderlich S

Bioengineering 2017, *4*(2), 38; Impact Factor: n/a

http://www.mdpi.com/2306-5354/4/2/38; doi:10.3390/bioengineering4020038

Publikation 5

Miniaturized Flow-Through Bioreactor for Processing and Testing in Pharmacology

Böhme A, Radke L, Schütze F, Schneider S, Liebscher T, Sauer S, Santo L, Quadrini F, Hummel M, Giese C, Frohme M, Foitzik A

Materials Science Forum 2017, 879: 236-243; Impact Factors: SJR 0.19 (2016), RG Journal Impact 0.28 (2016)

https://www.scientific.net/MSF.879.236

Cellular Immunology 272 (2012) 144–153

Contents lists available at SciVerse ScienceDirect

Cellular Immunology

journal homepage: www.elsevier.com/locate/ycimm

Induced cytokine response of human PMBC-cultures: Correlation of gene expression and secretion profiling and the effect of cryopreservation

Lars Radke [a,*], Diana A. López Hemmerling [a], Annika Lubitz [b], Christoph Giese [b], Marcus Frohme [a]

[a] Technische Hochschule Wildau (FH), Bahnhofstr. 1, 15745 Wildau, Germany
[b] ProBioGen AG, Goethestraße 54, 13086 Berlin, Germany

ARTICLE INFO

Article history:
Received 28 January 2011
Accepted 17 October 2011
Available online 28 October 2011

Keywords:
PBMC stimulation
Cytokine
Bead-based multiplex assay
mRNA profiling
Protein profiling
Cryopreservation

ABSTRACT

The immune system is regulated by the complex interaction of multiple cytokines, which are secreted signaling molecules affecting other cells. In this work, we studied the cytokine response to several well-known stimulants, such as OKT-3, Con A, PWM, and SEB. Healthy donor cells (PBMCs) were cultivated for up to 72 h and the mRNA levels and cytokine release of four key cytokines (IL-2, IL-4, IFN-γ, and TNF-α) were analyzed by RT-PCR and bead-based multiplex analyses. The generated cytokine profiles showed characteristic expression patterns and secretion kinetics for each cytokine and substance. PWM/SEB and OKT-3 led to a very fast and long-lasting immune response, whereas Con A induced the slowest cytokine production. Cytokine concentrations also differed greatly. The highest IFN-γ concentration was 1000 times higher than the respective IL-4 concentration. Gene expression and cytokine concentration profiles were strongly correlated during the time course.

The chronological response of the donors' cytokine profiles coincided, but showed individual characteristics regarding the strength of the cytokine release.

The comparison of stimulation experiments using freshly isolated and cryopreserved PBMCs showed that, for the observation of an immunological response at early points in time, gene expression experiments are more reliable than the measurement of cytokines in the cell culture supernatant. However, the freezing of cells influences the response significantly. The measurement of secreted proteins is the superior method at later points in time.

1. Introduction

Cytokines are regulatory soluble proteins, including interleukins, interferons, tumor necrosis factors, chemokines, and colony stimulating factors. They are secreted by leukocytes and other cells, act on the behavior of cells of the immune system and modulate inflammatory reactions, cell growth and signal transduction. Their effect is very diverse, and different cytokines can have overlapping functions [1]. Cytokines play an important role in inflammation, immune responses and immune homeostasis. Some of them modulate immune cell responses and cell activation at long and short distances without any direct cell-to-cell contact. Others induce the homing of leukocytes from the blood or lymph vessels to target tissues, e.g. to the source of infection or secondary lymphatic organs, and guide extravasation, migration and cell–cell interaction.

Cytokine secretion is strongly controlled by autocrine and paracrine regulations and feedback loops, and is typically downregulated in an immunological "standby-mode". Some diseases, e.g. autoimmune diseases, such as multiple sclerosis (MS) or rheumatoid arthritis (RA), are characterized by increased basal levels of inflammatory cytokines. Cytokines are often upregulated very fast during infection or disease. The primary impulse induces the short but fulminant first defence. T helper cells and their T_H1 and T_H2 cytokines refine the immune response towards cellular and humoral immunity.

Furthermore, the structural organization and steady state of primary and secondary immune organs, e.g. bone marrow, spleen or lymph nodes, is controlled by a complex local cytokine (and chemokine) microenvironment.

The simultaneous effects of multiple cytokines on cells can be antagonistic as well as synergistic; therefore, the reaction of the cell can be qualitatively diverse. Cytokines can react in cascades with other cytokines and lead to a higher or lower production or secretion of further cytokines. The constitutive production of cytokines (of nonactivated cells) is usually low and transient, and the effective radius of chemokines is typically small. Furthermore, the same cytokines can be produced by different non-cognitional cells [2].

Since cytokines act in a very complex manner, the analysis of cytokine profiles is useful to understand the response and activation of the immune system.

* Corresponding author.
E-mail address: lradke@tfh-wildau.de (L. Radke).

0008-8749/$ - see front matter © 2011 Elsevier Inc. All rights reserved.
doi:10.1016/j.cellimm.2011.10.018

In this context, cryopreservation is widely used to conserve and store sample material for later use in more comprehensive or comparable studies. Therefore, freezing should have as little effect on sample material as possible, and its impact on several parameters, such as cell viability [3,4], cell proliferation, surface markers [4–6], cell composition [4,7], or cytokine production [8,9], has been investigated. Not all of these studies were performed with human peripheral blood mononuclear cells (PBMCs) or used the same stimulants and this has led partly to diverse results for these reasons.

The aim of this study was to determine the level of cytokine response in healthy donors to several effector agents. We analyzed the gene expression modulation of four key cytokines and their secretion over time in cell cultures of PBMCs stimulated with several substances. The cytokines used were interleukin 2 (IL-2) and interferon-gamma (IFN-γ), both type 1 cytokines, interleukin 4 (IL-4), a type 2 cytokine, and tumor necrosis factor-alpha (TNF-α), a representative of the monokines. IFN-γ and TNF-α are typical for inflammatory processes, IL-2 for the cellular immune response and IL-4 for the humoral immune response.

The immune response was triggered *in vitro* with four stimulants in three experimental set-ups: (1) the lectin pokeweed mitogen together with Staphylococcal enterotoxin B (PWM/SEB), (2) OKT-3, which is a therapeutic monoclonal antibody against the CD-3 surface antigen of T-lymphocytes or (3) the lectin Concanavalin A (Con A).

The bacterial toxin SEB binds to MHC class II receptors [10,11] and interacts with particular TCR Vβ chains [12,13]. Lectins are complex glycoproteins which are able to bind specific carbohydrates onto cell membranes. All agents are substances commonly used to stimulate immune responses and cytokine secretion and have been well studied. Lectins and other mitogens, as well as endotoxins, lead to an unspecific activation of the immune system.

We also investigated the differences in stimulation experiments with the above-mentioned substances on freshly isolated PBMCs and cryopreserved PBMCs for all four key cytokines on the level of gene expression and for five additional cytokines (IL-5, IL-10, IL-12, IL-13, and GM-CSF – all related to T-cell activation) on the level of protein secretion to determine the influence of cryopreservation.

The modulation of cytokine levels can be quantified in several ways. The expression of mRNA in human cells can be determined with RT-qPCR (real time quantitative polymerase chain reaction). Secreted cytokines in cell culture supernatants can be analyzed with immunosorbent assays. Although ELISAs (enzyme linked immunosorbent assays) are standard for cytokine measurements, other techniques are more appropriate. A lot of systems have been developed to detect multiple cytokines in one sample using microparticles and flow cytometry [14–17]. The xMAP-technique (Luminex) allows multiplexing, is able to quantify whole cytokine patterns and shows high correlations of the measured values compared to an ELISA [16,18]. It offers a wider dynamic range (i.e. the fluorescent read-out is more direct, stable and sensitive than the colorimetric readout of an ELISA) and a higher reliability, because the data are calculated from the mean of at least 100 beads, each being an individual replicate. It theoretically allows the detection of 100 analytes in the same amount of sample required for one ELISA, and is, therefore, a time- and cost-saving method. The xMAP-technique uses flow cytometry and fluorescently-labeled beads of up to 100 classes discriminated by the ratio of the two intrinsic dyes. All beads of a class are functionalized with an antibody (or another binding molecule) to bind a specific analyte. A secondary biotinylated antibody and SAPE (streptavidin–phycoerythrin) are used to label the analyte and quantify it in a sandwich assay format. This technique can be easily adapted to individual analyte patterns [17], making it ideal for the measurement of cytokines in this case [15]. In this study, we used a BioPlex-200 System (BioRad) in combination with a Lightcycler 480 qPCR system (Roche) for the quantification of four key cytokines.

2. Materials and methods

2.1. Preparation of PBMCs

Whole blood or leukocyte concentrate of healthy adult donors was diluted 1:2 with PBS/EDTA (1 × PBS + 2 mM EDTA). The isolation of leukocytes was carried out by density gradient centrifugation: 20–30 ml of whole blood or leukocyte concentrate was overlaid on 20 ml of Biocoll leukocyte separation media (Biochrom AG) and centrifuged (35 min, 400×*g*). PBMC fractions were collected and washed three times with PBS/EDTA (10 min, 300×*g*, 200×*g* for the last washing step). The cell count and determination of viability was carried out with an automatic device (ViCell, Beckman Coulter).

Cells of one donor were divided into two aliquots for the cryopreservation experiments, one for instant testing with fresh PBMCs and one for cryopreservation, which were then resuspended in cold medium with 10% Dimethylsulfoxid (DMSO), 30% Fetal Calf Serum (FCS) and 60% Roswell Park Memorial Institute medium 1640 (RPMI 1640) final concentration. The vials were then transferred into a pre-cooled (4 °C) cryocontainer filled with isopropyl alcohol (IPA) and placed in a −80 °C freezer overnight. Thereafter, the vials were stored in a nitrogen vapor phase.

2.2. Cell cultivation

Cryopreserved PBMCs were thawed and rested for 1 day at 37 °C, 5% CO_2. The cells were then seeded in 24-well plates with 1 ml of RPMI 1640 medium supplemented with 10% fetal calf serum (FCS). The four stimulants were added immediately to the cultures. Pokeweed-Mitogen (PWM; Sigma) was added at 10 μg/ml to the cell suspension in combination with Pansorbin (Staphylococcus aureus, standardized, fixed suspension; SAC), which was diluted 1:10,000 in two steps and was purchased from Novabiochem. Concanavalin A (Con A; Sigma) was diluted to a final concentration of 2 μg/ml and OKT-3 (Muromonab-CD3; Novartis Pharma) to 50 ng/ml. After 1 h of incubation time, half of the medium in the OKT-3 stimulated wells was replaced with fresh medium six times to dilute the stimulant to a non-toxic concentration, since OKT-3 toxicity does not only depend on the concentration, but also on the exposition time. Some wells were left untreated (negative control). Supernatants were collected and cells were harvested after 1, 2, 4, 6, 8, 24, 34, 48, and 72 h of cultivation, and one well was completely harvested in each case. The secreted proteins accumulated within each well destined for later harvest. The supernatants were frozen at −20 °C for analyses of the cytokine levels. The cells were detached with PBS + EDTA, centrifuged (10 min, 230×*g*) and resuspended in RNA-protect Cell Reagent (Qiagen) for the analysis of RNA expression.

The cryopreservation experiments were carried out in a similar way with 1 day resting time for both fresh and cryopreserved cells. The cells were stimulated with OKT-3 and Con A in the same concentration as described above. The experiments were performed for 4 and 24 h for an early and a midterm response.

2.3. RT-PCR

The isolation of the total-RNA from PBMCs was carried out with RNeasy® Plus Mini Kit (Qiagen) and was performed as described by the manufacturer (Purification of total RNA from Animal Cells). The quality control of the RNA isolation was carried out with a 2100 Bioanalyzer (Agilent) using the Agilent RNA 6000 Pico Assay. Reverse transcription of the RNA was carried out with the

Transcriptor High Fidelity cDNA Synthesis Kit (Roche). In this step, 300 ng of RNA were used. Conventional PCR was used to verify the cDNA synthesis. The primers were designed using Roche's Universal-LibraryProbe (UPL) Software and Perl Primer (Table 1). PBGD (Porphobilinogendeaminase) was used as a housekeeping gene (UPL Human PBGD Gene Assay, Roche). The mastermix contained 2 μl Dream Taq buffer (Fermentas), 0.5 μl dNTPs, 1 μl primer mix (20 μM), 1 μl cDNA template, and 1 μl Taq polymerase (Dream Taq, Fermentas). DEPC-treated water was added to a final volume of 20 μl per reaction. The reaction was conducted in a Thermal Cycler (Mastercycler gradient, Eppendorf) with amplification under the following conditions: 1 min at 95 °C, 35 cycles at 95 °C for 10 s, 60 °C for 10 s, and 72 °C for 15 s, and extension for 10 min at 72 °C.

The same primers were used in the RT-PCR on the Roche LightCycler® 480 with SYBR® Green quantification (LightCycler® 480 SYBR Green I Master, Roche). RT-PCR was carried out as described in the Kit protocol, with 100 ng of total RNA. Results were analyzed with the LightCycler Software (Roche) using the relative quantification method.

2.4. Bead-based cytokine measurements

The cytokine concentrations in the cell culture supernatants were measured with a suspension array system (BioPlex-200, Bio-Rad) using commercially available kits (Bio-Plex Pro™ Human Cytokine Assay, 8-Plex Group I and Bio-Plex Human Cytokine Th1/Th2 Panel, both BioRad, Munich, Germany for the correlation experiments and the cryopreservation experiments, respectively). The assays were performed according to the manufacturer's protocol. The results were analyzed with the Bio-Plex Manager 6.0 using the logistic 5-point regression method.

3. Results

3.1. Standards

Relative gene (mRNA) expression values were obtained with the ΔΔct-method using the reference gene PBGD (Porphobilinogen deaminase). The samples and controls of the correlation experiments were measured in duplicates and in triplicates for the cryopreservation experiments. The relative expression values were normalized by using the means of the cp-values (crossing points) of the housekeeping gene and the samples in the equation of the ΔΔct-method:

$$R = \frac{(E_{tar})^{\Delta cp_{tar(Mean\ control - Mean\ sample)}}}{(E_{ref})^{\Delta cp_{ref(Mean\ control - Mean\ sample)}}}$$

PCR efficiencies of the target genes were 1.93 (IL-2), 1.86 (IFN-γ), 1.91 (TNF-α), and 2.04 for the reference gene PBGD. No PCR-efficiency could be determined due to the very low concentrations of IL-4 mRNA in the samples.

Eight samples (with 1:4 dilution steps) were measured in duplicates to generate the cytokine (protein) standard curves.

The coefficient of variation (%CV, the percentage of the standard deviation in reference to the mean of the values) of all values were between 0.59% and 19.99% (median of standards for each analyte: IL-2: 4.55%, IL-4: 6.33%, IFN-γ: 11.86%, and TNF-α: 7.08%). The standard curves had large dynamic ranges which differed from analyte to analyte. IL-2 and IFN-γ can be detected between approximately 5 and 25000 pg/ml, whereas the dynamic range of IL-4 is much lower (1–5000 pg/ml) and TNF-α is detectable in much higher concentrations (10–100,000 pg/ml). The samples did not have to be concentrated because of the large dynamic ranges.

3.2. The influence of cryopreservation

Cryopreserved and freshly isolated cells were stimulated with OKT-3 and Con A for 4 and 24 h to determine the changes in transcript rates at the beginning and at a later ongoing cultivation stage (Fig. 1). We could show with RT-qPCR that OKT-3 led to higher or even gene expression ratios in fresh PBMCs. In contrast, Con A tended to evoke higher gene expression values in cryopreserved PBMCs.

The following cytokines were analyzed in the bead-based assay: IL-2, IL-4, IL-5, IL-10, IL-12(p70), IL-13, GM-CSF, IFN-γ, and TNF-α. A comparable protein expression pattern could be observed at the early time point, as in the gene expression experiment, although only half of the cytokines of the panel examined could be detected.

Cytokine concentrations of IL-2, IL-10, GM-CSF, and IFN-γ in OKT-3 stimulated cells were higher in fresh PBMCs, with the exception of TNF-α, which was higher in cryopreserved cells (589–1098 pg/ml). Higher concentrations were observed for IL-2, TNF-α, GM-CSF, and IFN-γ in cryopreserved cells for the early time point and Con A stimulation. The proportions of secreted proteins for three of the four key cytokines coincided with the mRNA levels; IL-4 was not yet detectable (data available as Supplementary material).

The spectrum of cytokines expanded after 24 h of cultivation; IL-5 and IL-13 were now detected in both OKT-3 and Con A treated samples and, additionally, IL-4 and IL-12 only in OKT-3 treated samples. Clearly the variability of secreted cytokine levels between cryopreserved and fresh cells decreases in comparison to the early time point (Fig. 2). Fold-changes at 4 h were between 1.9 (TNF-α, OKT-3) and 19.6 (TNF-α, Con A), and after 24 h between 1.1 (IFN-γ, OKT-3) and 3.2 (IL-12, OKT-3). The degrees of correlation were calculated for every time point and every treatment by means of linear regression lines and are given as r^2-values. The coefficient of determination increased from 0.88 to 0.95 for OKT-3 treatment and from 0.51 to 0.97 for Con A treatment.

3.3. The time course of mRNA and protein expression

The mRNA expression was highly dynamic over the time course of 72 h after stimulation (Fig. 3). This refers to the strong regulation of the gene expression by the different signaling pathways of the mixed cell population, feedback loops and regulation of the cytokine production by other cytokines.

We observed a strong and fast reaction: IL-2 and IFN-γ, in particular, showed more than 1000 times elevated expression values (highest: ~80,000 fold IL-2, PWM/SEB, 6th hour, Donor 2). PWM/SEB showed the fastest reaction to a stimulus (detectable within

Table 1
Cytokine-primers.

Gene	Reverse	Forward
IL-2	5′-AAGTGAAAGTTTTTGCTTTGAGCTA	5′-AAGTTTTACATGCCCAAGAAGG
IL-4	5′-GCCCTGCAGAAGGTTTCC	5′-CACCGAGTTGACCGTAACAG
IFN-γ	5′-ATGTATTGCTTTGCGTTGGA	5′-AATTGGAAAGAGGAGAGTGAC
TNF-α	5′-GCCAGAGGGCTGATTAGAGA	5′-CAGCCTCTTCTCCTTCCTGAT

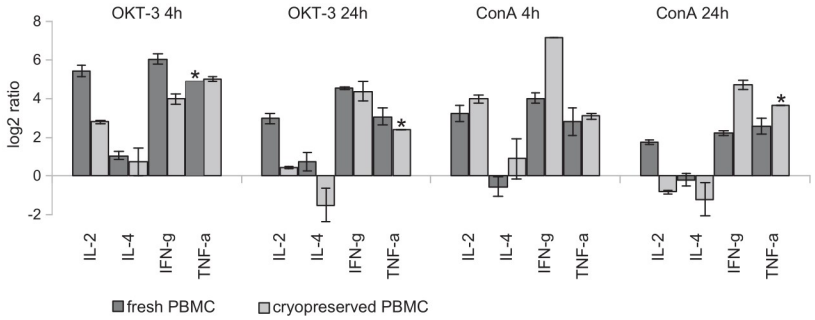

Fig. 1. Gene expression rates (determined by RT-qPCR) of IL-2, IL-4, IFN-γ, and TNF-α in freshly isolated and cryopreserved cells after 4 and 24 h of cultivation. PBMCs were stimulated with OKT-3 and Con A. The gene expressions are displayed as ratios of the logarithm to the basis 2 (a factor of 1 denotes a doubling of the gene expression, 10 corresponds to an increase of a factor of ca. 1000 referred to the reference gene PBGD). Asterisks mark results where no error bar could be calculated due to the exclusion of technical replicates.

the 1st hour), followed by OKT-3. Con A showed the slowest reaction with a delay of 4–6 h and a comparatively weak reaction (maximum upregulation 250 fold, IFN-γ, 24th hour).

The IL-4 data could not be normalized due to undetectable signals in the controls, but it was noticeable that IL-4 was downregulated after 24 h in all experimental settings.

Donor 2 showed a slightly higher upregulation overall.

The measured protein-concentrations of the cytokines are visualized in a digitized manner to facilitate the comparison of the donor profiles. Fig. 4 shows the results for all effectors and donors over the time.

The protein data show distinct patterns over the time course. The time points of the first cytokine release, and the duration and the magnitude of the cytokine release are clearly visible. These characteristics are clearly more related to the substance used than to the according cytokines. PWM/SEB and OKT-3 provoked the highest cytokine levels of the type 1 cytokines (with more than 100 ng/ml of IL-2 and IFN-γ), whereas stimulated cultures levels in Con A were at least one order of magnitude smaller.

The release of IL-4 was, with a maximum of 110 pg/ml, by far the weakest compared to the other cytokines.

The protein expression kinetics was also more related to the respective substance. The shape of the concentrations of the cells stimulated with PWM/SEB plotted over the time course is similar for all cytokines. The levels increased with individual slopes for each cytokine, reached a maximum level between the 8th and 24th hour and stayed at that elevated level due to accumulation. Alternatively, we observed decreasing concentrations towards the end of the time course after a maximum around the 34 h time point (e.g. for cytokines after stimulations with OKT-3). The cytokine kinetics of Con A stimulated cells seemed to be more complex. While the TNF-α level was constant at a particular level from the 24th hour on, IL-2 and IL-4 levels decreased after 48 h of cultivation and the IFN-γ level steadily increased in the last 48 h of the observation time.

The correlations of the gene expression (mRNA) and the concentrations of cytokines (protein) in the cell culture supernatants were studied for all samples; examples are presented in Fig. 5 for the IL-2 and IFN-γ of Donor 1.

According to the very late upregulation of the gene expression by Con A, the detection of cytokines was possible after 24 h, which was a time delay of more than 4 h. Pursuant to the minor gene expression ratios (maximum 260 fold upregulated: IFN-γ, hour 24, Donor 2), the measured cytokine concentrations were lower (maximum IL-2: 1.6 ng/ml, IL-4: 32 pg/ml, IFN-γ 18.5 ng/ml, TNF-α: 2.9 ng/ml) than with other stimuli.

Contrarily, OKT-3 led to an early regulation of the cytokines, starting in the 2nd hour. The release of cytokine followed, with a slight delay, and was detectable in most cases after 8 h of cultivation. The gene expression of IL-2, IL-4 and TNF-α was strongly upregulated at the 6th or 8th hour (for example, IL-2: 10,000 fold, 6 h, both Donors) and resulted in the declining cytokine concentrations. However, the gene expression of IFN-γ was upregulated, steadily increasing until the 48th hour of cultivation, leading to the very high and stable IFN-γ level.

PWM/SEB effected the earliest regulation with a similar diversity in the expression pattern to OKT-3, but upregulation was long-lasting for all other cytokines too. PWM/SEB provoked the highest ratios of gene-expression compared to all other substances

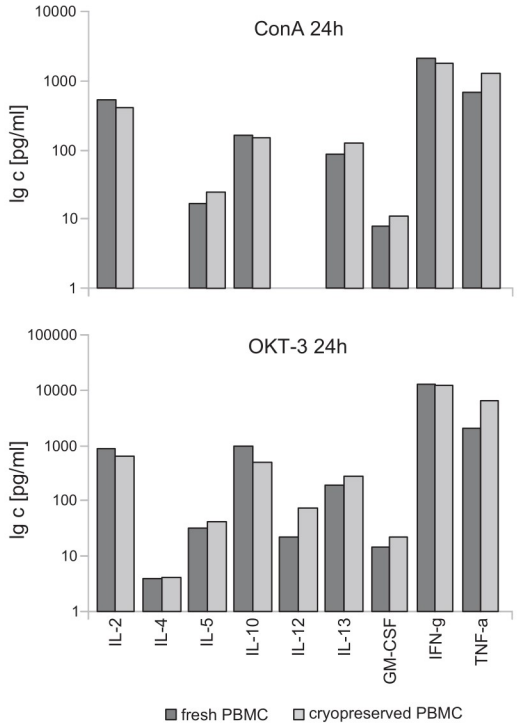

Fig. 2. Secreted cytokines in PBMCs stimulated with Con A and OKT-3 after 24 h of cultivation. Cytokine concentrations were measured with a bead-based suspension array system, and showed negligible differences between freshly isolated and cryopreserved cells.

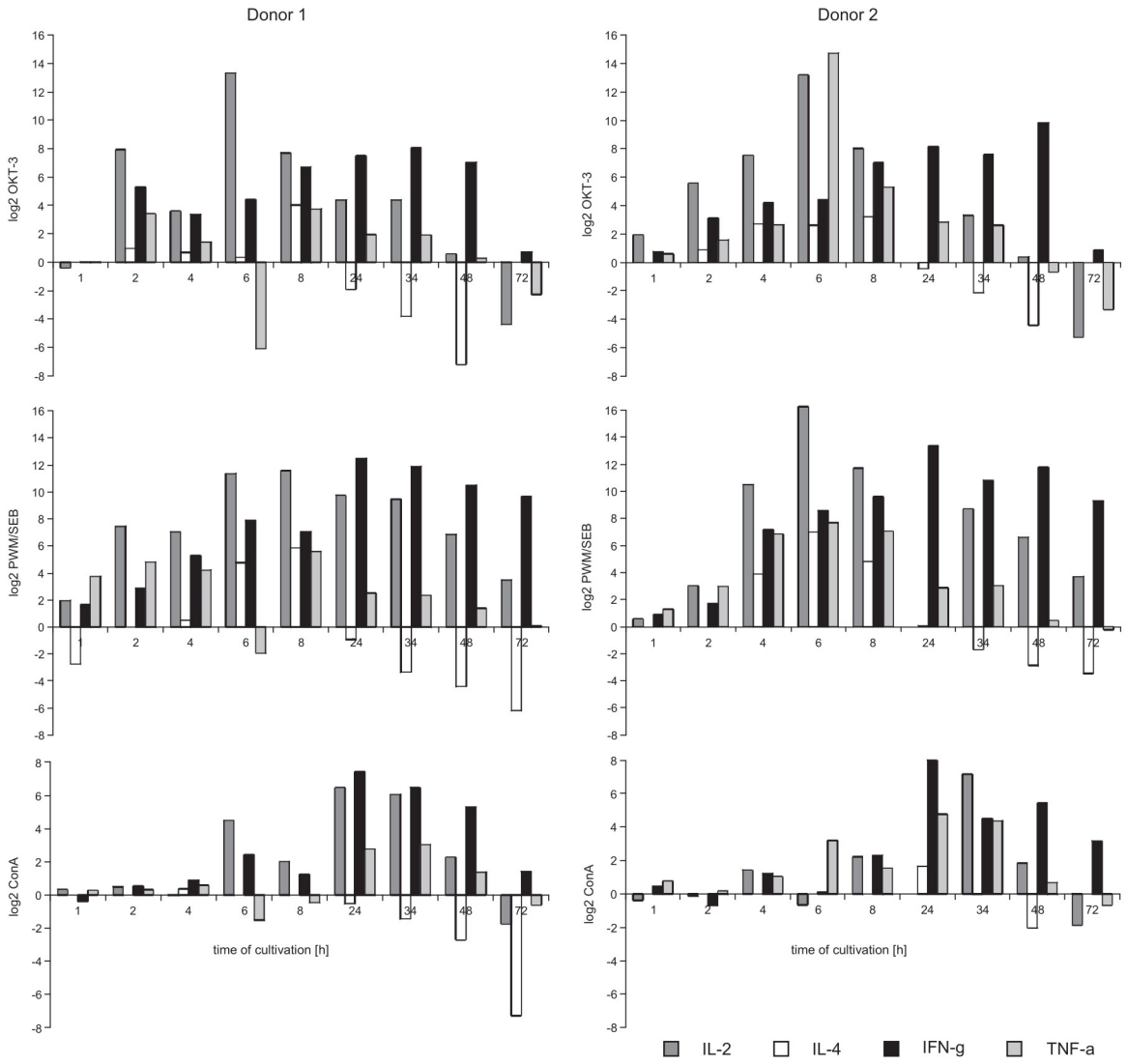

Fig. 3. Gene expression rates of IL-2, IL-4, IFN-γ and TNF-α of two healthy donors in a cell culture experiment with up to 72 h of cultivation. PBMCs were stimulated with different effectors (OKT-3, PWM/SEB and Con A). The gene expressions are displayed as normalized ratios of the logarithm to the basis 2 (a factor of 1 denotes a doubling of the gene expression, 10 corresponds to an increase of a factor of ca. 1000 referred to the reference gene PBGD). IL-4 data are not normalized. In a relative quantification of the gene expression, the housekeeping gene and controls are used to generate normalized gene expression ratios, so no controls are presentable.

(IL-2: 80,000 fold, IL-4: 130 fold, IFN-γ: 10,000 fold, and TNF-α: 200 fold). This led to the longest and highest release of cytokines of all compared substances with almost no delay. The maximum concentration of all cytokines was reached after 24 h of cultivation and stayed at the very high level (20–130 ng/ml, except IL-4 with 110 pg/ml) until the end of the observation.

The comparison of the results of both cytokine analyses showed an early expression for IL-2 (maximum at 6 h), except Con A, which led to a late regulation at all (maximum after 24 or 34 h). The release of cytokines followed with a very short delay, indicating that IL-2 was the fastest T cell cytokine without acting proinflammatorily.

IL-4 was often expressed for a short time with maxima after 6 or 8 h for PWM/SEB and OKT-3. No IL-4 expression could be observed after 34 h of cultivation. The secretion of the cytokine followed with a small delay and was very low, as mentioned previously.

The expression rate of IFN-γ over the time course showed no single peaks, such as for IL-2 or IL-4, but was slowly changing. The upregulation of the gene expression started with the 1st hour of cultivation and decreased depending on the substance used (except for Con A).

The expression rate of TNF-α was diverse, with a maximum after 6 h using OKT-3 or PWM/SEB. Donor 1 also showed an early peak after 2 h for these two substances. In contrast, the maximum for Con A appeared late. The maxima of the TNF-α expression rates were also irregular: they were mainly low (6–50-fold higher than the control), but Donor 2 showed significantly higher expression rates for PWM/SEB (200 fold) and OKT-3 (2000 fold). The release of the cytokines occured as a slow increase, detectable without a delay with the first measurable expression of the TNF-α gene. The TNF-α secretion decreased, except for PWM/SEB stimulation, showing the short lifetime (transient effect) of this cytokine.

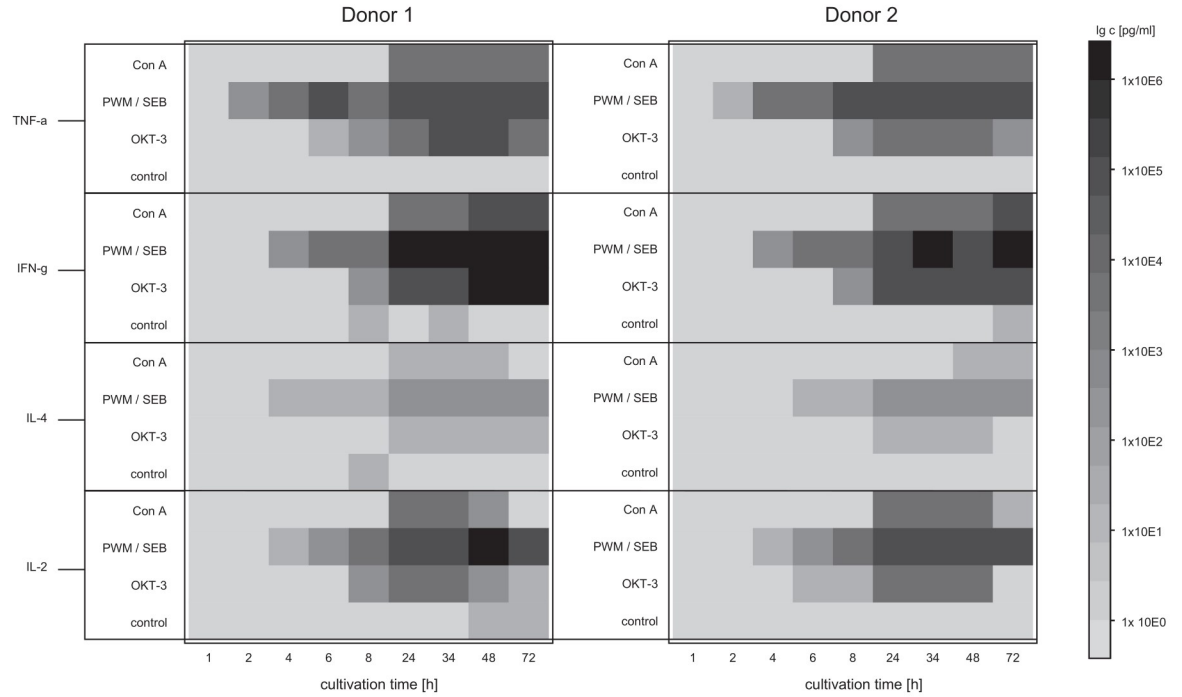

Fig. 4. Cytokine profiles of the cytokines IL-2, IL-4, IFN-γ, and TNF-α of two healthy donors. Cell culture supernatants of the single experiments were analyzed after the denoted time points. Immunologic stimulation was triggered with Concanavalin A (Con A), pokeweed mitogen mixed with Staphylococcal enterotoxin B (PWM/SEB) and OKT-3 (therapeutic anti-CD-3 antibody).

4. Discussion

We compared the gene expression and the cytokine secretion in freshly isolated and cryopreserved PBMC for the two stimulants OKT-3 and Con A to clarify the effect of freeze–thawing, since the data from the literature do not suffice to rule out that the use of frozen PBMCs provides reliable findings. The conflicting information of the literature results from studies analyzing different cytokines in various patient groups, using different methods and substances in highly diverse observation periods (hours to months).

It is crucial for comparable responses that there is no change in the cellular composition of the PBMCs, since the immune cells act together in a complex manner and single subsets are responsible for distinct reactions. Cryopreservation is assumed not to affect the cellular proportions of T cells, B cells, NK cells, and monocytes in PBMCs [4,7]. A decrease in the activity of NK cells was observed, but can be regained by resting the cells for some hours after thawing [19].

The duration of freezing and the thawing method were reported not to have an impact on the cell viability [8], but the freezing method and the temperature of the freezing medium, in particular, seems to influence the survival rate [20].

The proportion of activated $CD4^+$ and $CD8^+$ T cells in cryopreserved PBMCs, determined by CD25 expression, was found to be unaffected, except for $CD4^+$ T cells stimulated with Con A in which activation was delayed [4].

The proliferation of cryopreserved PBMCs was also investigated and was found to be unconcerned with a maximum after 3–5 days, but with a slightly lower capacity than fresh PBMCs [4].

We focussed in this study on two points in time to evaluate the effect of cryopreservation for the incipient immune reaction (4 h) and for the proceeding immune reaction (24 h). The gene expression of the four cytokines (IL-2, IL-4, IFN-γ, and TNF-α) showed strongly stimulant-related effects. OKT-3 led to the higher transcription of cytokines in fresh PBMCs, while stimulation with Con A led to higher gene expression ratios in cryopreserved cells (except IL-2 and IL-4 after 24 h). The analysis of the same cytokines in the cell culture supernatant showed high congruence for the 4 h time point. The higher protein levels for cryopreserved or fresh cells in the respective case resulted from the earlier onset of the immune reaction leading to higher transcript numbers measurable after 4 h.

After 24 h, the secreted cytokines reached equal levels for each stimulus independent of the state of the cells used. The high concordance was also shown by the high coefficient of determination (r^2) values of the linear regression. After 24 h, values of 0.95 for OKT-3 and 0.97 for Con A were assessed, denoting a close to perfect correlation.

Kreher et al. [20] also showed unimpaired antigen-specific cytokine recall responses for CD4+ and CD8+ cells in healthy human PBMCs after freezing for IL-2, IL-4, IL-5, and IFN-γ. Similar results were obtained by Jeurink et al. [4], who found no significant differences after stimulation with anti-CD3 plus anti-CD28 and Con A for the monocyte cytokines IL-10, IL-12 and TNF-α, and the T cell cytokines IL-4 and IL-13. They also investigated mRNA levels, but observation was limited to the first 6 h. Here they monitored significant differences as a subject of the substances used.

Kvarnström et al. [8] showed significant differences between fresh and cryopreserved PBMCs after stimulation for different groups of patients (multiple sclerosis, allergies and pregnancy) and for distinct points in time, both at the protein and the mRNA level. They also found an overall decrease of IL-4 in cryopreserved PBMCs. However, the two studies mentioned above correlate with

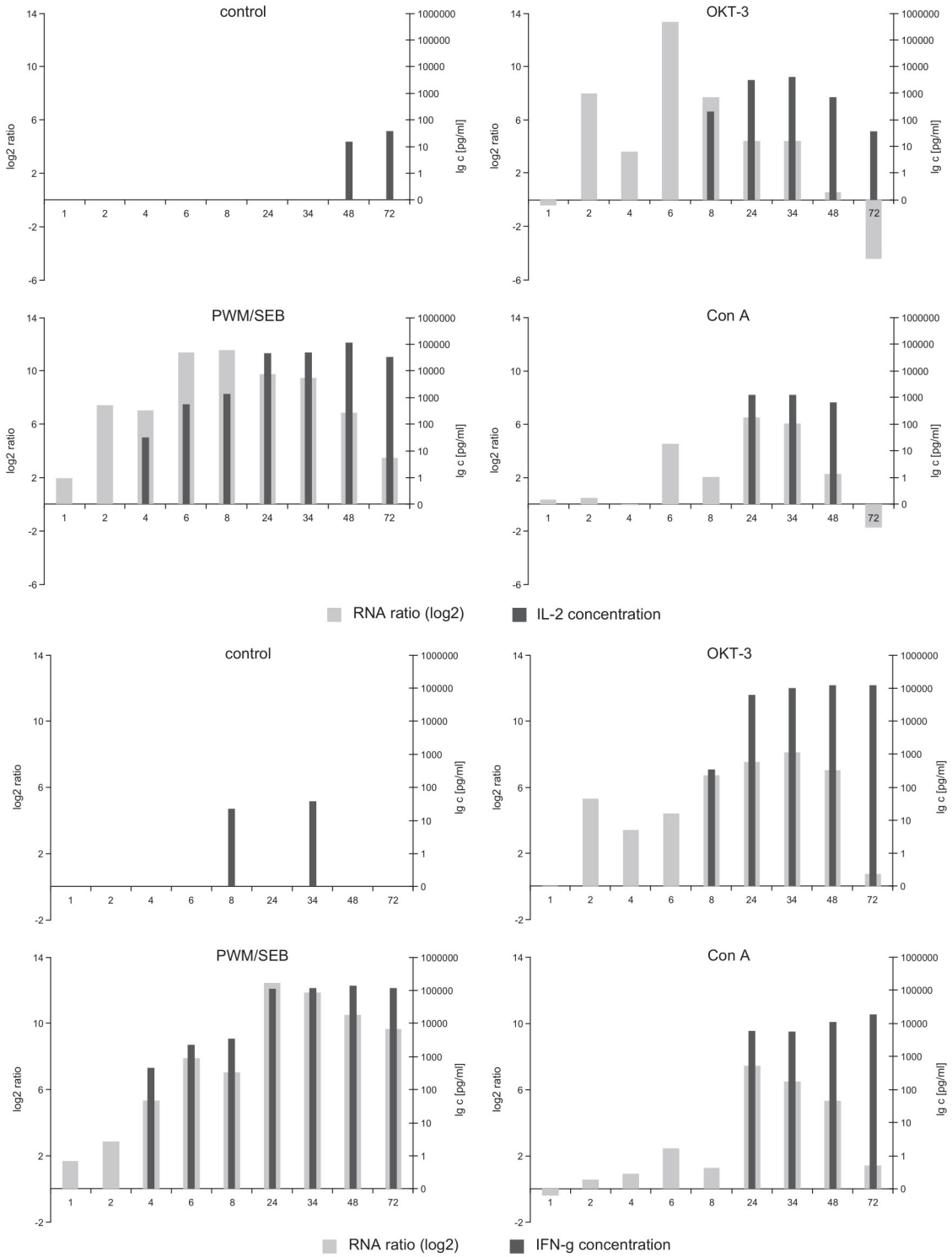

Fig. 5. mRNA and protein data shown exemplary for IL-2 and IFN-γ of Donor 1. The correlation of the chronological sequence and the strength of the gene expression and cytokine release are clearly recognizable. Gene expression values of the control samples were normalized to one. As a log2 ratio, they become zero and are, therefore, not apparent in the diagram of the control.

our data and did not show a consistent decrease of IL-4 in the PBMCs of healthy donors. Since IL-4 levels are low, it might be better to only use fresh cells for an analysis if possible.

In our study, the greatest difference between frozen and fresh cells was found for TNF-α, of which higher amounts were secreted by cryopreserved PBMCs. This was consistent for both stimuli and in line with Venkataraman [9].

Some of the proportions seem to be contradictory by comparing the ratios of gene expression and cytokine secretion between cryopreserved and fresh PBMCs after 24 h. However, given that the examination at 24 h only reflects a snapshot, it can be assumed that if low gene expression values and high protein levels are detected for a distinct data pair, the gene expression had already declined because an effectual level of cytokines had already been reached in the cell culture supernatant at an earlier point. Moreover, the high correlation of gene expression and cytokine secretion could be shown in this study over a longer period and a higher density of measuring points.

Profiles of the gene expression and the secretion for the four cytokines IL-2, IL-4, IFN-γ, and TNF-α were generated by the stimulation of PBMC cell cultures with four different stimulants (OKT-3, PWM/SEB, Con A). These were capable of inducing cytokine responses, differing in the extent of gene expression, the cytokine release and the appearance of first detectable effects.

Stimulated cytokine secretion is usually a process of hours or days. Highly dynamic releases peaking after a few hours are observed, as well as moderate but constant secretion profiles reaching a plateau. Typically, the dynamic behavior is controlled by autocrine and paracrine regulation and feedback loops, and secretion activity drops down to normal without continuous stimulation.

The secretion of cytokines is controlled by gene expression, the stability and activity of transcripts for biosynthesis, intracellular trafficking, and vesicular accumulation (reservoirs) and release. Lymphocytes have no reservoirs for cytokines, whereas other leukocytes, e.g. granulocytes, are characterized by a large amount of secretary vesicles. Therefore, the initial activation of transcription and biosynthesis in lymphocytes is strongly related to the consecutive secretion.

There is a clear relation in magnitude and time response between gene expression and the detectable amounts of cytokines in the cell culture supernatants. In individual cases, a time shift between the expression of the gene and the release of the corresponding cytokine ranging from almost instantaneous to up to 6–8 h of delay was observed.

The initial cytokine levels were very low, as can be seen in Fig 5. The resting time of 1 day before adding the substances to the cell cultures was sufficient to neutralize any cytokines originated from the stimulation of the cells by the preparation or by the donors. The cytokine levels of the controls remained very low over the whole investigation period, demonstrating the minimal influence of the cell culture process.

The cytokine profiles of both donors showed a typical shape of the concentration for each of the four cytokines investigated. While IL-2 was released for a short period only, IFN-γ and TNF-α concentrations stayed high for a longer time. The IL-4 profile has a similar shape, but at much lower concentrations.

The presence of protein concentration after 72 h does not imperatively mean a release of that cytokine at that time point. The experiments showed a process of accumulation and, therefore, an increase or an absence of cytokine release was only detectable with a stable protein concentration not implying cytokine production or degradation.

The two donors showed very few differences regarding the time response of gene regulation and cytokine secretion, but did differ in the levels of cytokine concentrations. The concentrations of TNF-α and IFN-γ of Donor 2 especially were significantly lower than those of Donor 1, although the gene expression rates of Donor 2 for both cytokines were higher compared to those of Donor 1. The variation of the individual response to stimulation over the time course has been monitored in various studies [20–23]: the IL-4 release in diluted whole blood was found to be stable over eight weeks in each donor. The IL-4 levels reached from 10 to 10,000 pg/ml after incubation with 100 ng/ml SEB for 72 h. Similar results were obtained for IL-2 with the same group [22] and for LPS-induced TNF release in whole blood over 30 days with a very small variation of ±0.6 ng TNF/ml [23]. This suggests individual donor characteristics for other cytokines too.

PBMC preparations are derived from whole blood samples. These preparations, as primary cell material, show donor to donor variations in the leukocyte composition and cellular activation levels, e.g. by individual infection status or other predispositions [22].

The expeditious upregulation of IL-2, IFN-γ and TNF-α after an initial activation with OKT-3 is in line with the findings of Fan et al. [21] and Hermann et al. [22], who used anti-CD3 monoclonal antibodies. In addition, they found a maximum accumulation of the mRNA of IL-2 for all stimuli used (CD3, PHA, PWM, and others) after 8 h. Our results can specify these findings with a maximum accumulation of activation with OKT-3 and PWM/SEB after 6 h because of the higher density of testing points at the beginning of the cultivation.

IL-2 and IFN-γ were more strongly upregulated by OKT-3 and PWM/SEB than by TNF-α. This is in line with Fan et al. [21]. According to this, the concentrations of IL-2 and IFN-γ in the cell culture supernatant are higher (more than 100,000 pg/ml) depending on the substance and donor. Both cytokines are produced by T_H1 cells amongst others. Contrary to Fan et al. [21], a specific effect of OKT-3 on T cells cannot be educed from those higher cytokine concentrations, since T cells represent the principal component of PBMCs. IL-4 is produced by T_H2 and T_H0 in the presence of IL-2 or IL-4. Since the amount of IL-4 at both mRNA and protein level is very low for all substances, T_H2 and T_H0 cells seem to be less present in the composition of donors' PBMCs. In general, the balance of PBMCs is shifted in favor of T_H1 cells (the T_H1/T_H2 ratio is often 2:1 [5,24]). In addition, T_H2 cells are rarely activated within this assay because no humoral immune response was induced. PBMCs do not contain the antigen-presenting cells (APC) which are necessary for a cell-mediated activation of T_H2 cells. However, a specific effect of OKT-3 on the T cells cannot be ruled out.

Yan et al. [25] investigated the effect of SEB on the TNF-α production. The TNF-α level in cell culture supernatants in their time course experiments increased after 4 h, reached the maximum level after 17 h and remained constant through 24 h, which is in line with our findings. We were able to recognize TNF-α earlier at lower concentrations using the bead-based technique to detect cytokines. They also found that the levels of TNF-α vary with the ratio of lymphocytes and monocytes, so individual donor characteristics in cytokine release may again refer to differences in the cell composition (lymphocyte/monocytes ratio).

Furthermore, they found a specific effect of SEB in low doses on T cells, which started TNF-α production [22]. This is mainly produced by monocytes and induced by SEB at much higher doses [26].

Cytokines were detectable even after 72 h of cultivation depending on the stimulus used, although a stable level could be detected in most cases, so the secretion at such a late time point is balancing the decay. PWM/SEB, especially, led to very high cytokine concentrations which stayed at the elevated levels after the 24th hour. The cytokine concentration with OKT-3 as the effector decreased in a larger part after 34 h due to decay or autocrin consumption. This is much longer than *in vivo*, which is based on the fact that the cytokines accumulate *in vitro* due to the absence of medium change. Experiments of Ferran et al. [27] showed that,

among others, IL-2, IFN-γ and TNF-α, after the addition of OKT-3, were no longer detectable after 12–24 h. In contrast, 37 pg IL-2/ml, 6700 pg TNF-α/ml and even 120,000 pg IFN-γ/ml were detectable in samples of Donor 1 after 72 h of cultivation. In spite of the decay and consumption of the cytokines, the decrease *in vitro* is much slower due to missing pathways, which are able to down-regulate the *in vivo* cytokine production very quickly.

In comparison, the stimulation of PBMCs with PWM/SEB and OKT-3 lead to very a similar cytokine pattern, whereas Con A also induced the lowest cytokine production compared to other effectors, such as LPS or zinc chloride [28].

In practice, the analysis of PBMCs is performed much more frequently with frozen PBMCs because samples from different occasions can be analyzed at the same time and inter-assay variations are eliminated. Therefore, the evaluation of differences in the responses of fresh and cryopreserved PBMCs is of high interest, especially when donors are dependants of different patient groups.

Additionally, the determination of the immune status of the donor is important prior to the cryopreservation of cells, since cellular subsets of subjects that are in a state associated with immune activation response are in a different manner during cryopreservation, leading to significant changes in the cytokine pattern after thawing [8].

The current literature seems to be inconclusive based on a multitude of factors. Comprehensive review work is needed which should take at least a few of the different factors, such as cytokines, observation periods, stimulations, detection methods, or patient groups, into account.

Fortunately, researchers have become more and more aware of the importance of proper cryopreservation of PBMCs, leading to guidelines [29] and quality assurance programs [30] in the recent past.

Aside from the effect of cryopreservation on cells modifying the response to stimulation, the freezing of cell culture supernatants also affects the concentration of cytokines measurable by immunosorbent assays. Less attention is given to this effect, although it is of the same importance since its effect is of individual strength on each cytokine [31].

Models with induced cytokine release are increasingly used to model inflammatory responses *in vitro* in order to detect the presence of pyrogenic contaminations and to monitor disease states or immunomodulatory treatments with different substances using the material of healthy donors *ex vivo* [22]. Several models with whole blood [22,23] or PBMCs [25,32] have been described. The kind of cytokines released depends on the substances used. Endotoxin-stimulated (lipopolysaccharide, LPS) models allow only the detection of monokines, because they signal (tlr) 4 (Gram-negative) or tlr 2 (e.g. lipoteichoic acid of Gram-positive) via the toll-like receptor. Such monokine-models have already led to a wide field of testing systems, e.g. pyrogen tests [33], or the characterization of various patient groups, such as multiple sclerosis [34], rheumatoid arthritis [35], HIV [36], cancer [32,37], or borreliosis [38].

Other substances, e.g. mitogens or enterotoxins such as SEB, are additionally able to induce lymphokine release. In our approach, different stimulants were used which were all able to induce cytokine response. In addition, the consideration of gene expression and the cytokine concentrations provides a detailed insight into cytokine kinetics and the regulation of the immune system.

If only the protein concentrations were to be addressed, the panel of cytokines in the bead-based multiplex approach could be expanded up to 27 or could be customized (Bio-Rad, Millipore, and others). This would enable complex applications, such as the determination of states of infection-status, and individual immune characteristics or the networking effect of immunotoxic or immunomodulatory substances.

Appendix A. Supplementary material

Supplementary data associated with this article can be found, in the online version, at doi:10.1016/j.cellimm.2011.10.018.

References

[1] A. O'Garra, K. Murphy, Role of cytokines in determining T-lymphocyte function, Curr. Opin. Immunol. 6 (1994) 458–466.
[2] J. Wilček, Introduction, in: A.W. Thomson, M.T. Lotze (Eds.), The Cytokine Handbook, vol. 1, 4th ed. Academic Press, San Diego, 2003, pp. 40–56 (Chapter 1).
[3] K.R. Fowke, J. Behnke, C. Hanson, K. Shea, L.M. Cosentino, Apoptosis: a method for evaluating the cryopreservation of whole blood and peripheral blood mononuclear cells, J. Immunol. Methods 244 (2000) 139–144.
[4] P.V. Jeurink, Y.M. Vissers, B. Rappard, H.F.J. Savelkoul, T cell responses in fresh and cryopreserved peripheral blood mononuclear cells: kinetics of cell viability, cellular subsets, proliferation, and cytokine production, Cryobiology 57 (2008) 91–103.
[5] D.D. Chaplin, 1. Overview of the immune response, J. Allergy Clin. Immun. 111 (2003) 442–459.
[6] J.W. Sleasman, B.H. Leon, L.F. Aleixo, M. Rojas, M.M. Goodenow, Immunomagnetic selection of purified monocyte and lymphocyte populations from peripheral blood mononuclear cells following cryopreservation, Clin. Diagn. Lab. Immunol. 4 (1997) 653–658.
[7] C.E. Allsopp, S.J. Nicholls, J. Langhorne, A flow cytometric method to assess antigen-specific proliferative responses of different subpopulations of fresh and cryopreserved human peripheral blood mononuclear cells, J. Immunol. Methods 214 (1998) 175–186.
[8] M. Kvarnström, M. Jenmalm, C. Ekerfelt, Effect of cryopreservation on expression of Th1 and Th2 cytokines in blood mononuclear cells from patients with different cytokine profiles, analysed with three common assays: an overall decrease of interleukin-4, Cryobiology 49 (2004) 157–168.
[9] M. Venkataraman, Effects of cryopreservation of immune responses. XI. Heightened secretion of tumor necrosis factor-alpha by frozen human peripheral blood mononuclear cells, Cryobiology 34 (1997) 276–283.
[10] T. Herrmann, R.S. Accolla, H.R. MacDonald, Different staphylococcal enterotoxins bind preferentially to distinct major histocompatibility complex class II isotypes, Eur. J. Immunol. 19 (1989) 2171–2174.
[11] M. Phillippa, J. Keppler, The Staphylococcal Enterotoxins and their relatives, Science 248 (1990) 705–711.
[12] J.E. Callahan, A. Herman, J.W. Kappler, P. Marrack, Stimulation of B10.BR T cells with superantigenic staphylococcal toxins, J. Immunol. 144 (1990) 2473–2479.
[13] J. White, A. Herman, A.M. Pullen, R. Kubo, J.W. Kappler, P. Marrack, The Vβ-specific superantigen Staphylococcal Enterotoxin B: stimulation of mature T cells and clonal deletion in neonatal mice, Cell 56 (1989) 27–35.
[14] R. Chen, L. Lowe, J.D. Wilson, E. Crowther, K. Tzeggai, J.E. Bishop, R. Varro, Simultaneous quantification of six human cytokines in a single sample using microparticle-based flow cytometric technology, Clin. Chem. 45 (1999) 1693–1694.
[15] W. de Jager, H. te Velthuis, B.J. Prakken, W. Kuis, G.T. Rijkers, Simultaneous detection of 15 human cytokines in a single sample of stimulated peripheral blood mononuclear cells, Clin. Diagn. Lab. Immun. 10 (2003) 133–139.
[16] C. Earle, E. King, A. Tsay, K. Pittman, B. Saric, L. Vailes, R. Godbout, K. Oliver, M. Chapman, High-throughput fluorescent multiplex array for indoor allergen exposure assessment, J. Allergy Clin. Immun. 119 (2007) 428–433.
[17] D.A.A. Vignali, Multiplexed particle-based flow cytometric assays, J. Immunol. Methods 243 (2000) 243–255.
[18] M.C. Jenmalm, M. Malit, J. Torrence, A. Zhang, Bio-plex cytokine immunoassays and ELISA: comparison of two methodologies in testing samples from asthmatic and healthy children, Bio-Rad. Lab. Appl. Note (2001).
[19] S. Fujiwara, M. Akiyama, M. Yamakido, T. Seyama, K. Kobuke, M. Hakoda, S. Kyoizumi, S.L. Jones, Cryopreservation of human lymphocytes for assessment of lymphocyte subsets and natural killer cytotoxicity, J. Immunol. Methods 90 (1986) 265–273.
[20] C.R. Kreher, M.T. Dittrich, R. Guerkov, B.O. Boehm, M. Tary-Lehmann, CD4+ and CD8+ cells in cryopreserved human PBMC maintain full functionality in cytokine ELISPOT assays, J. Immunol. Methods 278 (2003) 79–93.
[21] J. Fan, P. Nishanian, E.C. Breen, M. McDonald, J.L. Fahey, Cytokine gene expression in normal human lymphocytes in response to stimuli, Clin. Diagn. Lab. Immun. 5 (1998) 335–340.
[22] C. Hermann, S. von Aulock, K. Graf, T. Hartung, A model of whole blood lymphokine release for in vitro and ex vivo use, J. Immunol. Methods 275 (2003) 69–79.
[23] B.M.G. Wilson, A. Severn, N.T. Rapson, J. Chana, P. Hopkins, A convenient human whole blood culture system for studying the regulation of tumour necrosis factor release by bacterial lipopolysaccharide, J. Immunol. Methods 139 (1991) 233–240.
[24] Y. Qian, Q. Tang, Z. Wang, J. Sun, O. Li, Effect of allograft blood transfusion on Th1/Th2 balance and T cell surface antigens expression, Clin. Chim. Acta. 366 (2006) 361–362.

[25] Z. Yan, D.C.H. Yang, R. Neill, M. Jett, Production of tumor necrosis factor alpha in human T lymphocytes by Staphylococcal Enterotxin B correlates with toxin-induced proliferation and is regulated through protein kinase C, Infect. Immun. 67 (1999) 6611–6618.
[26] S. Matsuyama, Y. Koide, T.O. Yoshida, HLA class II molecule-mediated signal transduction mechanism responsible for the expression of interleukin-1 beta and tumor necrosis factor-alpha genes induced by a staphylococcal superantigen, Eur. J. Immunol. 23 (1993) 3194–3202.
[27] C. Ferran, K. Sheehan, M. Dy, R. Schreiber, S. Merite, P. Landais, L.H. Noel, G. Grau, J. Bluestone, J.F. Bach, Cytokine-related syndrome following injection of anti-CD3 monoclonal antibody: further evidence for transient in vivo T cell activation, Eur. J. Immunol. 20 (1990) 509–515.
[28] D. Pan, A.K. Bera, S. Das, S. Bandyopadhyay, T. Rana, S.K. Das, D. Bhattacharya, Use of zinc chloride as alternative stimulant for in vitro study of nitric oxide production pathway in avian splenocyte culture, Mol. Biol. Rep. 7 (2009) 2223–2226.
[29] A. Best, G. Hidalgo, K. Mitchell, J.R. Yannelli, Issues concerning the large scale cryopreservation of peripheral blood mononuclear cells (PBMC) for immunotherapy trials, Cryobiology 54 (2007) 294–297.
[30] A. Weinberg, R. Louzao, M.M. Mussi-Pinhata, M.L.S. Cruz, J.A. Pinto, M.F. Huff, A.C. de Castro, M.C. Sucupira, T.N. Denny, Quality assurance program for peripheral blood mononuclear cell cryopreservation, Clin. Vaccine Immunol. 14 (2007) 1242–1244.
[31] W. de Jager, K. Bourcier, G.T. Rijkers, B.J. Prakken, V. Seyfert-Margolis, Prerequisites for cytokine measurements in clinical trials with multiplex immunoassays, BMC Immunol. 10 (2009).
[32] U. Elsässer-Beile, S. von Kleist, H. Gallati, Evaluation of a test system for measuring cytokine production in human whole blood cell cultures, J. Immunol. Methods 139 (1991) 191–195.
[33] T. Hartung, I. Aaberge, S. Berthold, G. Carlin, E. Charton, S. Coecke, S. Fennrich, M. Fischer, M. Gommer, M. Halder, K. Haslov, M. Jahnke, T. Montag-Lessing, S. Poole, L. Schechtman, A. Wendel, G. Werner-Felmayer, Novel pyrogen tests based on the human fever reaction: The report and recommendations of ECVAM workshop 43. ATLA 29, 2001, pp. 99–123.
[34] M. Chofflon, C. Juillard, G. Gauthier, G.E. Grau, Predictive value of TNF-alpha production in patients with multiple sclerosis, Eur. Cytokine Network 3 (1992) 523–531.
[35] P.F. Zangerle, D. De Groote, M. Lopez, R.J. Meuleman, Y. Vrindts, F. Fauchet, I. Dehart, M. Jadoul, D. Radoux, P. Franchimont, Direct stimulation of cytokines (IL-1 beta, TNF-alpha, IL-6, IL-2, IFN-gamma and GM-CSF) in whole blood: II. Application to rheumatoid arthritis and osteoarthritis, Cytokine 4 (1992) 568–575.
[36] T. Hartung, D.L. Pitrak, M.A. Foote, E.M. Shatzen, S.C. Verral, A. Wendel, Filgrastim restores interleukin-2 production in blood from patients with advanced human immunodeficiency virus infection, J. Infect. Dis. 178 (1998) 686–692.
[37] L. Fliss-Jaber, R. Houissa-Kastally, K. Bouzouita, N. Khedrir, R. Khelifa, Cytokine and immunoglobulin production by PWM-stimulated peripheral and tumor-infiltrating lymphocytes of undifferentiated nasopharyngeal carcinoma (NPC) patients, BMC Cancer 4 (2004).
[38] I. Diterich, L. Härter, D. Hassler, A. Wendel, T. Hartung, Modulation of cytokine release in ex vivo-stimulated blood from Borreliosis patients, Infect. Immun. 69 (2001) 687–694.

Microchim Acta
DOI 10.1007/s00604-014-1221-x

ORIGINAL PAPER

Reference gene stability in peripheral blood mononuclear cells determined by qPCR and NanoString

Lars Radke · Christoph Giese · Annika Lubitz · Stephan Hinderlich · Grit Sandig · Michael Hummel · Marcus Frohme

Received: 5 September 2013 / Accepted: 28 February 2014

Abstract Quantitative real-time PCR (qPCR) is commonly used for gene expression analyses with defined documentation guidelines to compare published results. To minimize the impact of variances from qPCR performance, sample handling and processing reference genes are used. Their selection process cannot be completely aligned due to variations in experimental conditions. Furthermore, the named sources of error are also present when determining the stability of the reference genes themselves. Even software applications that are used to identify the best reference genes rarely coincide on their rankings and can be misleading under certain conditions. In previous experiments, peripheral blood mononuclear cells (PBMC) were analyzed to identify the most stable reference gene(s). Twelve of the 13 investigated genes showed sample type specific differences in the expression. Direct mRNA measurement was performed in the form of a NanoString analysis, a multiplexed absolute quantification method. The external validation showed a high concordance of the reference gene expression levels. However, it identified the same sample type specific expression pattern for only some of the tested reference genes. By comparing various combinations of reference genes with both methods we are able to suggest a set of well-performing reference genes.

Keywords Reference genes · qPCR · NanoString · PBMC · Validation

Introduction

The quantitative PCR (qPCR) is today the method of choice to study gene expression due to its high sensitivity and specificity, huge quantification range, and its ability for medium-throughput and multiplexing. It originated from reverse transcription polymerase chain reaction (RT-PCR) by the introduction of fluorescent dyes almost 20 years ago [1]. However, qPCR is a complex method frequently suffering from non-uniform enzymatic reactions, imprecise mRNA quantification and pipetting errors, particularly when performed as a two step reaction. This may cause substantial problems with sensitivity, reproducibility and specificity [2].

Reference genes are used to eliminate most of these errors and to adjust sample content. Therefore, imperatively the expression levels of these genes need to remain constant between all different experimental conditions or examined cell types even after stimulation, proliferation or differentiation. In particular, this does not hold true for former "standard" reference genes like glyceraldehyde-3-phosphate-dehydrogenase (GAPDH) [3] and Beta-actin (ACTB) [4, 5]. Therefore each reference gene needs to be tested—ideally concerning all experimental conditions (stimulation types, immunologic states, age, gender and other related aspects). Unfortunately, standardization guidelines like MIQE [6] do not intend to define methods, minimal numbers of samples or candidate genes that need to be evaluated and researchers are free to choose how much effort they put into this topic. The validation of reference genes has to be performed in addition to the

Electronic supplementary material The online version of this article (doi:10.1007/s00604-014-1221-x) contains supplementary material, which is available to authorized users.

L. Radke (✉) · M. Frohme
University of Applied Sciences Wildau, 15745 Wildau, Germany
e-mail: lradke@th-wildau.de

L. Radke · M. Hummel
Charité Berlin, 12203 Berlin, Germany

C. Giese · A. Lubitz
ProBioGen AG Berlin, 13086 Berlin, Germany

S. Hinderlich · G. Sandig
Beuth University of Applied Sciences Berlin, 13353 Berlin, Germany

Published online: 15 March 2014

virtual experiment and therefore is time consuming, costly and may not be feasible when samples and budgets are limited [7].

Reference genes are considered to compensate for artificially introduced variances and constitute a scale basis that can be used for inter-assay purposes. However, most of those errors also apply when the reference genes are tested themselves. Thus, the researcher cannot distinguish a differential gene expression from an introduced bias in the analytical method.

Software applications like Bestkeeper [8], Normfinder [9] or geNorm [10] are commonly used to identify most stable genes. However, many studies only mention which genes are considered best by the software without validation and only few compare the results of more than one of these software tools or perform additional statistics [11]. Moreover, all three software tools assume that stable genes are highly correlated. Therefore, they perform pairwise comparison of all analyzed genes or compare each gene to a calculated mean. Thus, these programs are error-prone when two unstable genes strongly coincide or many of the investigated genes show biased results. External validation on the mRNA level is needed to eliminate most sources of possible bias or to confirm the stimulation dependent nature of variable gene expression.

In a vaccine development project, the effectiveness of the vaccine candidates to stimulate T-cells is tested. Therefore, gene expression profiles of cultured PBMC are generated using qPCR. Those cells are widely used to investigate immunologic responses but tested reference gene panels in published studies are often small and since stimulation types and experimental set-ups differ greatly there are no universal reference genes available. Furthermore, the choice of a good reference gene is complicated because PBMCs are a mixture of lymphocytes, monocytes and macrophages which differ in their composition, immunologic state and response between donors [e.g. 12, 13]. Therefore, they make up a good system to show drawbacks and pitfalls of reference gene determination. Our previous exhaustive investigations of reference gene stability in PBMC cultures with standard stimulants revealed that most of the tested genes showed variation in their expression levels but coincided in their fluctuations. In this study, external validation with the nCounter® Analysis System (NanoString Technology) [14] was performed on a second set of vaccine stimulated samples to clarify whether these variations are caused by biased qPCR reactions or are PBMC specific.

The NanoString method is a multiplexed chip-based technology for direct mRNA quantification. It is intended to allow the analysis of tens to hundreds of genes on a large number of samples more rapidly and efficiently than qPCR, but with noise and cost characteristics more favorable than high-throughput methods [15]. Errors from sample handling are reduced due to a minimized number of pipetting steps within this method. RNA transcripts are barcoded with sets of color-coded nucleic acids and then detected via single molecule imaging. The high sensitivity allows the detection of single copies per cell. Since there are different predefined panels which profile e.g. immunology-related targets, this technique is well suited to screen for regulated genes in stimulation experiments with new substances. It is also a good technique to validate reference gene results from qPCR experiments because NanoString uses total RNA without the need of amplification or reverse transcription so that enzymatic errors can be ruled out.

Our aim was to identify reference genes with minimal variability for PBMC stimulated with vaccine candidates and to check if variations in reference gene expression are sample and stimulation dependent. Here we show gene expression data from qPCR and NanoString experiments for nine reference gene candidates (eight of them were available in the NanoString panel) in a reduced set of 12 samples as a proof of principle.

Material and methods

Preparation of PBMC and vaccines

Preparation of PBMC from whole blood and cryopreservation was carried out as described elsewhere [16].

For recombinant expression of the Respiratory Syncytial Virus (RSV)-Fusion (-F) protein a cDNA was constructed containing the N-terminal extracellular part of the protein fused to a C-terminal Factor Xa cleavage site and a 6xHis-tag. The cDNA was prepared as a synthetic gene and cloned into the vectors PBGGPEX1 for expression in Chinese hamster ovary (CHO) cells and in pFastBac1 for expression in insect (Sf9) cells, respectively. Protein expression was performed by standard procedures. The proteins were purified in mg scales by Ni-NTA affinity chromatography to apparent homogeneity in SDS-PAGE analysis.

Cell cultivation

Immature Dentritic Cells were generated from CD14+ cells by supplementation with Interleukin 4 and Granulocyte macrophage colony-stimulating factor after 24 h and 48 h. The development to mature Dentritic Cells (mDC) was triggered by the addition of the respective antigen after 7 days. A media exchange at day 8 removed all supplements.

Cryopreserved PBMCs were thawed and rested for 1 day at 37 °C, 5 % CO_2. $3*10^6 \cdot mL^{-1}$ PBMCs or $1.5*10^6 \cdot mL^{-1}$ PBMCs with mDCs were seeded in 12 well plates with 2 mL of RPMI 1640 medium supplemented with 10 % Fetal Calf Serum. RSV-F-vaccine candidates were added immediately to the cultures (F-Protein from CHO in ten fold dilution series ranging from 10 $\mu g \cdot mL$-1 to 0.1 $\mu g \cdot mL^{-1}$ and F-Protein from SF9 cells in 1 $\mu g \cdot mL^{-1}$ final concentrations).

Some wells were left untreated (negative control) and some wells were treated with Lipopolysaccharides (Sigma) at 1 μg·mL^{-1} (positive control). Cells were harvested after 24 h of cultivation, whereas in each case one well was completely harvested. Cells were detached with PBS+EDTA, centrifuged (10 min, 230×*g*) and resuspended in RNAprotect Cell Reagent (Qiagen) for the analysis of mRNA expression.

Sample preparation and qPCR

Isolation of total-RNA from stimulated cells was carried out with High Pure RNA Isolation Kit (Roche) and was performed as described by the manufacturer. For concentration, purity and quality control of the isolated RNA we used a Nanodrop 1000 (Nanodrop Instruments) and a 2100 Bioanalyzer (Agilent) using the Agilent RNA 6000 Pico Assay. Reverse transcription of 450 ng RNA was done with the Maxima Reverse Transcriptase (Fermentas, now Thermo).

qPCR was performed on the LightCycler 480 (Roche) in 384 well Plates. Five pmol of equimolar Primermix in 1 μL were placed on the bottom of each well and dried up by placing the plate for 30 min into a heating block. Samples were 1:50 diluted with double autoclaved DEPC treated water. Mastermixes containing 5 μl of LightCycler® 480 SYBR Green I Master (Roche) and 5 μL of sample for each reaction were mixed together and 10 μl were pipetted into the wells. qPCR experiments were conducted in triplicates under the following conditions: 10 min of pre-incubation at 95 °C followed by 45 amplification cycles with 10 s at 95 °C, 60 °C for 10 s and 72 °C for 15 s followed by melting curve acquisition from 65 °C to 97 °C with a ramp rate of 0.11 °C per sec.

Cq values were calculated with the second derivative maximum method within the LightCycler 480 Software 1.5.0 (Roche) and used for analyses in Bestkeeper (MS Excel Visual Basic macro) as well as Normfinder and geNorm within the GenEx 5.4.0.512 (MultiD) Software.

Primer

Primers (Table 1) were designed using PerlPrimer [17]. Despite the treatment with DNase I in the isolation of the RNA (in accordance to the protocol) special care was taken to ensure that one primer of a pair overlaps or at least the primer pair spans an intron/exon boundary to eliminate the possibility of genomic DNA amplification. Furthermore primer pairs were designed to have a similar GC content (40–60 %), an amplicon size up to 200 bp and similar melting temperatures (60 °C, +/− 1 °C). However, optimization of PCR for each primer pair led to increased annealing temperatures of 63 °C in the assays for the reference genes GAPDH, SDHA and TBP.

Efficiencies of amplification of each primer pair were determined with dilution series within the LightCycler 480 Software.

NanoString

RNA samples of vaccine stimulated experiments were analyzed with an nCounter® Gene Expression assay (NanoString Technologies). The prebuilt GX Immunology Panel analyzes 511 immunology-related human genes and 15 internal reference genes. In the chosen assay format, twelve samples were analyzed in parallel. RNA extracts were quantified with the Nanodrop 1000 and were diluted to a concentration of 100 ng·μL^{-1}. 10 μL of each sample were cooled to −80 °C and shipped for analyses on dry ice to NanoString Technologies (Seattle, WA, USA). For a better understanding, the method is described in detail: 100 ng (up to 5 μL) of each RNA sample are analyzed in special cartridges in sets of twelve. Samples are spiked with six different positive internal control probes at concentrations ranging from 128 f. to 0.125 f. in 4-fold dilution steps. Positive controls are used to determine the linearity of the assays and are used for normalization i.e. adjust for systematic variation from assay to assay. Another eight negative probes are used to control for carryover of reporter probes (background) since no RNA target is included for these probes. RNA samples are incubated for 16 h at 65 °C in hybridization buffer containing the CodeSet, which consists of reporter and capture probes and together with the target RNA forms a tripartite complex. Each reporter probe has a 5′ color code signal which is unique for each target RNA analyzed within the CodeSet. After hybridization, the complex is bound by its biotin-labeled capture probe on a streptavidin coated glass slide and is stretched within an electric field. Data acquisition is done by imaging on a digital analyzer. Raw counts are normalized using the positive controls and normally target genes are normalized to the internal reference genes. Due to the evaluation of reference gene expression in this study, normalization was done with the positive controls only i.e. by multiplying the raw values of one sample with a quotient generated from the geometric mean (GM) of the positive controls of this sample divided by GM of all 12 positive control GMs.

A direct comparison of NanoString and qPCR results is not possible since NanoString experiments return total counts for each transcript. Direct graphical visualization will create negatively correlating plots compared to qPCR data because high expression levels will result in huge transcript numbers but in small Cq values from qPCR. To enable statistical analysis and to facilitate the comparison of results, NanoString data was transformed into Cq equivalents (For calculation see Supplementary material). One DNA copy amplified with a perfect efficiency of 2.0 should reach Cq after about 35 PCR cycles. Using this empirical formula, which has also been described and used in calculations elsewhere [18, 19], Cq equivalents can be estimated. To raise accuracy differences in amounts of input material and amplification efficiencies were considered. The length of the

Table 1 Reference gene primers

Gene name	Refseq number	Function	Primer sequences	Amplicon size (bp)	Annealing temperature
ALAS1					
aminolevulinate, delta-, synthase 1	NM_000688	Heme synthesis	F TGTGATGAACTAATGAGCAGAC R GTGACTAGCAGATTCTCAAGG	148	60 °C
B2M					
beta-2-microglobulin	NM_004048	serum protein MHC I subunit	F ACTGGTCTTTCTATCTCTTGTACT R CTTCAAACCTCCATGATGCT	146	60 °C
GAPDH					
glyceraldehyde-3-phosphate dehydrogenase	NM_002046	Catalytic enzyme glycolysis	F CTCTGCTCCTCCTGTTCGAC R ACGACCAAATCCGTTGACTC	112	63 °C
HPRT1					
hypoxanthine phosphoribosyl-transferase 1	NM_000194	Transferase, nucleotide synthesis	F AGCCAGACTTTGTTGGATTT R ACTCAACTTGAACTCTCATCTTAG	178	60 °C
POLR2A					
RNA polymerase II polypeptide A	NM_000937	RNA Polymerase 2 subunit A	F CAGATGACCTTGAATACCTTCC R GCACAGAATATCCTTGGCTC	176	63 °C
POLR2F					
RNA polymerase II polypeptide F	NM_021974	RNA Polymerase 2 subunit F	F AATGCCGAAGAGGGAAGGCCA R CAGGGGCACACATCGCAATC	157	60 °C
PPIA					
peptidylprolyl isomerase A	NM_021130	Isomerase, protein folding	F TGAGAACTTCATCCTAAAGCATAC R CATCCAACCACTCAGTCTTG	115	60 °C
SDHA					
succinate dehydrogenase complex, subunit A	NM_004168	Oxidoreductase, respiratory chain	F TATATGGAAGGTCTCTGCGA R GTGTTCTTTGCTCTTATGCG	144	63 °C
TBP					
TATA box binding protein	NM_003194	RNA transcription	F TATTAACAGGTGCTAAAGTCAGAG R AACTCAACATCCATCTTCTCAC	200	63 °C

amplification products (which influences the accumulation of fluorescence signal in the SYBR Green assay) was neglected and a bias of less than one Cq was accepted in this transformation. Furthermore, any differences in the binding efficiencies of the Nanostring probes cannot be determined.

Results and discussion

qPCR assay evaluation

Prior to all further analyses, the efficiencies of the qPCR had to be examined in order to maintain the comparability of results. Thus, first the efficiencies of all primer pairs were analyzed in evaluation experiments with template dilution series and ranged between 74.6 and 97.6 % (see Supplementary material) when analyzed with the Roche LightCycler Software. Linearity (R^2) was between 0.89 and 0.98. Due to limited amounts of mRNA, dilution series only covered shortened dynamic ranges (four-point dilution series) for the low expressed reference gene TBP. The efficiencies are needed within Bestkeeper to calculate the reference gene stability and in the accurate calculation of the Cq equivalents.

Furthermore, specificities of qPCR assays were evaluated with melting curves analysis and gel electrophoresis. For all amplifications we observed distinct peaks and single bands of the correct size, respectively (data not shown).

Reference gene expression analyzed with qPCR

Two experimental set-ups were chosen to distinguish between the reaction of the innate and the adaptive immune system. Since antigen presenting cells are only a small proportion of PBMCs the adaptive immune response cannot be fully activated. Therefore the second set-up was complemented with matured dendritic cells. Both sample types are combined for analyzes in order to find stable and equally expressed reference genes. The identification of such genes would make the analysis of target gene expression comparable between both sample types.

There are huge differences in the median expression levels of the reference genes (shown as Boxplots in Fig. 1a) that range from Cq 17.0 (B2M) to Cq 29.0 (TBP). Furthermore, the expressions of the examined genes vary to a very different extent. The reference genes with the highest variation (SD >

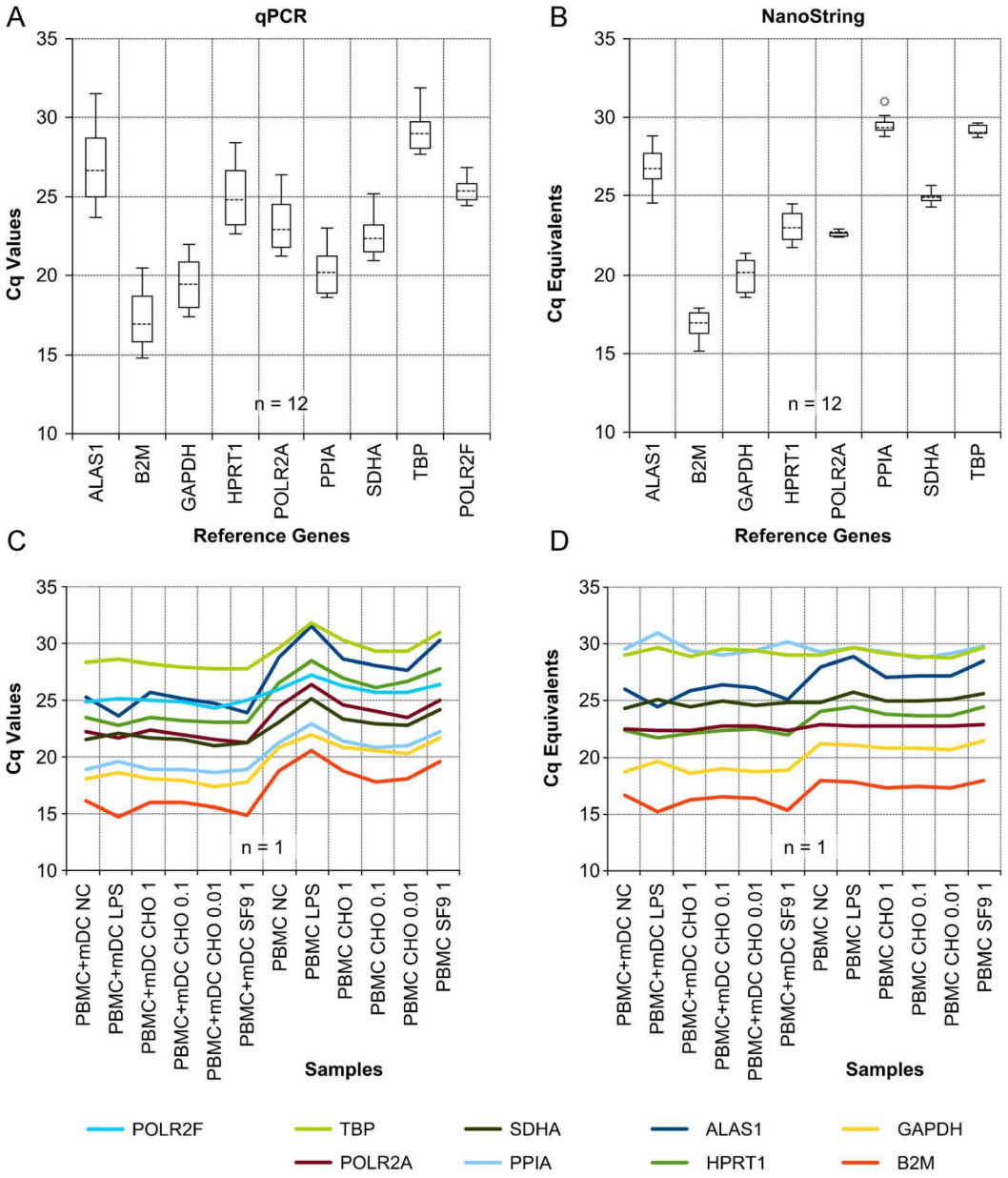

Fig. 1 Gene (**a**, **c**) and sample (**b**, **d**) specific variation of reference gene expression in qPCR and NanoString experiments. PBMC and PBMC supplemented with mDC were stimulated with different amounts (0.01 to 1 μg) of RSV F-Protein expressed in CHO and Sf9 cells and with LPS (positive control) or left untreated (NC). For easier comparability of both methods the NanoString data was transformed into Cq equivalents. Bottom and top of the boxplots are the 1st and 3rd quartile; bars of the whiskers are the highest and lowest occurring value within the 1.5 fold interquartile range; outliers are shown as individual points; dashed lines within the boxes denote the median. In sample specific plots (*bottom*) variances are only available for qPCR experiments since the NanoString experiment is conducted without any replicates. POLR2F data is only available for the qPCR experiment

2.0) were ALAS1 and HPRT1, whereas POLR2F showed the highest stability (see also Table 2).

Boxplots are widely used to depict reference gene variation. However, when sample types are combined they cannot illustrate whether the variation is caused by high variation within or between the sample types. They also cannot illustrate a possible co-regulation of genes. Therefore, the sample specific variation on the basis of the Cq value of each sample is shown for all reference genes in Fig. 1c.

The expression patterns of many genes correlate with each other. However, this is unlikely to occur due to co-regulation since the analyzed genes belong to different functional groups.

Table 2 Variation of reference gene expression in qPCR and NanoString

Gene name	qPCR		NanoString	
	Median Cq	SD	Median Cq equivalent	SD
ALAS1	26.65	2.60	26.70	1.31
B2M	16.96	1.93	16.93	0.93
GAPDH	19.46	1.68	20.19	1.12
HPRT1	24.82	2.14	23.04	1.03
POLR2A	22.91	1.64	22.71	0.18
POLR2F	25.39	0.72	–	–
PPIA	20.19	1.50	29.39	0.59
SDHA	22.39	1.27	24.95	0.42
TBP	28.97	1.35	29.08	0.34

It is more likely that variations in gene expression are sample dependent, especially in the PBMC sample subset. PBMC are derived from whole blood samples and may show donor to donor variations in their cellular composition and activation levels, e.g. by individual infection status or other predispositions [13]. To minimize these effects the serostatus of the donors is verified before use of the sample and the cellular composition is determined by flow cytometry. Since stimulants target receptors and pathways to a different extent, cellular subpopulations are activated and the cellular composition is shifted by differentiation or even proliferation.

For all tested genes the co-cultivation with dendritic cells leads to higher expression levels as in all PBMC samples (see Fig. 1c), although mRNA extraction, cDNA synthesis and qPCR were performed with the same number of cells or template concentrations, respectively. The lower abundance of antigen presenting cells in the experiment without mDC does not activate the T cells to the extent achieved by addition of mDC. This leads to the considerable lower expression of the reference genes in this experimental set up. In addition, mDC that are already activated by antigen contact are highly active cells and show an increased mRNA turnover. Even the expression levels of the co-cultured negative controls (PBMC+mDC NC) are higher than the positive controls (PBMC LPS) what can also be caused by the highly active mDC themselves.

Moreover, the variation within the PBMC subset is bigger than within the PBMC + mDC subset. Since unstimulated PBMCs are in a resting state the overall gene expression is very low. Activated PBMCs often produce high amounts of cytokines or antibodies and therefore transcribe lots of mRNAs. The higher transcription level of some subpopulations in PBMC contributes to a great extent to the analyzed material. This may obscure the signals from resting cells resulting in higher variability of the reference gene expression. The analyzed mRNA in this experiment is diluted to a constant quantity before transcription to cDNA and thus the number of virtual stable reference gene transcripts may be affected.

Both observation (higher expression in PBMC + mDC and higher variability in PBMC) are in concordance to preliminary screening experiments where PBMC and DC were activated with three common immunostimulants (Lipopolysaccharides, Cytomegalovirus and Polyinosinic-polycytidylic acid), that mimic distinct features of the used vaccine candidates.

Falkenberg et al. who analyzed reference gene stability in PBMC and whole blood, also attribute high variability of the reference genes POLR2A and EAR in PBMC to differences in cell populations, and the reduced variability in whole blood to the high percentage of a single cell type (neutrophils) [20].

From this background, the evaluation of reference genes in PBMC samples is difficult and makes a study specific search crucial to obtain valuable results. Validation with an amplification free method is required to rule out any bias from qPCR or erroneous sample handling and to attribute coinciding fluctuations of reference gene expression as a characteristic of PBMC. Therefore, the very same mRNA preparations were analyzed with the nCounter® Analysis System by NanoString Technologies.

Reference gene expression analyzed with NanoString

We initially applied the NanoString method to screen for differentially expressed genes in the PBMC and PBMC+mDC samples that were stimulated with the vaccine candidates. Here we compare the results from direct mRNA measurements and qPCR experiments to determine any sampling errors in qPCR experiments for eight of the available reference genes.

All twelve samples were analyzed in one cartridge system. Linearity of the six internal control probes (from 128 to 0.125 fM in 4-fold dilution steps) was $R^2>0.99$ and the 0.5 f. probe was detectable in all samples above background. The normalization factor for each sample is calculated from the reciprocal of the mean of the positive controls of that sample divided by the average of all those means from all samples. Normalization factor for all samples ranged from 0.64 to 2.25.

The normalized counts from the NanoString experiment were transformed into Cq equivalents. The spread of the genes and sample specific expression levels are compared in the transformed scale with the Cq values from the qPCR experiment for each gene in Fig. 1.

The proportion of the expression levels among the genes are comparable in both methods and the median Cq equivalents often differ very little from the median in the qPCR experiment (Table 2). Both SDHA (Δ median Cq of 4.7) and PPIA (Δ median Cq of 9.2) are much lower expressed when examined with the Nanostring assay. The variation of the expression of all reference genes is smaller in the NanoString experiment, especially that of POLR2A, PPIA, SDHA and TBP. These genes appear to have equal expression levels in

PBMC and PBMC+mDC. In contrast, ALAS1, B2M, GAPDH and HPRT1 show differences in the two sample types and the graphs are nearly identical to their qPCR equivalent. Due to the recurrence of these sample type specific expression pattern in the NanoString experiment, errors from sample handling in the qPCR experiment, which may have led to the co-regulating behavior of the reference genes can be ruled out. Moreover, it repeatedly indicates the induction of the gene expression of PBMC by the mDC or the overlapping signals by highly active mDC.

The huge difference in the expression level of PPIA may refer to differences in the analyzed target sequences. The quantification of PPIA can be hindered since there are by now seven PPIA-like genes and 30 pseudogenes known (The HUGO Gene Nomenclature Committee; http://www.genenames.org/) which are located on different chromosomes [21]. However, it is more likely that the difference of the expression level contributes to an underestimation of the amplification efficiency (which is needed for the transformation into Cq equivalents), since PPIA had the lowest (1.77) of all tested genes.

The gene with the smallest variation in the NanoString experiment is POLR2A showing equal expression in all sample types. This is in contrast to the POLR2A expression in the qPCR experiment where it shows the sample type specific difference in the expression pattern of most other genes. Regrettably, POLR2F is not available as a reference gene in the chosen nCounter® GX Immunology Panel. It was added as a candidate gene in the qPCR experiment due to its very high stability in preliminary experiments with standard stimulants (data not shown). The biological background of the expression levels of POLR2A and POLR2F are not identical, since POLR2A transcribes for the biggest subunit of the RNA polymerase II only, while the transcription product of POLR2F is also utilized in the assembly of RNA polymerase I and III.

Furthermore we analyzed the agreement of these two assays in a Bland-Altman plot (Fig. 2), in which the differences between two values of one sample are plotted as a function of their mean. Any bias between the two methods is represented by the mean value of all differences.

To be more rigorous in determining the 95 % limit of agreement (average difference±1.96 standard deviation of the difference) we excluded PPIA from the calculation. The average difference calculated within this plot is negligible (−0.038) and provides again evidence of the high correlation of the gene expression. In addition, the correctness of the transformation of the NanoString data into Cq Equivalents is indicated. Most of the datapoints are within the 95 % limit of agreement and suggest that the two methods may be used interchangeably. The plot shows proportional bias for each gene accentuated by regression curves. The slope of the inserted regression lines is steeper for reference genes that show sample type specific expression pattern in the qPCR but not in the NanoString experiment (i.e. POLR2A, PPIA, SDHA and TBP). However, there is no bias through the whole range of measurements which would indicate that the methods do not agree equally.

Reference gene stability

The stability of the reference genes within all twelve samples of this vaccine stimulation experiment were tested with three software tools in order to find overall suitable reference gene(s). The rankings from all tools for the results from the qPCR and NanoString measurement are shown in Table 3.

In the qPCR data set the rankings of geNorm and Bestkeeper correlate with the exception of POLR2F. Although this gene shows the smallest standard deviation (SD) of all genes it is ranked in the last places together with the genes with the highest SD (HPRT1, ALAS1) by geNorm and Normfinder. In contrast, it is ranked in first place by Bestkeeper followed by those genes that show equal expression levels in both sample types in the NanoString experiment. High variable genes like ALAS1, HPRT1 and B2M are ranked in the last positions by this tool.

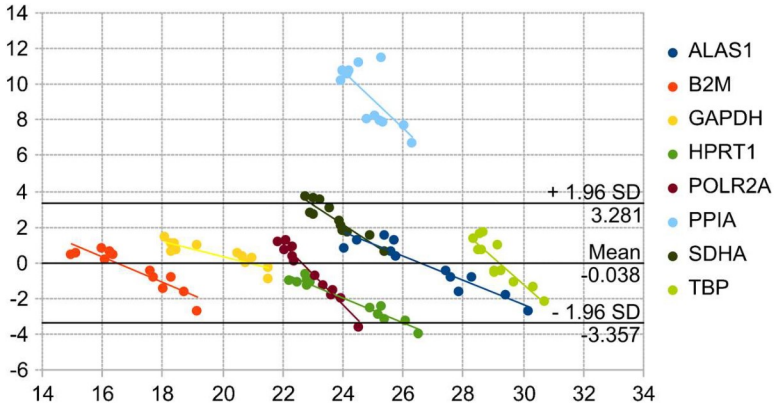

Fig. 2 Bland-Altman plot of Cq values (qPCR) and Cq equivalents (NanoString). Average mean of all differences and 95 % limits of agreement are depicted. PPIA was excluded from this calculation to be more stringent

Table 3 Ranking of reference gene candidates in qPCR and NanoString assays

	geNorm		Normfinder		Bestkeeper	
	Gene name	M-Value	Gene name	SD	Gene name	Power of HKG
qPCR	SDHA, TBP	0.2051	POLR2A	0.0598	POLR2F	1.32
	PPIA	0.3007	PPIA	0.161	SDHA	1.56
	GAPDH	0.3844	GAPDH	0.2802	TBP	1.56
	POLR2A	0.4199	TBP	0.4332	PPIA	1.68
	B2M	0.5097	B2M	0.451	GAPDH	1.79
	HPRT1	0.5787	SDHA	0.4519	POLR2A	1.80
	POLR2F	0.6678	HPRT1	0.6366	B2M	1.97
	ALAS1	0.7773	POLR2F	1.0469	HPRT1	2.14
			ALAS1	1.1539	ALAS1	2.42
NanoString	B2M, HPRT1	0.3808	SDHA	0.3276	PPIA	0.86
	ALAS1	0.4157	POLR2A	0.463	TBP	1.07
	GAPDH	0.5416	B2M	0.5346	POLR2A	1.16
	SDHA	0.7014	HPRT1	0.6123	SDHA	1.37
	POLR2A	0.7724	TBP	0.6627	B2M	2.25
	TBP	0.8199	GAPDH	0.7241	GAPDH	2.70
	PPIA	0.8934	ALAS1	0.8929	HPRT1	2.82
			PPIA	1.0479	ALAS1	3.02

Stability of reference gene as determined by three different software tools for the combination of vaccine candidate stimulated PBMC and PBMC + mDC samples from qPCR and NanoString experiments ordered by decreasing stability. Rankings of NanoString analysis depend on Cq equivalents and were calculated to show contrasts in the results of reference gene ranking algorithms. The reference genes with the lowest SD (see Table 2) are highlighted in grey. Gene stability is shown as M-Value for geNorm, as (internal) Standard Deviation (SD) for Normfinder and as Power of Housekeeping Gene (HKG) for Bestkeeper. The geNorm algorithm is based on pairwise comparison of genes and therefore not able to distinguish between the two best gene candidates which are put into one line

Since the reliability of the transformed Cq equivalents from the NanoString experiment is suggested by the high order of agreement (see Fig. 2), all three ranking tools were applied also on this data set. In this special case, the panel of tested reference genes consists of four relatively stable genes and four genes showing differences in the expression level of the two sample types. Thus, the results exemplify the relative weaknesses of some of these algorithms.

Normfinder ranks genes with low variability in the first but also in the very last position. In between, genes with high variable Cq equivalents are ranked. The results of geNorm are misleading since it ranks genes with low variability in the second half of the position table but all genes with sample type specific expression pattern in the first half. The rankings of Bestkeeper are exactly vice versa: The four genes with low variance are ranked best followed by the four genes with high variability. Actually, the ranks one to four of Bestkeeper are exactly inverse ordered as ranks five to eight of geNorm.

All three programs assume that correlating genes are highly stable. However they differ in their algorithms which are based on pairwise correlation of each reference gene or correlation with a calculated mean. Thus, these programs are error-prone when unstable genes strongly coincide or genes show biased results. Furthermore, the variation of each candidate gene and the strength of their correlation are scored differently by each program and rankings can be highly diverse. In this case Bestkeeper performs best because it excludes highly variable genes from the generation of the so called Bestkeeper-index, to which each gene is compared. Thus, only the comparison of genes with low variation results in high correlation.

Three of the four reference genes that were ranked best by Bestkeeper are identical in both methods. These genes (SDHA, PPIA and TBP) were combined to serve as reference in target gene normalization.

The three target genes chemokine (C-C motif) ligand 5 (CCL5), interleukin 12 subunit beta (IL12b) and Toll-like receptor 3 (TLR3) were analyzed to compare the performance of this normalization factor in both methods. These genes were chosen due to their different expression ranges (lowest Cq value of CCL is 20.5; highest Cq value of IL12B is 33.2).

The gene expression ratios strongly coincide between both methods and data points show high correlation in a simple linear regression analysis (slopes: 1.04 for CCL5, 0.93 for IL12b and 0.99 for TLR3; coefficients of determination: 0.99 for CCL5, 0.92 for IL12b and 0.60 for TLR3). The used normalization factor performs excellently for both methods

although PPIA showed huge differences in the strength of the gene expression between qPCR and NanoString. In contrast, the normalization with the combination of B2M, GAPDH and POLR2A—which are placed in the upper half of the rankings by all three software tools for the qPCR data—led to totally uncorrelated target gene expression ratios (slopes of linear regression analysis between −0.02 and −0.06; further data available in the Supplementary material). This finding also confirms the reliability of the result provided by Bestkeeper.

HPRT1 and ALAS1 were not tested due to their very high SD (Table 2) and low rankings. Both genes seem to be inapplicable for normalization purposes.

The present data of POLR2F is promising. Its value is even increased by the fact that its unmatched stability would allow the sole use of POLR2F as a normalizer. The calculation of the single control normalization error E in accordance to Vandesompele [10] and Falkenberg [20] revealed a distinct lower error rate for POLR2F than the combination of SDHA, PPIA and TBP (see Supplementary material). The use of POLR2F as a reference gene is not common practice but has been recommended for a wider range of cells and tissues before [22]. If the good performance of POLR2F is confirmed by additional studies, the use as single normalizer would be very beneficial to save money and sample material.

Applicability of NanoString for reference gene expression studies

The NanoString method has the potential to replace qPCR for medium throughput applications and is more favorable for extensive mRNA profiles studies. In contrast to mircoarray experiments, where the limited length of probes (25–100 bp) can result in nonspecific binding of transcripts [23], the dual probe system of the NanoString method results in more accurate signal capture, although the length of the capture and reporter probes is similar. This is ensured by three factors: first, both probes are present in solution allowing for more direct interaction with targets; second, the reaction is carried through to completion to ensure all targets are counted; and finally, the digital system provides less noisy results than analog systems [14, 15].

Prokopec et al. [15] compared the performance and technical aspects (e.g. processing time, throughput, required sample quantities, splicing variant coverage, unspecific hybridization, dynamic range, detection limit, price per sample) of NanoString, qPCR and OpenArray (Life Technology) as medium-throughput mRNA abundance measurement technologies. Their analyzed data showed good correlation between the platforms, as well as in comparison to microarray data. In compliance to our study they found that the qPCR data comprised significantly more variance than the other two platforms. In return to the lower variance NanoString results revealed a smaller dynamic range than qPCR. A very high correlation between NanoString and qPCR results for different sample types could be shown by Malkov et al. [24].

NanoString is also sought to measure reference gene stability by direct target detection. A very high comparability of the NanoString results with that of qPCR could be statistically shown (see Bland-Altman-Plot, Fig. 2). However, the direct comparison is hindered by the different result formats in Cq values and total counts. The application of existing software tools, used for gene stability evaluation for NanoString data, is only possible when results are converted to corresponding Cq values. A modification of these tools might be necessary since other techniques like digital PCR are emerging which also provide total counts as output. The determination of the stability by simply calculating the SD of each gene requires appropriate data normalization. For NanoString data, the preprocessing approaches are poorly described, although their variations can alter the experiment outcome [15]. There are several software packages available for NanoString data processing: nSolver is distributed by NanoString Technology itself, the NanoStringNorm R package has been developed by Waggot et al. [25] and Brumbaugh et al. [26] developed the web application NanoStriDE to normalize and analyze differential expression in NanoString nCounter data. We manually applied the normalization with positive controls only to assess variances in reference gene expression.

Our study shows a high concordance of the median expression of most reference genes and high correlation of target gene expression ratios when the normalizer is carefully chosen. However, the comparability of the results between NanoString and qPCR has limitations. The NanoString experiment was conducted to specify the observed variations as characteristics of PBMC and to rule out any bias. We found these sample type specific expression pattern only for four of the eight genes. The other four genes were stably expressed in both sample types. Differences in the binding efficiencies of the NanoString probes are unlikely but cannot be ruled out. Prokopec et al. also detected varying performance of reference genes between the examined platforms and led them back to slight differences in probe placement or specificity, leading to detection of distinct splice variants or other transcript isoforms [15]. If this holds true, special attention has to be turned on this issue to avoid the occurrence of platform-specific reference genes which would rule out any inter-platform validation.

Conclusion

We investigated the gene expression of nine reference gene candidates in two sets of PBMC samples (with or without addition of mDC with qPCR and NanoString) and analyzed the gene stability with three software tools. Biased reactions could be ruled out, since sample type specific variation pattern persists within direct mRNA measurement. Statistical

comparison of the reference gene expression showed that both methods could be used interchangeably and normalization with SDHA, TBP and PPIA showed highly correlating target gene expression ratios. Therefore NanoString has some value for validation as a bias-free method for reference gene expression but due to the different data output format, it has some limitations when being used with current ranking tools. POLR2F needs to be implicitly included into future NanoString experiments to clarify its use.

Acknowledgements This work was done within the Project "IPoGly - Potentiation of Vaccines by targeted Design of the Glycosylation" which is supported by the German Federal Ministry of Education and Research as grant a "FHProfUnt" in the line of funding "Forschung an Fachhochschulen" (grant number 17025B10,). We thank Ulrich Tillich for helpful discussions and advice.

References

1. Higuchi R, Fockler C, Dollinger G, Watson R (1993) Kinetic PCR analysis: real-time monitoring of DNA amplification reactions. Biotechnology 11(9):1026–1030
2. Bustin SA (2000) Absolute quantification of mRNA using real-time reverse transcription polymerase chain reaction assays. J Mol Endocrinol 25(2):169–193
3. Meyer-Siegler K, Rahman-Mansur N, Wurzer JC, Sirover MA (1992) Proliferative dependent regulation of the glyceraldehyde-3-phosphate dehydrogenase/uracil DNA glycosylase gene in human cells. Carcinogenesis 13(11):2127–2132
4. Elder PK, Schmidt LJ, Ono T, Getz MJ (1984) Specific stimulation of actin gene transcription by epidermal growth factor and cycloheximide. Cell Biol 81:7476–7480
5. Leof EB, Proper JA, Getz MJ, Moses HL (1986) Transforming growth factor type β regulation of actin mRNA. J Cell Physiol 127: 83–88
6. Bustin SA, Benes V, Garson JA, Hellemans J, Huggett J, Kubista M, Mueller R, Nolan T, Pfaffl MW, Shipley GL, Vandesompele J, Wittwer CT (2009) The MIQE guidelines—minimum information for publication of quantitative real-time PCR experiments. Clin Chem 55(4):611–622
7. Small BC, Murdock CA, Bilodeau-Bourgeois AL, Peterson BC, Waldbieser GC (2008) Stability of reference genes for real-time PCR analyses in channel catfish (Ictalurus punctatus) tissues under varying physiological conditions. Comp Biochem Physiol B 151: 296–304
8. Pfaffl MW, Tichopad A, Prgomet C, Neuvians TP (2004) Determination of stable housekeeping genes, differentially regulated target genes and sample integrity: BestKeeper—excel-based tool using pair-wise correlations. Biotechnol Lett 26:509–515
9. Andersen CL, Jensen JL, Ørntoft TF (2004) Normalization of real-time quantitative reverse transcription-pcr data: a model-based variance estimation approach to identify genes suited for normalization, applied to bladder and colon cancer data sets. Cancer Res 64:5245–5250
10. Vandesompele J, De Preter K, Pattyn F, Poppe B, Van Roy N, De Paepe A, Speleman F (2002) Accurate normalization of real-time quantitative RT-PCR data by geometric averaging of multiple internal control genes. Genome Biol 3(7), RESEARCH0034
11. Setiawan AN, Lokman PM (2010) The use of reference gene selection programs to study the silvering transformation in a freshwater eel Anguilla australis: a cautionary tale. BMC Mol Biol 11:75
12. Leifer CA, Verthelyi D, Klinman DM (2003) Heterogeneity in the human response to immunostimulatory CpG oligodeoxynucleotides. J Immunother 26(4):313–319
13. Hermann C, von Aulock S, Graf K, Hartung T (2003) A model of whole blood lymphokine release for in vitro and ex vivo use. J Immunol Methods 275:69–79
14. Geiss GK, Bumgarner RE, Birditt B, Dahl T, Dowidar N, Dunaway DL, Fell HP, Ferree S, George RD, Grogan T, James JJ, Maysuria M, Mitton JD, Oliveri P, Osborn JL, Peng T, Ratcliffe AL, Webster PJ, Davidson EH, Hood L, Dimitrov K (2008) Direct multiplexed measurement of gene expression with color-coded probe pairs. Nat Biotechnol 26(3):317–325
15. Prokopec SD, Watson JD, Waggott DM, Smith AB, Wu AH, Okey AB, Pohjanvirta R, Boutros PC (2013) Systematic evaluation of medium-throughput mRNA abundance platforms. RNA 19:51–62
16. Radke L, López Hemmerling DA, Lubitz A, Giese C, Frohme M (2011) Induced cytokine response of human PMBC-cultures: correlation of gene expression and secretion profiling and the effect of cryopreservation. Cell Immunol 272(2):144–153
17. Marshall OJ (2004) PerlPrimer: cross-platform, graphical primer design for standard, bisulphite and real-time PCR. Bioinformatics 20(15):2471–2472
18. Karlen Y, McNair A, Perseguer S, Mazza C, Mermod N (2007) Statistical significance of quantitative PCR (Additional File 4). BMC Bioinforma 8:131
19. Wilhelm J, Pingoud A, Hahn M (2003) Validation of an algorithm for automatic quantification of nucleic acid copy numbers by real-time polymerase chain reaction. Anal Biochem 317:218–225
20. Falkenberg VR, Whistler T, Murray JR, Unger ER, Rajeevan MS (2011) Identification of *Phosphoglycerate Kinase 1* (PGK1) as a reference gene for quantitative gene expression measurements in human blood. BMC Res Notes 4:324
21. Willenbrink W, Halaschek J, Schuffenhauer S, Kunz J, Steinkasserer A (1995) Cyclophilin A, the major intracellular receptor for the immunosuppressant cyclosporin A, maps to chromosome 7p11.2-p13: four pseudogenes map to chromosomes 3, 10, 14, and 18. Genomics 28(1):101–104
22. Hoerndli FJ, Toigo M, Schild A, Götz J, Day PJ (2004) Reference genes identified in SH-SY5Y cells using custom-made gene arrays with validation by quantitative polymerase chain reaction. Anal Biochem 335(1):30–41
23. Zhang J, Day IN, Byrne CD (2002) A novel medium throughput quantitative competitive PCR technology to simultaneously measure mRNA levels from multiple genes. Nucleic Acids Res 30(5):e20
24. Malkov VA, Serikawa KA, Balantac N, Watters J, Geiss G, Mashadi-Hossein A, Fare T (2009) Multiplexed measurements of gene signatures in different analytes using the Nanostring nCounter™ assay system. BMC Res Notes 2:80. doi:10.1186/1756-0500-2-80
25. Waggott D, Chu K, Yin S, Wouters BG, Liu FF, Boutros PC (2012) NanoStringNorm: an extensible R package for the pre-processing of NanoString mRNA and miRNA data. Bioinformatics 28:1546–1548
26. Brumbaugh CD, Kim HJ, Giovacchini M, Pourmand N (2011) NanoStriDE: normalization and differential expression analysis of NanoString nCounter data. BMC Bioinforma 12:479

bioengineering

MDPI

Article

In Vitro Evaluation of Glycoengineered RSV-F in the Human Artificial Lymph Node Reactor

Lars Radke [1,2], Grit Sandig [3], Annika Lubitz [4], Ulrike Schließer [4], Hans Henning von Horsten [5], Veronique Blanchard [6], Karolin Keil [1], Volker Sandig [4], Christoph Giese [4], Michael Hummel [2], Stephan Hinderlich [3] and Marcus Frohme [1,*]

1 Molecular Biotechnology and Functional Genomics, Technical University of Applied Sciences Wildau, Hochschulring 1, Wildau 15745, Germany; lars.radke@charite.de (L.R.); keil@th-wildau.de (K.K.)
2 Institute of Pathology, Charitè-University Medicine Berlin, Augustenburger Platz 1, Berlin 13353, Germany; michael.hummel@charite.de
3 Laboratory of Biochemistry, Department of Life Sciences and Technology, Beuth University of Applied Sciences, Seestraße 64, Berlin 13347, Germany; Grit.Sandig@HTW-Berlin.de (G.S.); hinderlich@beuth-hochschule.de (S.H.)
4 ProBioGen AG, Goethestraße 54, Berlin 13086, Germany; Annika.Lubitz@Probiogen.de (A.L.); Ulrike.Schliesser@Probiogen.de (U.S.); Volker.Sandig@Probiogen.de (V.S.); Christoph.Giese@Probiogen.de (C.G.)
5 Department of Life Science Engineering, HTW Berlin University of Applied Sciences, Wilhelminenhofstraße 75a, Berlin 12459, Germany; HansHenning.vonHorsten@htw-berlin.de
6 Institute of Laboratory Medicine, Clinical Chemistry and Pathobiochemistry, Charité Medical University Berlin, Augustenburger Platz 1, Berlin 13353, Germany; veronique.blanchard@charite.de
* Correspondence: mfrohme@th-wildau.de; Tel.: +49-3375-508-249

Academic Editor: Anthony Guiseppi-Elie
Received: 1 April 2017; Accepted: 3 August 2017; Published: 15 August 2017

Abstract: Subunit vaccines often require adjuvants to elicit sustained immune activity. Here, a method is described to evaluate the efficacy of single vaccine candidates in the preclinical stage based on cytokine and gene expression analysis. As a model, the recombinant human respiratory syncytial virus (RSV) fusion protein (RSV-F) was produced in CHO cells. For comparison, wild-type and glycoengineered, afucosylated RSV-F were established. Both glycoprotein vaccines were tested in a commercial Human Artificial Lymph Node in vitro model (HuALN®). The analysis of six key cytokines in cell culture supernatants showed well-balanced immune responses for the afucosylated RSV-F, while immune response of wild-type RSV-F was more Th1 accentuated. In particular, stronger and specific secretion of interleukin-4 after each round of re-stimulation underlined higher potency and efficacy of the afucosylated vaccine candidate. Comprehensive gene expression analysis by nCounter gene expression assay confirmed the stronger onset of the immunologic reaction in stimulation experiments with the afucosylated vaccine in comparison to wild-type RSV-F and particularly revealed prominent activation of Th17 related genes, innate immunity, and comprehensive activation of humoral immunity. We, therefore, show that our method is suited to distinguish the potency of two vaccine candidates with minor structural differences.

Keywords: Glycoengineering; fucosylation; RSV; F-Protein; NanoString

1. Introduction

In recent years, the process of vaccine development has evolved drastically. Yet, the main requirement on vaccines have not changed: the establishment of a long-lasting and pathogen-specific immunological memory as a result of a concerted immune response. Subunit vaccines are highly

focused and specific, but often suffer from reduced immunogenicity, low reactogenicity, and limited availability of innate defense triggers [1]. Although adjuvants are applied to compensate for these deficiencies by activation of different cell types or by a long-lasting release of antigen, the frequently-used aluminum salts and mineral oil lead to diminished immune responses or side effects [2]. Recently, in vitro experiments showed that the adjuvant component α tocopherol elevated the risk of narcolepsy after H1N1 vaccination [3]. Covalent linkage of immunogenic agents with the vaccines, e.g., by cross-linking, could be used for the enhancement of efficacy. Recombinant protein vaccines opened a way to introduce immunogenic agents immediately during the production process. This could be done by additional immunogenic peptides, which are bound N- or C-terminally to the protein backbone, or by introduction of non-human posttranslational modifications, e.g., via glycosylation in the case of glycoprotein vaccines [4]. These foreign glycosidic structures are able to interact with the conserved Toll-like receptors and, by that, stimulate the immune system comprehensively. Therefore, they can be used as adjuvants in vaccine development which mainly boost the recognition of very small inoculants, like toxins, subcellular components, or viral proteins. In this study a subunit vaccine candidate against the respiratory syncytial virus (RSV) was used as a model. It was recombinantly produced in its native and afucosylated forms. However, glycans with and without fucose are both common in humans and, therefore, a direct adjuvant role is highly unlikely. This is in contrast to monosaccharides artificial to humans, e.g., N-glycan-bound xylose, which may work as adjuvants [4–6].

RSV causes infections of the lower respiratory tracts and has a prevalence of nearly 100% within the first 24 months of life [7]. The virus is a certain threat to prematurely-born children and immunocompromised people. According to estimates, 600,000 people die as a result of RSV infections each year [8]. The common antibody treatment with Palivizumab is of short protective effect, cost intensive, and restricted to infants of high risk. DeVincenzo et al. developed an oral RSV entry inhibitor (named GS-5806) which lowered the viral load and the disease symptoms in a double-blind placebo-controlled exposition study [9]. However, until now, there has been no vaccine available and, recently, a phase III study by Novavax failed to confirm vaccine efficacy [10].

The RSV envelope consists of two major proteins, RSV-G (where G stands for glycoprotein) and the "fusion" protein RSV-F. Both proteins have been used as targets in previous attempts (e.g., [11,12]). In this study, we focused on the highly-conserved RSV-F which is responsible for virus spreading by fusing with neighboring healthy cells. It contains three N-glycans playing a critical role in this process [13]. For vaccine production, a soluble variant of RSV-F was constructed lacking the transmembrane region, but fused with a C-terminal Factor Xa cleavage site and a 6xHis-tag. The construct contains two furin cleavage sites that allow proteolytic processing of RSV-F within the trans-Golgi. This mechanism results in the native active form (disulfide-linked F1 and F2 subunits) and release of the p27 peptide.

It became obvious in recent years that the predictive value of substance testing in animals is limited and the phylogenetic distance between laboratory animals and humans is considerable [14]. RSV vaccines are often tested in mice or cotton rats which, in part, mimic human responses. However, there is no single globally-accepted animal-model for the study of RSV vaccines and none in which RSV disease fully matches that of humans [15]. Several studies failed to transfer positive results from rodents, or even primates [16], to humans. In addition, animal studies are outside the scope of this (preliminary) study. In vitro models exist that, e.g., mimic the pediatric bronchial epithelum via a 3D air-liquid interface model [17] or investigate the growth of RSV in primary cells from the human respiratory tract [18]. However, these models cannot display the well-concerted interaction of immune cells. Therefore, we determined the immunogenic potential of the produced vaccine candidates with the altered glycosylation pattern by performing stimulation experiments in a highly-specialized perfusion reactor system named the Human Artificial Lymph Node reactor (HuALN®, ProBioGen AG, Berlin, Germany) [19]. It has been developed to model the human

immune system in vitro for testing of biopharmaceuticals and vaccines, assessing immunomodulation, immunogenicity, and immunotoxicity.

The reactor allows long-term co-cultivation of primary human peripheral blood mononuclear cells (PBMCs) and matured dendritic cells (mDC). In a 3D hydrogel matrix cells can migrate to form immune-competent micro-organoid structures and dendritic cells form a network in which B- and T-cells can swarm and cluster. The HuALN® enables the analysis of cellular and humoral immunity on the basis of various read-out parameters, e.g., cytokine profiles, histological studies and the cells can be harvested for further analysis, like gene expression profile studies [20].

Here, we performed standard HuALN® 28-day cultivation experiments, where cells of healthy donors were repeatedly stimulated with mDC and RSV-F variants and cell culture supernatants were collected on a daily basis. The concentrations of six key cytokines were quantified with a bead-based suspension assay (BioPlex, BioRad). These key cytokines were identified in previous studies [21] and cover cellular (IL-2) and humoral (IL-4) immune response, as well as pro- (IFN-g, TNF-a) and anti-inflammatory (IL-10) cytokines and growth factors (GM-CSF). Since cells can only be harvested at the end of the trial, the same experiment was conducted in a fed batch microtiter plate with a comparable stimulation pattern. For a comprehensive gene-expression analysis mRNA was analyzed with a Nanostring nCounter® Gene Expression panel covering more than 500 immunology genes. The most stable expressed reference genes in this experimental set-up were identified in an extensive study beforehand and have been cross-checked with quantitative polymerase chain reaction (qPCR) results [22].

2. Materials and Methods

2.1. Production and Analysis of Recombinant RSV-F Protein

Cells for expression of soluble RSV-F were obtained according to Sandig et al. [5]. In brief, a cDNA was constructed containing the N-terminal extracellular part of RSV-F, an N-terminal Mellitin signal sequence, and a C-terminal Factor Xa cleavage site fused with a 6xHis-tag. CHO DG44 cells were transfected with the respective vector and selected by puromycin methotrexate. For protein production CHO RSV-F cells were cultivated for 14 days, and RSV F was purified by Ni-NTA affinity chromatography. To obtain glycoengineered RSV-F the cDNA for RMD (GDP-6-deoxy-D-lyxo-4-hexulose reductase) from *Pseudomonas aeruginosa* was co-expressed in CHO RSV-F cells using the GlymaxX® technology [23], resulting in knock-down of the endogenous fucosylation pathway of CHO DG44 cells. In the following we, therefore, indicate RSV-F from CHO DG44 cells as "fucosylated RSV-F" and RSV-F from CHO DG44/RMD cells as "afucosylated RSV-F" or "RSV-F Fuc-".

The integrity of RSV-F proteins was verified by Western blot analysis using a Penta-His HRP antibody (1:2000, Qiagen, Hilden, Germany). The monosaccharide composition of the proteins was analyzed using high-performance anion exchange chromatography with pulsed amperiometric detection (HPAEC-PAD), as described in [24], and N-glycan patterns by matrix-assisted laser-desorption/ionization time-of-flight (MALDI-TOF) mass spectrometry, as described before [25,26].

2.2. Stimulation Experiments

In the cell culture stimulation experiment CD14 (−) PBMC were co-cultured with mDC. Therefore, CD14 (+) and CD14 (−) cells were enriched from whole blood of healthy donors, as described before [21]. Immature dendritic cells (iDC) were differentiated from enriched CD14 (+) cells by the addition of interleukin 4 (IL-4) and granulocyte-macrophage colony-stimulating factor (GM-CSF), 800 U/mL each (both Miltenyi Biotec, Bergisch Gladbach, Germany), on day 1 and 2. Antigen-specific maturation was done on day 7 (1 μg/mL of each antigen). On day 8 all supplements were removed by a media exchange.

Stimulation experiments were conducted simultaneously in three HuALN® reactors to collect and analyze supernatants on a daily basis, as well as in 96-well microtiter plates to harvest cells for a comparative gene expression study of the initial immune response. In two HuALN® reactors CD14 (−) cells were cultivated with mDC and the respective vaccine (fucosylated wild-type RSV-F from parental CHO or afucosylated RSV-F from CHO-RMD). A third HuALN® reactor served as a negative control and was left untreated (no vaccine-specific mDC, and the bolus is media at the days of stimulation).

Cryopreserved PBMCs were thawed and rested for one day at 37 °C, 5% CO_2. On the next day cells were harvested and adjusted to the following concentrations: each matrix (5 mg/mL agarose and 1.3 mg/mL collagen final concentration) with 500 µL total volume contained 1.7×10^7 DCs (with or without stimulation) and 2×10^8 CD14 (−) cells. Matrices were placed in the HuALN® reactors and perfused with 45.15 µL/h in three intervals of 15 µL/min.

One hundred microliters of supernatants from HuALN® reactors were taken on a daily basis for 28 days (with the exception of days 4, 12, 19, and 25). (Re-) stimulation took place always after collection of supernatants on days 0, 7, 14, and 21.

For the gene expression study 3×10^6/mL CD14 (−) cells with autologous mDCs were seeded in 96-well plates in 200 µL of RPMI 1640 medium supplemented with 10% fetal calf serum. RSV-F variants (1 µg/mL), as well as LPS (10 µg/mL) as a positive control, were added immediately to the cultures. Due to the high cell density, the medium needed to be partially replaced every day as follows: after 24 h, 100 µL cell culture supernatant was taken and 200 µL of new media with stimulants was added to a final volume of 300 µL. Every following media replacement included the collection of 200 µL of supernatant and the addition of 200 µL new media also including stimulants. On day 5 the cells were restimulated with mDC, additionally. After 48 h, five-day and seven-day cells from each treatment were collected by harvesting all cells of a respective well.

2.3. Cytokine Analysis

Supernatants from HuALN® reactors were collected over a period of 28 days. Since (re-) stimulation took place after the collection of supernatants, changes in cytokine secretion can be detected one day later, at the earliest. Supernatants were analyzed with a multiplexed suspension array system (Bio-Plex 200, Bio-Rad, Munich, Germany). A Bio-Plex Express assay (Bio-Rad) for six custom analytes was used to quantify the cytokines IL-2, IL-4, IL-10, GM-CSF, IFN-γ, and TNF-α. The assay was performed according to the manufacturer's protocol, but conducted fully-automated on a Tecan Freedom Evo 200 (Tecan, Männedorf, Switzerland) with an in-house-developed Tecan Freedom EVOware® script in order to lower the variance from manual handling [27]. All samples were tested in duplicate. The results were analyzed with Bio-Plex Manager 6.1 (Bio-Rad, Munich, Germany) using the logistic five-point regression method.

2.4. RNA Preparation and NanoString Measurement

Cells from microtiter plates were stored as cell pellets at −80 °C. Extraction of total RNA was performed with a High Pure RNA Isolation Kit (Roche, Mannheim, Germany). The purity of the total RNA was verified with a Nanodrop ND-1000 (Nanodrop Instruments, Wilmington, DE, USA) by determining the spectral absorption quotients 260/280 and 260/230. RNA integrity was checked with a DNF-472 High-Sensitivity RNA Analysis Kit on a Fragment Analyzer™ (Advanced Analytical Technologies, Heidelberg, Germany). Analysis was performed as described by the manufacturer with the exception of an extended runtime of an additional 20 min to be able to detect any remaining contamination with genomic DNA.

RNA samples of vaccine stimulation experiments were analyzed with an nCounter® Gene Expression assay (NanoString® Technologies, Seattle, WA, USA) in duplicate. The prebuilt Human Immunology v2 panel analyzes 579 immunology-related human genes and 15 reference genes in parallel in a special cartridge. RNA samples were quantified with the Qubit® RNA HS AssayKit

(Molecular Probes, Eugene, Oregon, USA) immediately prior to preparation for the NanoString experiment. Due to a slight fragmentation of some RNA samples, 150 ng of total RNA was used. NanoString experiments were performed on an nCounter® Dx Analysis System with FLEX Configuration, as described [22].

Data was normalized using nSolver Analysis Software 3.0 (NanoString® Technologies). To estimate the general difference between stimulation types, normalized and log transformed counts of all samples (including the negative control) were utilized for a cluster analysis using hclust in R (version 3.3.2).

Duplicates were grouped and fold-change estimates were calculated within the nSolver software. To test the significance of differentially-expressed genes between both RSV-F variants, the recently-published R package NanoStringDiff [28] was used, which is specially-developed for nCounter assays, where t-test-based approaches do not fit. Herein, counts are normalized, as in the nSolver Analysis Software, and transferred into a generalized linear model of the negative binominal family. An empirical Bayes shrinkage approach is utilized to estimate the dispersion parameters in the used model and differentially-expressed genes are identified using a likelihood ratio test.

Finally, genes were clustered by their function when they were of primary immunologic interest or when they were identified as significantly differentially expressed.

3. Results and Discussion

3.1. Production and Analysis of RSV-F Proteins

Two glycosylation variants of soluble RSV-F were recombinantly expressed in CHO DG44 and CHO DG44/RMD cells. Proteins were purified from cell culture supernatants by Ni-NTA affinity chromatography. Western blot analysis of the purified proteins displayed proteins of a size of 70 kDa under non-reducing conditions (Figure 1A). Obviously, there are two forms of the RSV-F2 subunit visible under the reducing conditions. We cannot completely rule out that the double band indicates different glycosylation variants [29]. However, it is more likely that differently-processed proteins exist. Although both furin cleavage sites are obviously recognized by the protease, part of RSV-F might only be processed by one furin cleavage and still contain the pep27 peptide, whereas the lower band seems to represent the fully-processed F2 subunit after double furin cleavage. Densitometric estimation of RSV-F and RSV-F Fuc- revealed a ratio of about 70:30 of the upper band (singly-cleaved protein) and the lower band (doubly-cleaved protein) for both samples. The production conditions of RSV-F, therefore, seem to hamper complete posttranslational modification by furin, most likely due to the high expression rate of the recombinant protein and its limited retention time in the Golgi. However, there is no significant effect of fucosylated or afucosylated glycans on furin cleavage efficacy.

Reduction of the fucose level of the RSV-F protein from CHO DG44/RMD cells was proven by monosaccharide analysis via HPAEC-PAD (Figure 1B). The N-glycan patterns of both RSV-F variants were analyzed by MALDI-TOF mass spectrometry. Figure 1C predominantly shows fucosylated N-glycans of RSV-F from CHO DG44 cells. In contrast, analysis of RSV-F from CHO DG44/RMD cells reveals a pattern of comparable N-glycans, but without fucose. These data indicate that RSV-F could be produced successfully as a glycoengineered, non-fucosylated variant in CHO DG 44/RMD cells.

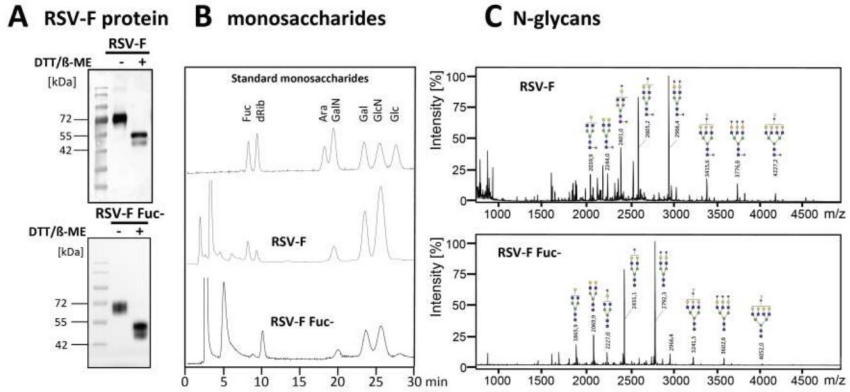

Figure 1. Soluble RSV-F was stably expressed in CHO DG44 cells, as well as in fucose-deficient CHO DG44 cells. RSV-F proteins were purified from cell culture supernatants and analyzed by Western blot. (**A**) Fucose levels of purified and acid-hydrolyzed proteins (15 µg) were analyzed by HPAEC-PAD. (**B**) Peaks were compared to standard monosaccharides: 2-deoxy-D-ribose (dRib), L-fucose (Fuc), D-arabinose (Ara), D-galactosamine (GalN), D-galactose (Gal), D-glucosamine (GlcN), and D-glucose (Glc). N-glycans of the RSV-F proteins were permethylated and masses were obtained by MALDI-TOF mass spectrometry. (**C**) Structures were verified using Glycoworkbench 2.0 [30].

3.2. Cytokine Analysis

Three HuALN® reactors were run with fucosylated RSV-F, RSV-F Fuc-, and one negative control. Quantification of the secreted cytokines in the cell culture supernatants was used to evaluate the extent of the humoral and cellular activation of the immune cells. Since only 100 µL of supernatants were available per day, multiplexed assays were required to quantify the six key cytokines IL-2, IL 4, IL-10, GM-CSF, IFN-γ, and TNF-α. Bead-based suspension assays allow the quantification of up to 100 analytes in as little as 50 µL, thus enabling the measurement of duplicates. Bio-Plex Express Kits were used with the help of an automated liquid handling robot in order to achieve very high precision and repeatability. Mean recovery rates of spike-in-controls were between 91% and 122%, and for 70% of all data points error limits were below 20% (median error rate 10.4%). The time course of the cytokine secretion is shown for all stimulation experiments in Figure 2.

The cytokine pattern reveals differences in the mode of stimulation of the immune system. Overall, RSV-F Fuc- generates a stronger pro-inflammatory and Th2-based response, while RSV-F strongly suppresses the inflammation process and the T-cell response is more Th1-pronounced. Details of the cytokine pattern are discussed below.

Only in the initial phase of the cultivation can a stronger pro- and anti-inflammatory response be observed for RSV-F-stimulated cells. After restimulations at day 7, 14, and 21 the pro- and anti-inflammatory cytokine secretions show individual characteristics, especially differences in the particular duration of their release. In general, the pro-inflammatory response is higher in the afucosylated viral antigene than in the fucosylated one. In particular, TNF-α secretion clearly correlates with the time points of restimulation. In contrast, the anti-inflammatory IL-10 response is more strongly pronounced in RSV-F. As a result, the IFN-γ response is suppressed after the first restimulation on day 7 in the wild-type control. IL-10 shifts the immune response indirectly in favor of Th2 cells, B-cells, and the humoral response, while IFN-γ suppresses the same. In RSV-F Fuc- stimulated cells the Th2 activation is mediated via the immunologically-relevant secretion of IL-4. While its initial secretion is low, the response to restimulations is well-modulated and indicates a highly specific mode of action for the afucosylated RSV-F protein. RSV-F stimulated cells lack this prominent Th2 activating response. Overall, the observed concentrations of Th1 activating IL-2 are unexpectedly low. RSV-F treatment always shows elevated IL-2 levels one day after restimulation. In contrast, the highest IL-2 concentration is reached on day 7 after RSV-F Fuc- treatment and is heavily delayed from the initial stimulation. IL-2 is bound to the IL-2 receptor during T-cell proliferation, which might lead to lower

IL-2 concentrations in the cell culture supernatant. In contrast, IFN-γ secretion, which is one of the effector cytokines of activated Th1 cells, is elevated. Hence, activation of Th1 cells can be concluded and a well-balanced Th1/Th2 response is demonstrated. Finally, GM-CSF secretion of RSV-F Fuc- stimulated cells corresponds with each restimulation, but shows decreasing concentrations. GM-CSF promotes the development of monocytes and granulocytes and, thus, facilitates the cellular response and adaptive immunity, since monocytes can mature into dendritic cells.

Unstimulated cells (negative control) exhibit two stress responses. Within the first days of cultivation levels of TNF-α and IL-10 are already increased, which is true for all cytokines, with the exception of TNF-α, from day 16. The initial release of proinflammatory cytokines and chemokines can be induced by overnight resting (e.g., after thawing the cells) and is reported for TNF-α, but not for IFN-γ, by Kutscher et al. [31]. Secondly, the bolus for negative controls contained medium in the same volume as for the vaccine stimulations. Thus, necrotic cells may be whirled up, disintegrated at once, and raise interferon levels of healthy cells nonspecifically. As a result, IL-2 concentration increases at day 21. More importantly, PBMCs react or die spontaneously at this time point due to the absence of any kind of stimulation. This is in line with the normal lifespan of naïve and resting T-cells in vitro, which need to be stimulated with cytokines for survival or proliferation [32,33].

3.3. Quality of RNA Preparations and Nanostring Assays

The nCounter immunology panel contains a broad range of genes, covering cytokines, their respective receptors, proteins from signaling pathways, as well as humoral and cellular, or innate and adaptive, immunity-related factors. Thus, a deep and precise insight into the immunologic processes can be gained and modes of action are revealed.

For NanoString experiments 50 to 100 ng of RNA are required. Cells from stimulation experiments in multititer plates yielded RNA in sufficient concentrations (25.8 to 61.7 ng/μL; >20 ng/μL) are required in good quality and purity. In Nanodrop 1000 measurements all samples were within the required ranges for the absorption ratios of 260/280 and 260/230, with the exception of four. However, these samples showed clear peaks for 28S and 18S rRNA and yielded high RNA quality numbers when analyzed with the Fragment Analyzer. Since other samples with good performance in the Nanodrop measurement showed slight fragmentation or low concentrations, we followed the manufacturer's advice to increase the quantity of RNA used for the NanoString measurement to 150 ng (quantified with Qubit directly before the NanoString sample preparation).

Finally, quality control within the nSolver analysis software showed no flags indicating fragmentation, but consistent binding densities from lane to lane, as well as consistent RNA concentration, indicated by low normalization factors (0.85–1.69). Dilutions of the positive spike in controls showed high linearity within each sample ($R^2 > 0.9875$). The reference genes *GAPDH*, *OAZ1*, and *TUBB* were excluded from the panel of used reference genes due to their high coefficient of variation (>75%), as well as the commonly-used reference gene *B2M*, known to be regulated by IFN-γ [34].

3.4. Gene Expression Analysis

To get a general idea of changes of the gene expression between stimulants we performed a cluster analysis (Figure 3) using hclust in R (version 3.3.2). As expected, these clusters are mainly time-dependent, with the exception of LPS. Both RSV-F protein-stimulated cells show higher dissimilarity of LPS samples compared to the unstimulated negative control, due to the different mode of action of LPS. Interestingly, after 48 h of cultivation, RSV-F Fuc- is clustered outside the closer-related fucosylated RSV-F and negative control. This indicates that the onset of immunologic reactions is stronger for the afucosylated viral antigene.

To analyze differences of gene expression pattern of this time point in more detail, fold-change estimates were built from the nCounter assay for each stimulation type. We did not use any specific thresholds to identify genes with a particularly strong fold change, but identified significantly

differentially-expressed genes between both RSV-F protein treatments with the help of NanoStringDiff R package. Clusters of genes that are functionally associated with the identified genes or of primary immunologic function were grouped and further analyzed. In accordance with the hclust analysis the early response after 48 h of cell stimulation showed the most prominent and informative differences in gene expression (Figure 4), whereas data of day 5 and 7 often showed transient effects over time (data not shown).

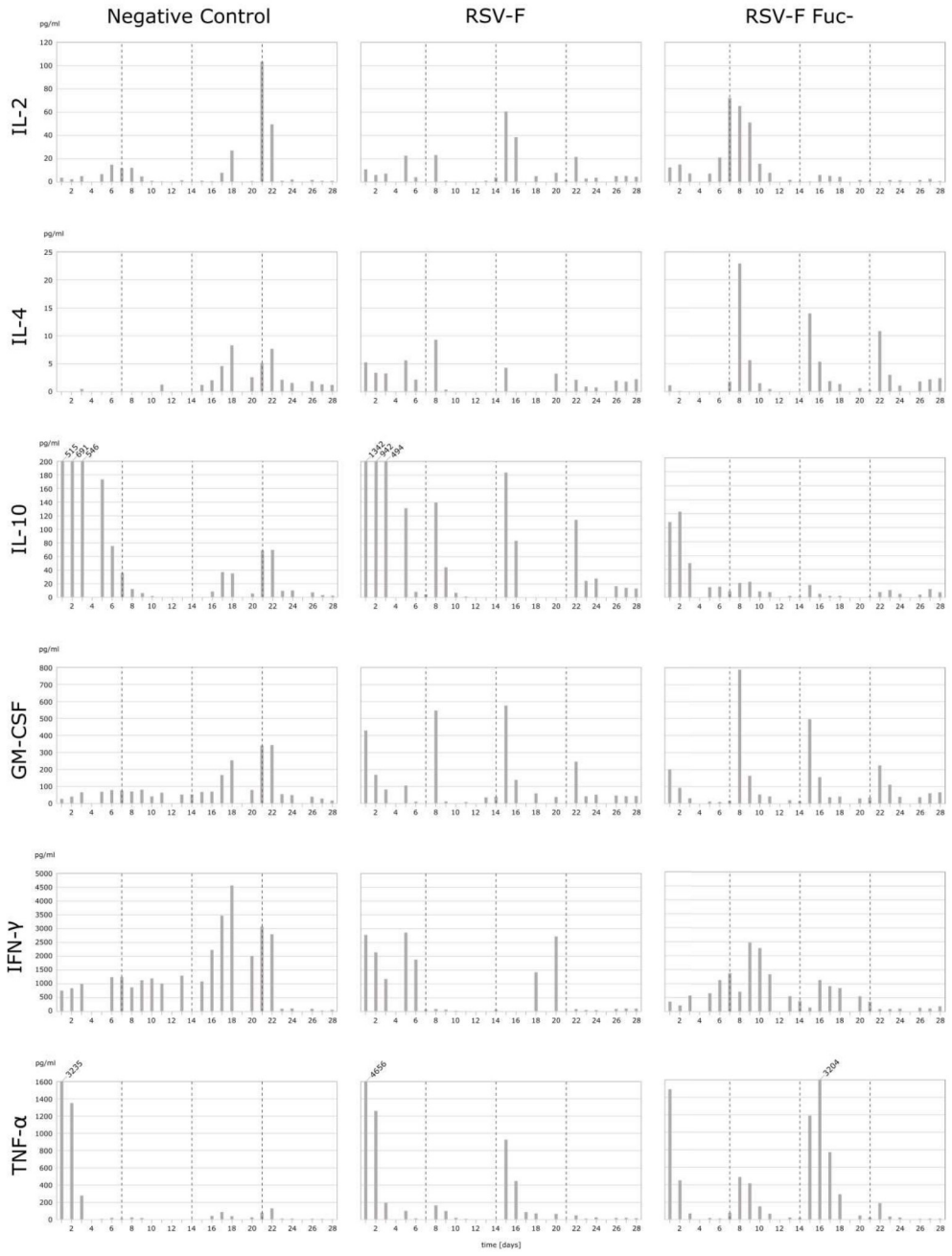

Figure 2. Cytokine secretion (in pg/mL) of PBMC in HuALN® reactors with repeated stimulations. PBMC were incubated for 28 days and stimulated with RSV-F protein variants and the according maturated DC at days 0, 7, 14, and 28 (dotted lines). Some maximum values are cut off (IL-10 and TNF-α) for better resolution of lower concentrations. Since both cytokines can act in an autocrine-like manner, the height of the values is of minor importance, immunologically, if a certain threshold is exceeded.

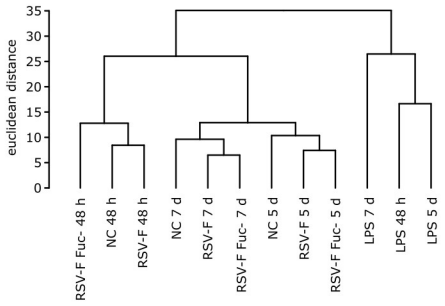

Figure 3. Hierarchical clustering of stimulated samples with normalized and log transformed counts from the NanoString experiment. Samples show time-dependent and stimulus-dependent similarity. Notably, after 48 h the gene expression pattern of cells stimulated with the afucosylated RSV-F protein shows less similarity to the pattern of the wild-type RSV-F-stimulated cells than the latter one to that of the unstimulated negative control (NC).

Figure 4. Fold change ratios of stimulated cells in functionally-ordered clusters. Significance is calculated for gene expression of RSV-F Fuc- vs. RSV-F. NanoString nCounter assays were performed in duplicate. Since PBMC are a mixture of cells, higher p-values were depicted, as well: $p \leq 0.001$: ***; $p \leq 0.01$: **; $p \leq 0.05$: *; $p \leq 0.1$: +; and $p \leq 0.2$: o.

Several clusters show comprehensive upregulation of gene expression for RSV-F Fuc- but not for RSV-F, stimulation after 48 h of stimulation. These clusters cover cellular, humoral, innate, and adaptive immunity, as well as the related transcription factors or activation markers and are discussed in detail.

To augment the cytokine analysis, clusters of Th1-, Th2-, and Th17-related genes were analyzed. Apparently, differences in the expression of Th1-associated genes are negligible, however, IL2 and IFNG (coding for IL-2 and IFN-γ) were upregulated—providing evidence that RSV-F Fuc- evokes a certain Th1 response, although IL-2 concentrations were comparably low in cell culture supernatants of RSV-Fuc- treated cells. In the Th2 panel all interleukins and transcription factors are upregulated in RSV-F Fuc-, but not in RSV-F, which is in compliance to the cytokine data from the HuALN® experiment. The Th17 panel shows the most significant differences in the expression of Interleukin 17 subunits and Th17 associated transcription factors (RORC, STAT3). Activation of Th17 cells is favorable, since they play critical roles in host defense against pathogens at mucosal sites [35], where RSV infections takes place. Both Th2, as well as Th17, promote B cell development and interact closely with B cells in response to pathogens. Th17 cells are involved in B cell recruitment, and Th17 activity may encourage antibody production [36], which is promising since a high titer of neutralizing antibodies is often seen as an indicator for successful RSV protection [37].

B cell development markers show significantly higher expression by the afucosylated viral protein than in wild-type RSV-F. Among them is, e.g., BLNK, which plays a critical role in orchestrating the pro-B cell to pre-B cell transition. Furthermore, genes that code for receptors for the Fc region (*FCGRs* and *FCAR*) of monomeric or complexed immunoglobulins (Ig) are partially activated. They have comprehensive functions in innate, adaptive, and humoral immune responses by modulating subsequent effector and regulatory processes, like phagocytosis of immune complexes and antibody production. The upregulation of these genes proves that immune cells respond to the inflammatory reaction by going into an alert state and expect a humoral immune reaction. The upregulation of IgG and IgA, but not IgE is of interest, since both classes of antibodies transcytose across the epithelial cells to enter the lumen of the respiratory tract, bathes the mucosal lining, and can protect against RSV disease [38,39].

Along with this, there is an overall increased expression of observable genes associated with the activation, differentiation or proliferation of T cells and DCs in RSV-F Fuc-. This is accompanied with a generally stronger activation of parts of the innate immune system comprising antiviral and antimicrobial components, as well as lectins in cells stimulated with RSV-F Fuc-, but not in wild-type RSV-F-stimulated cells. Moreover, the expression of chemotactic ligands and receptors is more pronounced in the afucosylated RSV-F protein. Lastly, RSV-F Fuc- shows a comprehensive upregulation of signaling molecules of the JAK/STAT and NFKB pathway, which leads to broad activation of transcription factors.

LPS, a widely used inflammation control, worked efficiently in this study. It generated a strong pro-inflammatory response and also activated LPS-induced genes like *CD14* (a co-receptor of TLR 4) and other typical LPS-induced chemokines (CCL2, CCL19, and CCL20). However, in comparison to both RSV-F proteins, it failed to activate the Fc receptor expression. In further studies, a more specialized positive control can be used, consisting of a mix of different stimulants which, themselves, address distinct cell types and their pathways. Thus, an encompassing activation of the immune system may be elicited.

Since PBMCs are a mixture of cells, differential gene expression may be masked and a strong activation of a small fraction of cells cannot be distinguished as significant. Thus, we accepted somewhat lower *p*-values within the analysis of differential gene expression. Optimally, cells need to be separated (e.g., into Th1, Th2, Th17, and DC) and analyzed individually to allow an exact assignment of significant changes in the gene expression. A higher number of tests will be necessary; however, smaller individual gene sets will be appropriate in subsequent experiments.

The humoral immune response can be further investigated in the HuALN® system. The experimental setup was not designed for a deeper analysis of B-cells and any generated antibodies. Nevertheless,

we see an upregulation of the Recombination Activating Gene 2 (*RAG2*) after 48 h of stimulation for the afucosylated F-protein, but not for the wild-type F-protein. However, the expression of *RAG1* and Activation-Induced Cytidine Deaminase (AICDA), which is heavily involved in somatic hypermutation, is downregulated. This may represent a kind of intermediate incomplete activation status due to the lack of additional factors (e.g., stromal cells). Recently, the physiology of the HuALN® system has been further improved by establishing a differentiation protocol to generate lymph node stromal-like cells from mesenchymal stromal cells for co-cultivation in the existing allogenic PBMC and mDC system [40]. We believe that this improvement can further enhance the analysis of relevant glycoengineered viral antigenes.

Investigation of the glycosylation pattern of the produced antibodies or other immunologically-important molecules is highly interesting in itself, since it correlates with the vaccine's mode of action. Mahan et al. revealed that distinct glycosylation patterns are programmed, and even remembered, after immunization, when adjuvant stimulation addressed Toll-like receptors (TLRs) [41]. However, the responsible glucuronyltransferases are only partially covered by the used NanoString panel, and have to be analyzed with custom assays in the future.

The analysis of cytokines and of the gene expression within suggests different modes of activation between both RSV-F types, which can be attributed to the fucosylation state of the RSV-F protein. Afucosylation led to a much stronger pro-inflammatory Th2 and Th17 based activation. However, in this study we were unable to address the molecular mechanism of this effects experimentally. It is known, that the interaction of immune receptors could be mediated by the degree of fucosylation of ligand glycans. The most prominent example is the improved binding of fucose-deficient IgG1 to human FcγRIIIA [42]. Furthermore, fucosylation of glycans may influence the conformation of the RSV-F proteins. In this context, unmasking of complete epitopes is unlikely due to the small size of fucose, but increasing accessibility of epitopes by the immune system might be possible. A second explanation for the observed small, but significant, differences in immunogenic potency of RSV-F and RSV-F Fuc- might be the proportion of remaining pep27 at the purified proteins. Although we cannot detect significant differences by semiquantitative densitometry, an influence of pep27 on immunogenicity is suggested. An immunomodulatory role has been found for bovine RSV pep27 [43]; however, no such role has been attributed to the human RSV intervening peptide, which does not share a sequence similarity with its bovine counterpart.

However, most importantly, in this study we showed that the HuALN® reactor and the downstream analysis methods are able to discriminate the effects caused by very small modifications of the glycan structure.

Recently, Rosenlöcher et al. reported the gradual fucosylation of recombinant glycoproteins by exploiting the salvage pathway of the same cells used in this study [24]. Supplementation of the culture media with distinct concentrations of fucose could allow a fine tuning of the Th1/Th2 balance and the strength of the inflammatory process. Furthermore, by supplementing immunogenic fucose analogues in the culture media, the immunogenicity of recombinant protein vaccines could be further modulated.

4. Conclusions

The complementary quantification of cytokines in the cell culture supernatant and analysis of the gene expression by extensive nCounter panels provided the possibility to analyze the extent of the activation of the immune system broadly. Altogether, we proved with the chosen methods that viral proteins with varying glycan structures are able to trigger the immune system in a slightly different way. Afucosylated RSV-F reveals stronger activation of the innate immune system, generates a moderate inflammation response, and activates, via Th2 and Th17, the humoral immune system.

We suggest that through gradual afucosylation of the RSV-F protein N-glycans a balance between Th1 and Th2 response might even be more controllable. Further characterization of the adjuvant and the RSV vaccine has to concentrate on the analysis of the produced antibodies.

Acknowledgments: This research was supported by the Bundesministerium für Bildung und Forschung (BMBF) within the program "Forschung an Fachhochschulen". The authors want to thank Hedwig Lammert (Charité-University Medicine Berlin, Germany) for her time and effort in conducting the nCounter analyses.

Author Contributions: Volker Sandig, Christoph Giese, and Stephan Hinderlich conceived the glycosylation approach. Henning von Horsten designed the RSV-F gene construct. RSV-F proteins were produced and analyzed by Grit Sandig. Glycan analysis was carried out by Grit Sandig and Veronique Blanchard. Annika Lubitz performed the cell culture experiments. Karolin Keil conducted automated cytokine analysis. nCounter experiments were performed by Lars Radke within the group of Michael Hummel. Lars Radke, Ulrike Schließer, and Christoph Giese reviewed analyzed and interpreted gene expression and cytokine data. Lars Radke, Grit Sandig, and Stephan Hinderlich wrote the paper. Marcus Frohme supervised the analysis of the cells and supernatants and the article writing. All authors commented on the manuscript.

Conflicts of Interest: Christoph Giese and Volker Sandig are employees of ProBioGen AG, the developer and owner of the HuALN® technology. The founding sponsors had no role in the design of the study; in the collection, analyses, or interpretation of data; in the writing of the manuscript, and in the decision to publish the results.

References

1. Strugnell, R.; Zepp, F.; Cummingham, A.; Tantawichien, T. Vaccine antigens. *Perspect. Vaccinol.* **2011**, *1*, 61–88. [CrossRef]
2. Israeli, E.; Agmon-Levin, N.; Blank, M.; Shoenfeld, Y. Adjuvants and Autoimmunity. *Lupus* **2009**, *18*, 1217–1225. [CrossRef] [PubMed]
3. Masoudi, S.; Ploen, D.; Kunz, K.; Hildt, E. The adjuvant component α-tocopherol triggers via modulation of Nrf2 the expression and turnover of hypocretin in vitro and its implication to the development of narcolepsy. *Vaccine* **2014**, *32*, 2980–2988. [CrossRef] [PubMed]
4. Zimmermann, S.; Lepenies, B. Glycans as Vaccine Antigens and Adjuvants: Immunological Considerations. *Methods Mol. Biol.* **2015**, *1331*, 11–26. [PubMed]
5. Sandig, G.; von Horsten, H.H.; Radke, L.; Blanchard, V.; Frohme, M.; Giese, C.; Sandig, V.; Hinderlich, S. Engineering of CHO Cells for the production of recombinant glycoprotein vaccines with xylosylated N-glycans. *Bioengineering* **2017**, *4*, 38. [CrossRef]
6. Brzezicka, K.; Vogel, V.; Serna, S.; Johannssen, T.; Lepenies, B.; Reichardt, N.C. Influence of Core β-1,2-Xylosylation on Glycoprotein Recognition by Murine C-type Lectin Receptors and Its Impact on Dendritic Cell Targeting. *ACS Chem. Biol.* **2016**, *11*, 2347–2356. [CrossRef] [PubMed]
7. Glezen, W.P.; Taber, L.H.; Frank, A.L.; Kasel, J.A. Risk of primary infection and reinfection with respiratory syncytial virus. *Am. J. Dis. Child.* **1986**, *140*, 543–546. [CrossRef] [PubMed]
8. Thorburn, K. Pre-existing disease is associated with a significantly higher risk of death in severe respiratory syncytial virus infection. *Arch. Dis. Child.* **2009**, *94*, 99–103. [CrossRef] [PubMed]
9. DeVincenzo, J.P.; Whitley, R.J.; Mackman, R.L.; Scaglioni-Weinlich, C.; Harrison, L.; Farrell, E.; McBride, S.; Lambkin-Williams, R.; Jordan, R.; Xin, Y.; et al. Oral GS-5806 Activity in a Respiratory Syncytial Virus Challenge Study. *N. Engl. J. Med.* **2014**, *371*, 711–722. [CrossRef] [PubMed]
10. Press Release—Novavax. Available online: http://ir.novavax.com/phoenix.zhtml?c=71178&p=irol-newsArticle&ID=2202271 (accessed on 30 March 2017).
11. Groothuis, J.R.; King, S.J.; Hogerman, D.A.; Paradiso, P.R.; Simoes, E.A. Safety and immunogenicity of a purified F protein respiratory syncytial virus (PFP-2) vaccine in seropositive children with bronchopulmonary dysplasia. *J. Infect. Dis.* **1998**, *177*, 467–469. [CrossRef] [PubMed]
12. Power, U.F.; Plotnicky, H.; Blaecke, A.; Nguyen, T.N. The immunogenicity, protective efficacy and safety of BBG2Na, a subunit respiratory syncytial virus (RSV) vaccine candidate, against RSV-B. *Vaccine* **2003**, *22*, 168–176. [CrossRef]
13. McDonald, T.P.; Jeffree, C.E.; Li, P.; Rixon, H.W.; Brown, G.; Aitken, J.D.; MacLellan, K.; Sugrue, R.J. Evidence that maturation of the N-linked glycans of the respiratory syncytial virus (RSV) glycoproteins is required for virus-mediated cell fusion: The effect of α-mannosidase inhibitors on RSV infectivity. *Virology* **2006**, *350*, 289–301. [CrossRef] [PubMed]
14. Leist, M.; Hartung, T. Inflammatory findings on species extrapolations: Humans are definitely no 70-kg mice. *Arch. Toxicol.* **2013**, *87*, 563–567. [CrossRef] [PubMed]
15. Hurwitz, J.L. Respiratory syncytial virus vaccine development. *Expert Rev. Vaccines* **2011**, *10*, 1415–1433. [CrossRef] [PubMed]

16. Karron, R.A.; Wright, P.F.; Crowe, J.E., Jr.; Clements-Mann, M.L.; Thompson, J.; Makhene, M.; Casey, R.; Murphy, B.R. Evaluation of Two Live, Cold-Passaged, Temperature-Sensitive Respiratory Syncytial Virus Vaccines in Chimpanzees and in Human Adults, Infants, and Children. *J. Infect. Dis.* **1997**, *176*, 1428–1436. [CrossRef] [PubMed]
17. Parker, J.; Sarlang, S.; Thavagnanam, S.; Williamson, G.; O'donoghue, D.; Villenave, R.; Power, U.; Shields, M.; Heaney, L.; Skibinski, G. A 3-D well-differentiated model of pediatric bronchial epithelium demonstrates unstimulated morphological differences between asthmatic and nonasthmatic cells. *Pediatr. Res.* **2010**, *67*, 17–22. [CrossRef] [PubMed]
18. Wright, P.F.; Ikizler, M.R.; Gonzales, R.A. Growth of respiratory syncytial virus in primary epithelial cells from the human respiratory tract. *J. Virol.* **2005**, *79*, 8651–8654. [CrossRef] [PubMed]
19. Giese, C.; Demmler, C.D.; Ammer, R.; Hartmann, S.; Lubitz, A.; Miller, L.; Müller, R.; Marx, U. A human lymph node in vitro—Challenges and progress. *Artif. Organs* **2006**, *30*, 803–808. [CrossRef] [PubMed]
20. Giese, C.; Lubitz, A.; Demmler, C.D.; Reuschel, J.; Bergner, K.; Marx, U. Immunological substance testing on human lymphatic micro-organoids in vitro. *J. Biotechnol.* **2010**, *148*, 38–45. [CrossRef] [PubMed]
21. Radke, L.; López Hemmerling, D.A.; Lubitz, A.; Giese, C.; Frohme, M. Induced cytokine response of human PMBC-cultures: Correlation of gene expression and secretion profiling and the effect of cryopreservation. *Cell. Immun.* **2012**, *272*, 144–153. [CrossRef] [PubMed]
22. Radke, L.; Giese, C.; Lubitz, A.; Hinderlich, S.; Sandig, G.; Hummel, M.; Frohme, M. Reference gene stability in peripheral blood mononuclear cells determined by qPCR and NanoString. *Microchim. Acta* **2014**, *181*, 1733–1742. [CrossRef]
23. Von Horsten, H.H.; Ogorek, C.; Blanchard, V.; Demmler, C.; Giese, C.; Winkler, K.; Kaup, M.; Berger, M.; Jordan, I.; Sandig, V. Production of non-fucosylated antibodies by co-expression of heterologous GDP-6-deoxy-D-lyxo-4-hexulose reductase. *Glycobiology* **2010**, *20*, 1607–1618. [CrossRef] [PubMed]
24. Rosenlöcher, J.; Böhrsch, V.; Sacharjat, M.; Blanchard, V.; Giese, C.; Sandig, V.; Hackenberger, C.P.R.; Hinderlich, S. Applying Acylated Fucose Analogues to Metabolic Glycoengineering. *Bioengineering* **2015**, *2*, 213–234. [CrossRef]
25. Reinke, S.O.; Bayer, M.; Berger, M.; Blanchard, V.; Hinderlich, S. Analysis of cell surface N-glycosylation of the human embryonic kidney 293t cell line. *J. Carbohydr. Chem.* **2011**, *30*, 218–232. [CrossRef]
26. Frisch, E.; Kaup, M.; Egerer, K.; Weimann, A.; Tauber, R.; Berger, M.; Blanchard, V. Profiling of endo H-released serum N-glycans using CE-LIF and MALDI-TOF-MS-application to rheumatoid arthritis. *Electrophoresis* **2011**, *32*, 3510–3515. [CrossRef] [PubMed]
27. Keil, K.; Radke, L.; Tillich, U.; Frohme, M. Automatisierung des Bio-Plex Pro Analyseverfahrens. *Wissenschaftliche Beiträge 2015* **2015**, *19*, 15–19. (In German) [CrossRef]
28. Wang, H.; Horbinski, C.; Wu, H.; Liu, Y.; Stromberg, A.J.; Wang, C. A Negative Binomial Model-Based Method for Differential Expression Analysis Based on NanoString nCounter Data. *Nucleic Acids Res.* **2016**, *44*, e151. [PubMed]
29. Sugrue, R.J.; Brown, C.; Brown, G.; Aitken, J.; McL Rixon, H.W. Furin cleavage of the respiratory syncytial virus fusion protein is not a requirement for its transport to the surface of virus-infected cells. *J. Gen. Virol.* **2001**, *82*, 1375–1386. [CrossRef] [PubMed]
30. Ceroni, A.; Maass, K.; Geyer, H.; Geyer, R.; Dell, A.; Haslam, S.M. GlycoWorkbench: A Tool for the Computer-Assisted Annotation of Mass Spectra of Glycans. *J. Proteome Res.* **2008**, *7*, 1650–1659. [CrossRef] [PubMed]
31. Kutscher, S.; Dembek, C.J.; Deckert, S.; Russo, C.; Körber, N.; Bogner, J.R.; Geisler, F.; Umgelter, A.; Neuenhahn, M.; Albrecht, J.; et al. Overnight Resting of PBMC Changes Functional Signatures of Antigen Specific T- Cell Responses: Impact for Immune Monitoring within Clinical Trials. *PLoS ONE* **2013**, *8*, e76215. [CrossRef] [PubMed]
32. Röth, A.; Schneider, L.; Himmelreich, H.; Baerlocher, G.M.; Dührsen, U. Impact of culture conditions on the proliferative lifespan of human T cells in vitro. *Cytotherapy* **2007**, *9*, 91–98. [CrossRef] [PubMed]
33. Sprent, J. T-cell survival and the role of cytokines. *Immunol. Cell Biol.* **2001**, *79*, 199–206. [CrossRef] [PubMed]
34. Samarajiwa, S.A.; Forster, S.; Auchettl, K.; Hertzog, P.J. INTERFEROME: The database of interferon regulated genes. *Nucleic Acids Res.* **2009**, *37*, D852–D857. [CrossRef] [PubMed]
35. Guglani, L.; Khader, S.A. Th17 cytokines in mucosal immunity and inflammation. *Curr. Opin. HIV AIDS* **2010**, *5*, 120–127. [CrossRef] [PubMed]

36. Crome, S.Q.; Wang, A.Y.; Levings, M.K. Translational Mini-Review Series on Th17 Cells: Function and regulation of human T helper 17 cells in health and disease. *Clin. Exp. Immunol.* **2009**, *159*, 109–119. [CrossRef] [PubMed]
37. Walsh, E.E.; Falsey, A.R. Humoral and mucosal immunity in protection from natural respiratory syncytial virus infection in adults. *J. Infect. Dis.* **2004**, *190*, 373–378. [CrossRef] [PubMed]
38. Rojas, R.; Apodaca, G. Immunoglobulin transport across polarized epithelial cells. *Nat. Rev. Mol. Cell Biol.* **2012**, *3*, 944–956. [CrossRef] [PubMed]
39. He, W.; Ladinsky, M.S.; Huey-Tubman, K.E.; Jensen, G.J.; McIntosh, J.R.; Björkman, P.J. FcRn-mediated antibody transport across epithelial cells revealed by electron tomography. *Nature* **2008**, *455*, 542–546. [CrossRef] [PubMed]
40. Sardi, M.; Lubitz, A.; Giese, C. Modeling Human Immunity In Vitro: Improving Artificial Lymph Node Physiology by Stromal Cells. *Appl. In Vitro Toxicol.* **2016**, *3*, 143–150. [CrossRef]
41. Mahan, A.E.; Mattoo, H.; Dionne, K.; Tedesco, J.; Pillai, S.; Alter, G. IgG Glycosylation Is Programmed and Remembered after Immunization with TLR Stimulating Adjuvants. *AIDS Res. Hum. Retrovir.* **2014**, *30*, A65. [CrossRef]
42. Shields, R.L.; Lai, J.; Keck, R.; O'Connell, L.Y.; Hong, K.; Meng, Y.G.; Weikert, S.H.A.; Presta, L.G. Lack of Fucose on Human IgG1 N-Linked Oligosaccharide Improves Binding to Human FcγRIII and Antibody-dependent Cellular Toxicity. *J. Biol. Chem.* **2002**, *277*, 26733–26740. [CrossRef] [PubMed]
43. Zimmer, G.; Rohn, M.; McGregor, G.P.; Schemann, M.; Conzelmann, K.K.; Herrler, G. Virokinin, a bioactive peptide of the tachykinin family, is released from the fusion protein of bovine respiratory syncytial virus. *J. Biol. Chem.* **2003**, *278*, 46854–46861. [CrossRef] [PubMed]

bioengineering

MDPI

Article

Engineering of CHO Cells for the Production of Recombinant Glycoprotein Vaccines with Xylosylated *N*-glycans

Grit Sandig [1], Hans Henning von Horsten [2], Lars Radke [3], Véronique Blanchard [4], Marcus Frohme [3], Christoph Giese [5], Volker Sandig [5] and Stephan Hinderlich [1,*]

1 Laboratory of Biochemistry, Department of Life Sciences and Technology, Beuth University of Applied Sciences Berlin, Seestrasse 64, 13347 Berlin, Germany; Grit.Sandig@htw-berlin.de
2 Department of Life Science Engineering, HTW Berlin University of Applied Sciences, Wilhelminenhofstraße 75a, 12459 Berlin, Germany; HansHenning.vonHorsten@htw-berlin.de
3 Molecular Biotechnology and Functional Genomics, Technical University of Applied Sciences Wildau, Hochschulring 1, 15745 Wildau, Germany; lradke@th-wildau.de (L.R.); mfrohme@th-wildau.de (M.F.)
4 Institute of Laboratory Medicine, Clinical Chemistry and Pathobiochemistry, Charité Medical University Berlin, Augustenburger Platz 1, 13353 Berlin, Germany; veronique.blanchard@charite.de
5 ProBioGen AG, Goethestrasse 54, 13086 Berlin, Germany; christoph.giese@probiogen.de (C.G.); volker.sandig@probiogen.de (V.S.)
* Correspondence: hinderlich@beuth-hochschule.de; Tel.: +49-30-4504-3910

Academic Editor: Anthony Guiseppi-Elie
Received: 31 March 2017; Accepted: 24 April 2017; Published: 28 April 2017

Abstract: Xylose is a general component of *O*-glycans in mammals. Core-xylosylation of *N*-glycans is only found in plants and helminth. Consequently, xylosylated *N*-glycans cause immunological response in humans. We have used the F-protein of the human respiratory syncytial virus (RSV), one of the main causes of respiratory tract infection in infants and elderly, as a model protein for vaccination. The RSV-F protein was expressed in CHO-DG44 cells, which were further modified by co-expression of β1,2-xylosyltransferase from *Nicotiana tabacum*. Xylosylation of RSV-F *N*-glycans was shown by monosaccharide analysis and MALDI-TOF mass spectrometry. In immunogenic studies with a human artificial lymph node model, the engineered RSV-F protein revealed improved vaccination efficacy.

Keywords: CHO; glycoengineering; respiratory syncytial virus; vaccine; xylose

1. Introduction

Glycosylation is one of the most important post-translational modifications. Proteins can be decorated with glycans, which are linked either with asparagine residues via an *N*-glycosidic linkage (*N*-glycans) or with serine or threonine residues via an *O*-glycosidic linkage (*O*-glycans) [1]. The majority of *N*- and *O*-glycans consists of six different monosaccharides, namely mannose, galactose, *N*-acetylglucosamine (GlcNAc), *N*-acetylgalactosamine (GalNAc), fucose and sialic acids. Xylose is a rare monosaccharide component of *O*-glycans [2], and it is part of the linker between glycosaminoglycans and proteins [3]. Furthermore, pentose, together with glucuronic acid, is one of the two monosaccharide components of a heteropolymer linked to α-dystroglycan in muscle cells [4], where it mediates its interaction with the extracellular matrix component laminin. In *N*-glycans xylose is only found in plants and helminth [5,6]. There it is usually β1,2-linked to the central mannose residue of the *N*-glycan core.

For mammals, xylosylated *N*-glycans are alien structures. Parenteral introduction of glycoproteins carrying this kind of *N*-glycans into mammals therefore leads to strong immune reactions [5,7].

For the production of recombinant therapeutic glycoproteins in plant cells immunogenicity of the *N*-glycans is therefore an issue [7]. To date, plant cell lines used for recombinant glycoprotein productions are engineered by knock-out of the respective β1,2-xylosyltransferase [8,9]. However, the metabolic pathway for the synthesis of xylose and its activated nucleotide sugar UDP-xylose, respectively, is present also in mammalian cells [10]. UDP-xylose is synthesized from UDP-glucose in two steps; first by oxidation of the C-6 atom, resulting in UDP-glucuronic acid. The same C-6 atom is then decarboxylated, and the pentose xylose is generated, which is bound to UDP in the furanose form. UDP-xylose is then transported to the Golgi apparatus, where it serves as substrate for xylosyltransferases.

Altered glycans may increase or modulate the immunogenicity with potential benefits for recombinant glycoprotein vaccines [11,12]. Introduction of core β1,2-xylosylation is one promising approach [13]. In this study we have used a protein of the human respiratory syncytial virus (RSV) as a model vaccine. RSV is the main cause of lower respiratory tract infections in infants and the elderly, and also affects high-risk adults [14,15]. Although several strategies, including use of vaccines and therapeutic antibodies, have been tested for treatment of RSV infections in the last few decades, no highly efficient prevention therapy is presently available [16]. RSV vaccines based on recombinant proteins could benefit from the two major surface proteins RSV-F (fusion protein) and RSV-G (glycoprotein). In this study we used a truncated form of RSV-F, which only contains the extracellular part. RSV-F has five *N*-glycosylation sites, whereby two of them are released together with a 27 amino acid peptide by intracellular cleavage by the Golgi protease furin [17]. Mature RSV-F therefore consists of two disulfide-bridged polypeptide chains with *N*-glycans at the positions Asn-23, Asn-66 and Asn-497 [17–19]. The recombinant RSV-F protein was produced in glycoengineered CHO DG44 cells, co-expressing the β1,2-xylosyltransferase (XylT) from *Nicotiana tabacum*. We were able to show that RSV-F from glycoengineered cells contains xylosylated *N*-glycans, and that this recombinant vaccine, compared to RSV-F with non-xylosylated *N*-glycans, displays stronger immunogenicity in a human artificial lymph-node (HuALN) model.

2. Materials and Methods

2.1. Materials

CDC4 medium with 4.5 g/L glucose was obtained from ProBioGen AG, Berlin, Germany, Dulbecco's phosphate buffered saline (DPBS) from PAN-Biotech GmbH (Aidenbach, Germany), adenovirus expression medium (AEM) from Life Technologies GmbH (Darmstadt, Germany), fetal calf serum (FCS) superior from Merck Millipore (Darmstadt, Germany). Unless otherwise stated, all chemicals were purchased from Carl Roth GmbH + Co. KG (Karlsruhe, Germany) or Sigma-Aldrich GmbH (Taufkirchen, Germany).

2.2. Cell Culture

Standard cultivation of all cells was performed in CDC4 medium supplemented with 6 mM L-glutamine, 50 ng/mL IGF and 100 µg/mL penicillin/streptomycin (100 U/mL) within a 8% CO_2 atmosphere at 36.5 °C. Stably RSV-F-expressing CHO-DG44 cells and additional XylT expressing CHO-DG44 cells were cultivated under serum-free conditions in CDC4 medium supplemented with 6 mM L-glutamine, 1% penicillin/streptomycin (100 U/mL, 100 µg/mL) and insulin-like growth factor (50 ng/mL).

2.3. Construction of Expression Vectors

The RSV-F cDNA was constructed corresponding to Ternette et al. [20], with the exception that the signal sequence was replaced by the mellitin signal sequence (according to Acc. No. P01501; MKFLVNVALVFMVVYISYIY). It is followed by the ectodomain of the RSV-F protein (amino acids 26 to 530; according to Acc. No. EF566942), a Factor Xa cleavage site (IEGR), and a GSGS linker fused

to a 6xHis-tag (HHHHHH). The gene was codon optimized for *Cricetulus griseus* and synthesized with flanking EcoRI and BamHI restriction by Gene Art (Regensburg, Germany). The gene was cloned into the EcoRV restriction site of the vector pBGGPEX1 (ProBioGen AG, Berlin, Germany) by EcoRI/BamHI digestion, and followed by DNA polymerase Klenow (Roche, Mannheim, Germany) treatment resulting in the pBGGPEX1-RSV-F vector.

The gene of *Nicotiana tabacum* XylT (Acc. No. AJ627182) was synthetized by Gene Art (Regensburg, Germany) with a codon-optimized sequence for *Cricetulus griseus*, flanked by BglII/EcoRI restriction sites. The gene was cloned into the expression vector EF2flag neo (ProBioGen) using the BglII/EcoRI restriction sites resulting in the vector EF2flag XylT. Plasmids were prepared by the QIAprep® Spin Miniprep kit (Qiagen, Hilden, Germany) and EndoFree® Plasmid Maxi kit (Qiagen).

2.4. Transfection of CHO Cells

The CHO-DG44 cells were transfected with pBGGPEX1-RSV-F vector by electroporation using the Neon® Transfection system (Thermo Fisher, Schwerte, Germany). Selection of transfected has been carried out for 17 days in serum-free C8862 medium supplemented with puromycin and methotrexate (MTX). The resulting CHO RSV-F cells were additionally transfected with the EF2flag XylT vector by lipofection using the Freestyle Max Reagent (Thermo Fisher) in Optipro medium (Thermo Fisher). CHO-F-XylT clones were selected with Neomycin (G418). The expression of the RSV-F protein has been verified by western blot analysis using a Penta-His HRP antibody (Qiagen, 1:2000). The expression of the XylT was detected on the transcription level by RT-PCR with specific primers (forward 5′-GAGAACCACCACGACAAC-3′, reverse 5′-CTGTTCCTCGTTGGACAG-3′). The resulting PCR product of 1077 bp was visualized by agarose gel electrophoresis.

2.5. Protein Production

Serum free fed-batch culture of transfected CHO cells producing modified RSV-F protein was carried out in 50 mL bioreactor tubes containing CD-C4 growth medium supplemented with L-glutamine. Bioreactor tubes were inoculated at a starting cell density of 4×10^5 cells/mL and incubated at 146 rpm, 37 °C, 8% CO_2. Performance of the fed-batch cultures was monitored for 14 days and supernatant containing the RSV-F protein was harvested after declining of cell viability down to 75%. The supernatant was analyzed for RSV-F production by western blotting.

2.6. Purification of Proteins

RSV-F protein purification was performed by a one-step purification using a 5 mL Ni-NTA cartridge (Machery & Nagel, Düren, Germany). 250 mL of the sterile filtered supernatant from batch production was twice concentrated using an Amicon Filter device (300 mL) and diluted in binding/washing buffer (20 mM sodium phosphate, 0.5 M NaCl, 20 mM imidazole, pH 7). After equilibration of the column with 5 volumes binding buffer the sample was loaded and the column washed with 10 volumes of binding/washing buffer. Protein was eluted in one step by 5 mL elution buffer (20 mM sodium phosphate, 0.5 M NaCl, 500 mM imidazole, pH 7), dialysed against PBS, sterile filtered and stored at 4 °C. Protein concentration was quantified by BCA protein assay for total quantification and RSV-F proteins were analyzed by western blotting.

2.7. High-pH Anion-Exchange Chromatography with Pulsed Amperometric Detection (HPAEC-PAD) Monosaccharide Analysis

20 μg of purified proteins was hydrolyzed in 2 M trifluoroacetic acid (TFA) for 4 h at 100 °C. A blank sample was used as negative control. As internal standards 200 pmol 2-deoxy-D-ribose (DR), D-fructose (Fruc) and D-melibiose (Mel) (each from Sigma-Aldrich, Taufkirchen, Germany) were used. As external standards a set of monosaccharides, including 100 pmol L-fucose (Fuc), D-arabinose (Ara), D-galactosamine (GalN), D-galactose (Gal), D-glucosamine (GlcN), D-glucose (Glc), D-Xylose (Xyl) and D-Mannose (Man), was used and run prior to the protein samples. HPAEC-PAD was performed on

an ICS-3000 Ion Chromatography System (Thermo Fisher) using a Dionex CarboPac® PA200 column. Monosaccharides were separated by isocratic 2.25 mM NaOH elution while post-column addition of 200 mM NaOH provided the conditions for pulsed amperometric detection.

2.8. Release and Separation of N-Linked Glycans

Tryptic digestion was performed twice (for 4 h at 37 °C and overnight, respectively) using 2.5 μg trypsin (Sigma-Aldrich) per 30 μg of glycoprotein. After trypsin inactivation, samples were treated with 0.5 U of *N*-glycosidase F from Flavobacterium meningospeticum (Roche Diagnostics, Mannheim, Germany) and incubated at 37 °C. After 4 h additional enzyme was added, the sample was incubated overnight followed by inactivation (5 min, 95 °C). *N*-Glycans were separated from the peptide fraction using reversed-phase C18 cartridges and a subsequent desalting step on graphitized cartridges (Grace Davison Discovery Sciences, Worms, Germany) as described before [21]. Purified *N*-glycans were lyophilized and stored at −20 °C.

2.9. Permethylation and Matrix-Assisted Laser Desorption/Ionization Time-of-Flight (MALDI-TOF) Mass Spectrometry

Prior to mass spectrometric (MS) analysis, *N*-glycan samples were permethylated in order to stabilize sialic acids and to improve the efficiency of positive ion formation [22]. The derivatization procedure followed standard protocols of the solid sodium hydroxide technique [22,23] with minor modifications. Incubations were carried out under continuous shaking at room temperature. The iodomethane reaction was stopped by the addition of chloroform and subsequent washing steps with water until achieving a neutral pH of the aqueous phase.

For MALDI-TOF-MS analysis dried permethylated *N*-glycans were dissolved in 75% (v/v) acetonitrile in water and mixed with super-dihydroxybenzoic acid (sDHB) matrix (Sigma-Aldrich). Recording of mass spectra on an Ultraflex III MALDI-TOF/TOF spectrometer (Bruker Daltonik, Bremen, Germany) and subsequent data processing was realized as reported previously [24]. Structures were assigned to related peaks according to the Glycoworkbench 2.0 database, or constructed by the same software if not available. Fragmentation analysis was performed by the integrated Lift method of the mass spectrometer. Fragment sizes were compared to the theoretically determined size of the glycans using Glycoworkbench 2.0. Schematic representation of glycan structures are according to the symbol nomenclature of the Consortium for Functional Glycomics [25]: green circle, mannose; yellow circle, galactose; blue square, GlcNAc; yellow square, GalNAc; red triangle, fucose; purple diamond, *N*-acetylneuraminic acid; star, xylose.

2.10. Cytokine and Gene Expression Analysis

Stimulation experiments were performed in a HuALN (ProBioBen AG; [26,27]) In brief, RSV-F and RSV-F Xyl+ were cultivated in the presence of CD14(-) cells and mature dendritic cells prior to addition of PBMC and matrix. HuALN reactors were run for 28 days and re-stimulation took place at days 7, 14 and 21. Cell culture supernatants were taken daily and analyzed with a bead-based multiplexed immune assay (Luminex® technology, Thermo Fisher). A custom Bio-Plex® Express Aassay (Bio-Rad, München, Germany) was used to quantify the six analytes IL-2, IL-4, IL-10, GM-CSF, IFN-γ and TNF-α. The assay was performed in duplicates as described by the manufacturer, but conducted automated on a pipetting robot (Freedom Evo 200; Tecan, Crailsheim, Germany). Quantification of samples based on a logistic 5-point regression method using standard curves with 8 point 4-fold dilution series with analyte-specific concentration ranges. Error limits of data more than twice as much as the detection limit were below 20%.

To investigate the first response of the immunologic reaction comprehensively, gene expression was analyzed with a Human Immunology v2 nCounter® Gene Expression assay (NanoString® Technologies, Seattle, WA, USA) covering 579 immunology related genes. Therefore, PBMC of healthy donors were stimulated for 48 h with antigen-specific mDC and the according proteins, or were left

untreated (negative control). Total RNAs of cells were extracted with a High Pure RNA Isolation Kit (Roche Diagnostics). Concentration and purity of total RNAs were controlled with a Nanodrop 1000 (Thermo Fisher) using the spectral absorption quotients 260/230 and 260/280. RNA Quality Numbers (RQN) were determined on a Fragment Analyzer™ (Advanced Analytical Technologies, Heidelberg, Germany) with a DNF-472 High Sensitivity RNA Analysis Kit, using extended runtimes of 60 min per sample to be able to detect any remaining genomic DNA contaminations. The nCounter technology [28] is a multiplexed method that quantifies mRNA on single molecule level by using fluorescent barcoding probes and is described in detail in [29]. NanoString experiments were performed according to the manufacturer protocol. Due to slight fragmentation of RNA increased amounts of input material (150 ng) were used in the experiment. RNAs were quantified with Qubit® RNA HS AssayKit (Thermo Fisher), immediately before the nCounter experiment was conducted. The nSolver™ Analysis Software 3.0 (NanoString®) was used to perform data handling, including automated background subtraction, spike-in-control normalization and reference gene normalization. Furthermore, datasets from duplicates were grouped and fold change estimates were calculated by building ratios with the unstimulated negative control. Since analysis could be performed in duplicates only, somewhat higher p-values were accepted to keep data sets for broad immunologic parts descriptive.

3. Results and Discussion

3.1. Co-Expression of RSV-F and XylT in CHO DG44 Cells

For expression of the soluble version of RSV-F, the synthetic gene consisting of the extracellular domain of RSV-F equipped with the mellitin signal peptide and C-terminally linked with a factor X cleavage site followed by a hexa-His tag was cloned into the pBGGPEX1 vector and transfected into CHO DG44 cells. The melitin signal peptide is commonly used in insect cells but also functions well in mammalian cells (ProBioGen AG, unpublised). Transfectants were selected with puromycin and MTX and stable clones were generated. SDS-PAGE analysis of cell supernatant displayed a 72 kDa band, indicating successful production of the full-length RSV-F protein. Next, a codon-optimized cDNA of XylT was generated as an artificial gene and cloned into the E2Fflag vector. CHO DG44/RSV-F cells were transfected, selected with Neomycin (G418) and stable cell clones were isolated. Four of these clones were analyzed by RT-PCR for XylT mRNA, and by Western blot for RSV-F (Figure 1). All four clones revealed expression of XylT and maintained RSV-F protein expression, indicating successful co-expression of both proteins. RSV-F protein derived from these clones was labeled "RSV-F Xyl+".

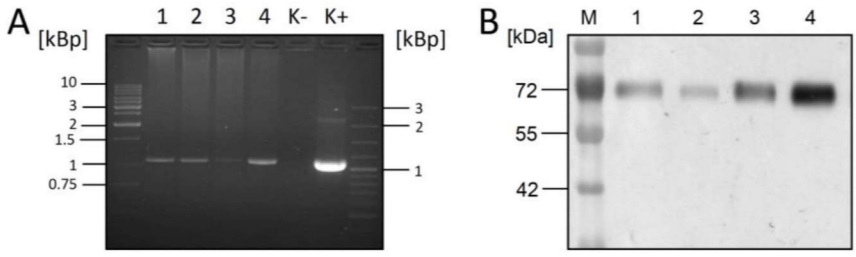

Figure 1. Detection of XylT mRNA and RSV-F-protein in four different CHO-XylT clones. (**A**) XylT mRNA was detected by RT-PCR. Clones 1–4 were compared to non-transfected CHO cells as negative control (K−), and the E2Fflag/XylT vector as RT-PCR template as positive control (K+); (**B**) Maintenance of RSV-F expression in clones 1–4 was verified by western blotting using anti-His antibody.

3.2. Monosaccharide Analysis

RSV-F and RSV-F Xyl+ were purified from cell culture supernatants by Ni-NTA affinity chromatography; 50 mL of supernatant resulted in about 11 mg of protein with a purity higher than 98%. 25 to 50 μg of protein was subjected to monosaccharide analysis by HPAEC-PAD. Samples were treated with strong acid hydrolysis, leading to the cleavage of acetyl groups from amino sugars,

and used for chromatographic separation of monosaccharides in the presence of standards (Figure 2). Chromatograms for RSV-F showed the typical monosaccharide composition of *N*-glycosylated proteins. Monosaccharides from RSV-F Xyl+ displayed a comparable composition, but an additional peak at about 34 min, which could clearly be assigned to xylose when comparing to standards. The peak at about 19 min in RSV-F and RSV-F Xyl+ samples might indicate the presence of GalN, in other words GalNAc before hydrolysis, which is a typical monosaccharide of O-glycosylation. Gruber and Levine [17] previously speculated about the presence of O-glycans in RSV proteins in 1985. However, there is no experimental proof for O-glycosylation of RSV-F to date. The peak for Glc, which is larger in the RSV-F Xyl+ sample compared to the RSV-F sample, does not really indicate O-glcosylation, suggesting more of a typical contamination in this kind of analysis. Finally, O-glycans contain only small amounts of xylose, which could not explain the amount of this monosaccharide found in RSV-F Xyl+ samples.

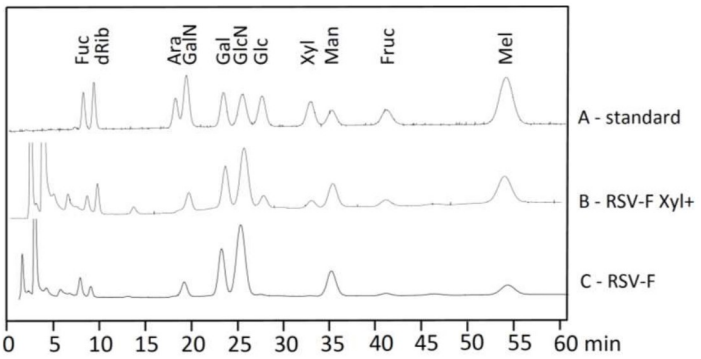

Figure 2. Monosaccharide composition of RSV-F glycans analyzed by HPAEC-PAD. Peaks were compared to standard monosaccharides (A). Xylose could only be found in RSV-F Xyl+ (B) and not in RSV-F (C).

3.3. Analysis of N-glycans of RSV-F Proteins

The *N*-glycans of both proteins were released by PNGase F, permethylated to allow detection of sialic acid, and analyzed by MALDI-TOF mass spectrometry (Figure 3). For RSV-F five biantennary, three triantennary and two tetraantennary complex *N*-glycans could be found. Most of the *N*-glycans are core-fucosylated and highly sialylated. This *N*-glycan pattern is typical for recombinant glycoproteins from CHO cells [30]. For RSV-F Xyl+ seven *N*-glycans of RSV-F could regained. Furthermore, eight new *N*-glycans could be identified, which carried an additional xylose residue. These data show that the xylose, which was found by monosaccharide analysis, is integrated into *N*-glycans by the action of heterologously expressed XylT. Quantification of *N*-glycans revealed that the biantennary xylosylated *N*-glycans are predominant compared to their non-xylosylated counterpart. On the other hand, reduction or disappearance of tri- and tetraantennary *N*-glycans could be observed. This might be due to strong activity of XylT in the medial Golgi, where branching of *N*-glycans is determined, and the respective GlcNAc transferases IV and V for the formation of the third and fourth antenna [31] have reduced activity by competing with XylT.

MALDI-TOF analyses (Figure 3) suggest the incorporation of xylose in the *N*-glycans isolated from RSV-F Xyl+. We therefore performed fragmentation analysis to confirm and localize the presence of xylose by comparing the peak m/z 3127.1 with its non-xylosylated counterpart m/z 2966.9 (Figure 4). The spectrum of the latter shows characteristic fragment ions of a biantennary complex *N*-glycan. The fragmentation pattern of the xylosylated *N*-glycan m/z 3127.1 reveals an additional mass of 160 Da of all fragments containing the core mannoses, correlating to the mass of an additional xylose moiety. These data indicate that xylose is bound to the central core mannose, and most likely in a β1,2-linkage, as it is catalyzed by *Nicotiana tabacum* XylT in its original target organism. Similar fragment patterns were obtained for peaks m/z 2765.8 vs. non-xylosylated m/z 2605.7 and

peaks m/z 2404.6 vs. non-xylosylated m/z 2244.5 (data not shown). Taken together, we have shown that heterologous expression of *Nicotiana tabacum* XylT results in formation of xylosylated complex *N*-glycans in CHO cells. We have detected also sialylated and triantennary *N*-glycans which does not occur in plants [6], with a core xylose. The action of XylT in CHO cells is therefore independent from the *N*-glycan structure.

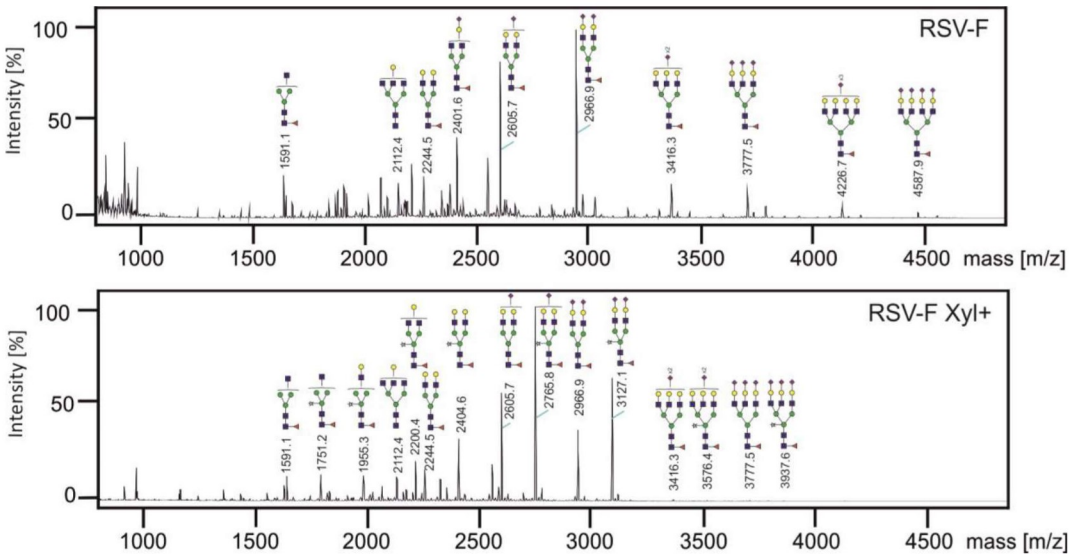

Figure 3. Mass spectrometric analysis of RSV-F *N*-glycans. *N*-glycans were prepared from RSV-F (upper panel) and RSV-F Xyl+ (lower panel), permethylated and analyzed by MALDI-TOF-MS. Structures were assigned to related peaks; xylosylated structures, which are not found in the database, have been constructed using Glycoworkbench 2.0.

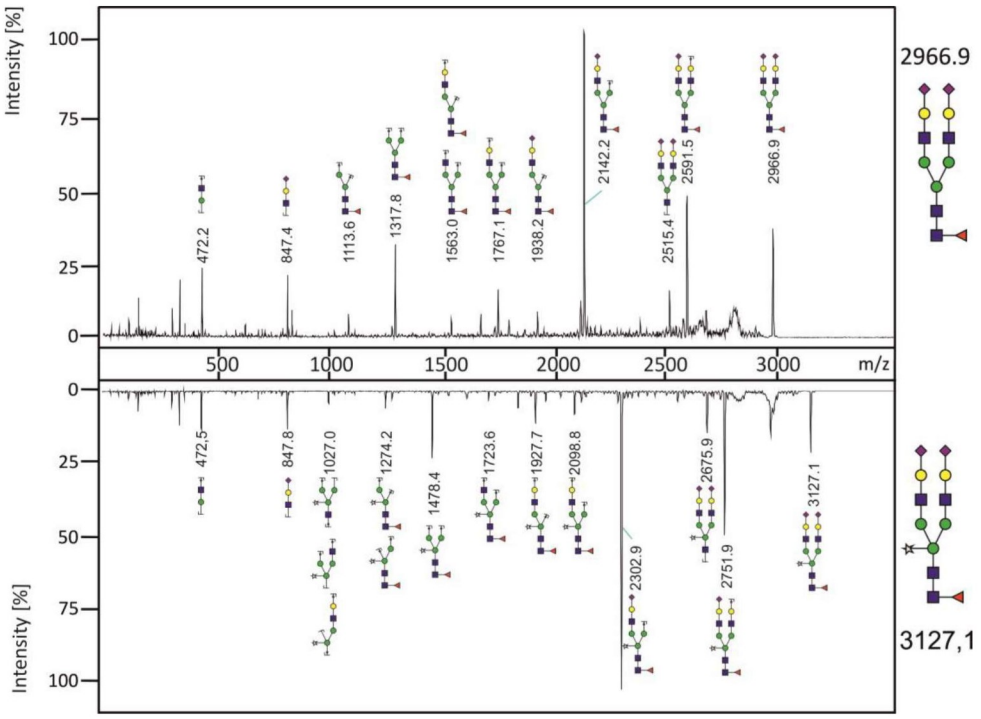

Figure 4. Fragmentation analysis of permethylated *N*-glycans. Fragments were obtained from the peaks m/z 2966.9 (RSV-F) and m/z 3127.1 (RSV-F Xyl+). Note the diagnostic mass differences of 160.1 Da for xylose.

3.4. Stimulation of Immune Cells with RSV-F Proteins

In order to investigate potential immune activation of RSV-F proteins, HuALN reactors were run in the presence of RSV-F and RSV-F Xyl+. Cytokine concentrations were detected in the collected cell culture supernatants with Bio-Plex Express Kits using an automated liquid handling robot (Figure 5). Cytokine expression of the immune cells clearly responded to the time-points of (re-)stimulation in both experiments. In general, cytokine secretion is stronger or more accentuated by cells stimulated with RSV-F Xyl+. IFN-γ levels are substantially high, and twice as high after restimulation. TNF-α concentration peaks after restimulation before returning to a basic level, leading to an overall strong pro-inflammatory response. This is in concordance with the lower level of anti-inflammatory IL-10 (603, 27, 11 and 38 pg/mL, respectively, at days after (re-)stimulation), compared to RSV-F (1342, 140, 184 and 114 pg/mL, respectively). Taken together, these data demonstrate a strong activation of Th1 cells. Besides the inhibiting effect of IL-10 on Th1 cytokines it enhances B-cell survival, proliferation and antibody production. In connection with IL-4, which is more strongly provoked by RSV-F Xyl+ (concentrations are 2.0-fold, 3.1-fold and 8.1-fold higher at days of restimulation), there is evidence for a potent Th2 and humoral response as well. IL-2 levels induced by stimulation with xylosylated RSV-F are continuously present in the first two weeks. However, IL-2 levels are relatively low for both vaccines, compared to studies with other stimulants [32]. Finally, GM-CSF peaks are higher (e.g., 6.9 fold and 9.0 fold higher at day 22 and 23) in the days after restimulation for cells treated with RSV-F Xyl+, indicating an enhancing effect on the cellular response and adaptive immunity, since monocytes can mature into dendritic cells.

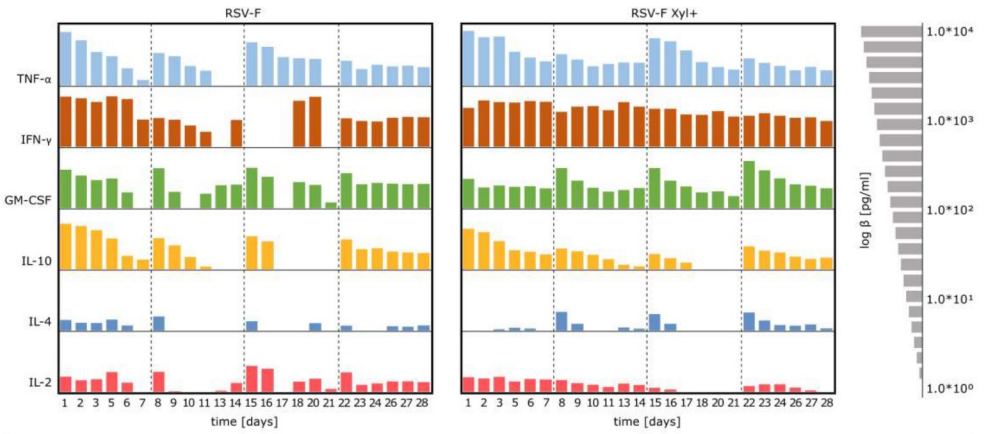

Figure 5. Cytokine secretion pattern in cell culture supernatants of long-term stimulation experiments. PBMCs were stimulated with RSV-F Xyl+ (right) and wildtype RSV-F protein (left) and the according antigen-specific mDC. Concentrations are log10 transformed. (Re-)stimulation took place at day 0, 7, 14 and 21 (dotted line). Supernatants were collected on a daily basis (exceptions at day 4, 12 and 19).

In addition to the long-term cultivation in the HuALN reactors, stimulation experiments were conducted to investigate the immunologic first response in high detail on genetic level. PBMCs were stimulated with the vaccine candidates and the respective mDC for 48 h in duplicates. mRNAs were extracted from harvested cells. Concentrations between 16.8 and 42.2 ng/µL, and sufficient purity were obtained, with exception of one sample. Slightly increased concentrations of input material were therefore used in nCounter experiments. The automatic quality control within the nSolver Software was passed by all samples. Due to their high coefficient of variation (>75%) within the analyzed samples GAPDH, OAZ1 and TUBB were excluded from the panel of used reference genes.

Gene expression ratios for cells stimulated with RSV-F and RSV-F Xyl+ were based on calculating fold changes compared to negative control. Within the clusters of functionally ordered genes, which are related to the activation of the different T-cell populations, the key cytokines are significantly

more activated by RSV-F Xyl+ (Figure 6). More precisely, IL-2 is expressed in much higher amounts within the Th1 subset, IL-4 and IL-5 are strongly upregulated in the Th2 subset and IL-17-related genes are upregulated in the TH17 subset, while the same genes are down-regulated by RSV-F treatment. However, the genes of the related STAT signaling pathways (STAT1, STAT3, STAT4, STAT6) are mostly unaffected at the analyzed time-point, as well as genes of T-cell (CD40, CD44) and DC (CD80, CD83 and CD86) activation. Overall concentrations of Th1, Th2 and Th17 key cytokines were relatively low. Probably, these cytokines are mostly bound to their respective receptors. The expression of those receptors (e.g., IL2RA and B, IL4R) is slightly downregulated. This might indicate a sufficient activation, which is already mitigated (weakened) by decreased receptor expression. Furthermore, gene expression of pro-inflammatory IFNγ and TNF is relatively low, but strong IL17 up-regulation works synergistically to these two cytokines [33].

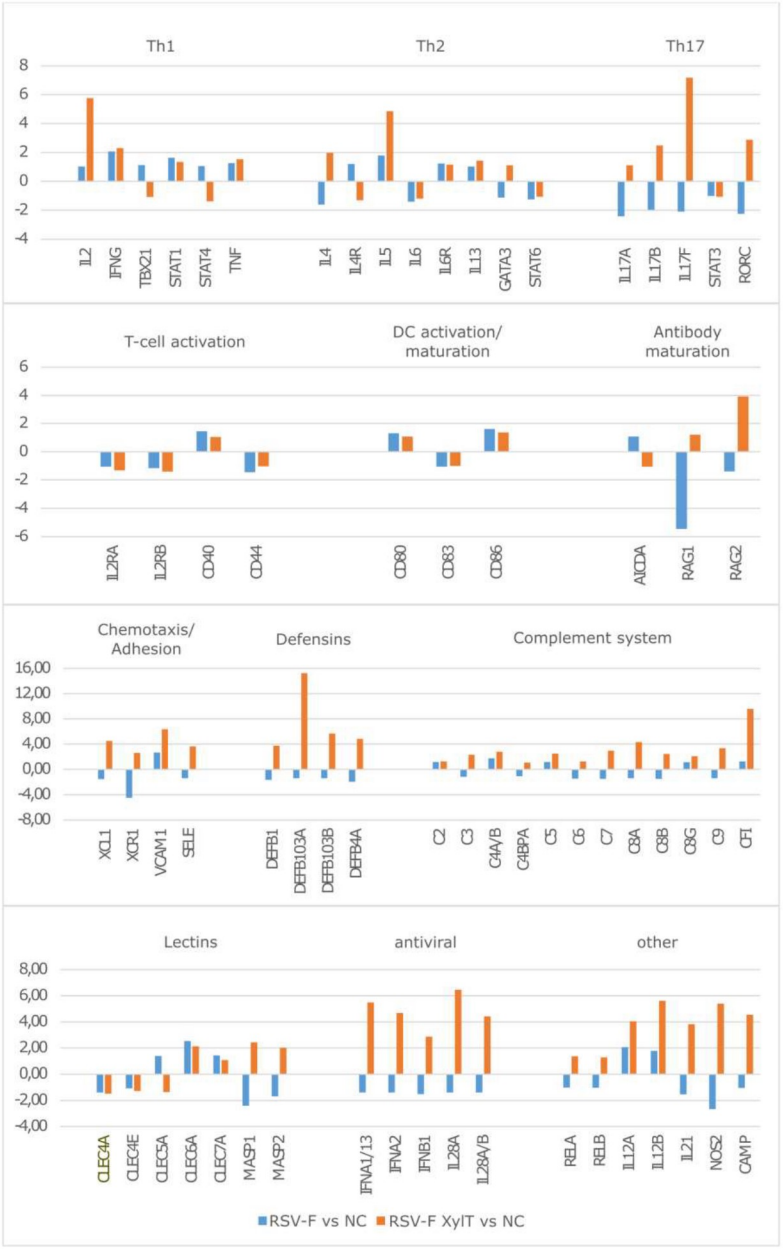

Figure 6. Gene expression ratios of PBMC stimulated for 48 h with RSV-F and RSV-F Xyl+ and maturated DC. Log2-fold changes are shown. NC—negative control without RSV-F treatment.

Genes related to antibody maturation show diverse regulation pattern: while the expression of AICDA—a key player in somatic hypermutation and immune globulin class switch—is not significantly altered, RAG 1 and RAG2 (Recombination Activation Genes 1 and 2) are upregulated by stimulation with RSV-F Xyl+, indicating the onset of antibody maturation, but downregulated by RSV-F treatment. Next to the activation of cellular and humoral components by RSV-F Xyl+, we recognized the activation of entire components of the innate immune systems, like defensins or the complement system. The latter one seems to be activated via the lectin pathway by the mannose binding lectins, MASP1 and MASP2. The role of C-type lectin receptors in activation of murine DC by stimulation with core β1,2-xylosylated glycoprotein was investigated by Brzezicka et al. [34]. They report enhanced uptake, presentation and subsequent T-cell activation by artificially glycosylated ovalbumin; however, xylosylated glycans did not significantly enhance the activation potential in this experimental setup. In our experiments the broad activation of antimicrobial defensins and complement system is complemented by the activation of genes with antiviral functions like IFNα, IFNβ or IL28. Thus, RSV-F Xyl+ seem to initiate a general activation of the immune system while RSV-F does not. Expression patterns of RELA and RELB, which are parts of the NFκB complex, as well as the proinflammatory factors NOS2, CAMP (coding for the multifunctional Cathelicidin Antimicrobial Peptide) or IL21 underline the immune activation by RSV-F Xyl+.

4. Conclusions

In this study we successfully glyco-engineered CHO cells for the production of xylosylated *N*-glycans. *Nicotiana tabacum* XylT was functionally expressed in a mammalian cell system, where it was localized in the correct Golgi compartment, had access to endogenous UDP-xylose and could transfer xylose to the *N*-glycan core of a recombinant, co-expressed viral glycoprotein. We were able to show that xylosylated *N*-glycans had strong adjuvant effects in a well-established human organoid immune model, indicating the usefulness of this approach for in vivo models and for vaccination strategies in general. Furthermore, glyco-engineering of CHO cells by the methodology presented here could be extended to other glycan structures with antigenic and therefore adjuvant potency—for example, α1,3-linked core-fucose natively occurring in plant and insect *N*-glycans [5,6,13], or the non-human sialic acid *N*-glycolylneuraminic acid [35].

Acknowledgments: This research was supported by the Bundesministerium für Bildung und Forschung (BMBF) within the program "Forschung an Fachhochschulen". The authors want to thank Detlef Grunow (Charité Medical University Berlin) for excellent technical and practical assistance concerning the mass spectrometry and HPAEC-PAD analyses.

Author Contributions: G.S., H.H.v.H, V.S., M.F. and S.H. conceived and designed the experiments; G.S., L.R. and C.G. performed the experiments; all authors analyzed the data; V.B. contributed analysis tools; G.S., L.R. and S.H. wrote the paper.

Conflicts of Interest: C.G. and V.S. are employees of ProBioGen AG, the developer and owner of the HuALN technology. The founding sponsors had no role in the design of the study; in the collection, analyses, or interpretation of data; in the writing of the manuscript, and in the decision to publish the results.

References

1. Varki, A. Biological roles of oligosaccharides: All of the theories are correct. *Glycobiology* **1993**, *3*, 97–130. [CrossRef] [PubMed]
2. Brockhausen, I.; Schachter, H.; Stanley, P. O-GalNAc Glycans. In *Essentials of Glycobiology*, 2nd ed.; Varki, A., Ed.; Cold Spring Harbor Laboratory Press: Cold Spring Harbor, NY, USA, 2009; Chapter 9.
3. Götting, C.; Kuhn, J.; Kleesiek, K. Human xylosyltransferases in health and disease. *Cell. Mol. Life Sci.* **2007**, *64*, 1498–1517. [CrossRef] [PubMed]
4. Inamori, K.; Yoshida-Moriguchi, T.; Hara, Y.; Anderson, M.E.; Yu, L.; Campbell, K.P. Dystroglycan function requires xylosyl- and glucuronyltransferase activities of LARGE. *Science* **2012**, *335*, 93–96. [CrossRef] [PubMed]

5. Altmann, F. The role of protein glycosylation in allergy. *Int. Arch. Allergy Immunol.* **2007**, *142*, 99–115. [CrossRef] [PubMed]
6. Strasser, R. Plant protein glycosylation. *Glycobiology* **2016**, *26*, 926–939. [CrossRef] [PubMed]
7. Yao, J.; Weng, Y.; Dickey, A.; Wang, K.Y. Plants as Factories for Human Pharmaceuticals: Applications and Challenges. *Int. J. Mol. Sci.* **2015**, *16*, 28549–28565. [CrossRef] [PubMed]
8. Strasser, R.; Altmann, F.; Mach, L.; Glössl, J.; Steinkellner, H. Generation of Arabidopsis thaliana plants with complex *N*-glycans lacking beta1,2-linked xylose and core alpha1,3-linked fucose. *FEBS Lett.* **2004**, *561*, 132–136. [CrossRef]
9. Castilho, A.; Steinkellner, H. Glyco-engineering in plants to produce human-like N-glycan structures. *Biotechnol. J.* **2012**, *7*, 1088–1098. [CrossRef] [PubMed]
10. Bakker, H.; Oka, T.; Ashikov, A.; Yadav, A.; Berger, M.; Rana, N.A.; Bai, X.; Jigami, Y.; Haltiwanger, R.S.; Esko, J.D.; et al. Functional UDP-xylose transport across the endoplasmic reticulum/Golgi membrane in a Chinese hamster ovary cell mutant defective in UDP-xylose Synthase. *J. Biol. Chem.* **2009**, *284*, 2576–2583. [CrossRef] [PubMed]
11. Gornik, O.; Pavić, T.; Lauc, G. Alternative glycosylation modulates function of IgG and other proteins—Implications on evolution and disease. *Biochim. Biophys. Acta* **2012**, *1820*, 1318–1326. [CrossRef] [PubMed]
12. Nishat, S.; Andreana, P.R. Entirely Carbohydrate-Based Vaccines: An Emerging Field for Specific and Selective Immune Responses. *Vaccines (Basel)* **2016**, *4*, E19. [CrossRef]
13. Brzezicka, K.; Echeverria, B.; Serna, S.; van Diepen, A.; Hokke, C.H.; Reichardt, N.C. Synthesis and microarray-assisted binding studies of core xylose and fucose containing *N*-glycans. *ACS Chem. Biol.* **2015**, *10*, 1290–1302. [CrossRef] [PubMed]
14. Glezen, W.P.; Taber, L.H.; Frank, A.L.; Kasel, J.A. Risk of primary infection and reinfection with respiratory syncytial virus. *Am. J. Dis. Child.* **1986**, *140*, 543–546. [CrossRef] [PubMed]
15. Thorburn, K. Pre-existing disease is associated with a significantly higher risk of death in severe respiratory syncytial virus infection. *Arch. Dis. Child.* **2009**, *94*, 99–103. [CrossRef] [PubMed]
16. Anderson, L.J.; Dormitzer, P.R.; Nokes, D.J.; Rappuoli, R.; Roca, A.; Graham, B.S. Strategic priorities for respiratory syncytial virus (RSV) vaccine development. *Vaccine* **2013**, *31* (Suppl. 2), B209–B215. [CrossRef] [PubMed]
17. Gruber, C.; Levine, S. Respiratory syncytial virus polypeptides. IV. The oligosaccharides of the glycoproteins. *J. Gen. Virol.* **1985**, *66*, 417–432. [CrossRef] [PubMed]
18. Scheid, A.; Choppin, P.W. Two disulfide-linked polypeptide chains constitute the active F protein of paramyxoviruses. *Virology* **1977**, *80*, 54–66. [CrossRef]
19. Arumugham, R.G.; Hildreth, S.W.; Paradiso, P.R. Interprotein disulfide bonding between F and G glycoproteins of human respiratory syncytial virus. *Arch. Virol.* **1989**, *105*, 65–79. [CrossRef]
20. Ternette, N.; Tippler, B.; Uberla, K.; Grunwald, T. Immunogenicity and efficacy of codon optimized DNA vaccines encoding the F-protein of respiratory syncytial virus. *Vaccine* **2007**, *25*, 7271–7279. [CrossRef] [PubMed]
21. Reinke, S.O.; Bayer, M.; Berger, M.; Blanchard, V.; Hinderlich, S. Analysis of cell surface N-glycosylation of the human embryonic kidney 293t cell line. *J. Carbohydr. Chem.* **2011**, *30*, 218–232. [CrossRef]
22. Wada, Y.; Azadi, P.; Costello, C.E.; Dell, A.; Dwek, R.A.; Geyer, H.; Geyer, R.; Kakehi, K.; Karlsson, N.G.; Kato, K.; et al. Comparison of the methods for profiling glycoprotein glycans—HUPO Human Disease Glycomics/Proteome Initiative multi-institutional study. *Glycobiology* **2007**, *17*, 411–422. [CrossRef] [PubMed]
23. Dell, A.; Khoo, K.H.; Panico, M.; McDowell, R.A.; Etienne, A.T.; Reason, A.J.; Morris, H.R. FAB-MS and ES-MS of glycoproteins. In *Glycobiology: A Practical Approach*; Fukuda, M., Kobata, A., Eds.; IRL Press at Oxford University Press: Oxford, UK, 1993; pp. 187–222.
24. Frisch, E.; Kaup, M.; Egerer, K.; Weimann, A.; Tauber, R.; Berger, M.; Blanchard, V. Profiling of endo H-released serum *N*-glycans using CE-LIF and MALDI-TOF-MS–application to rheumatoid arthritis. *Electrophoresis* **2011**, *32*, 3510–3515. [CrossRef] [PubMed]
25. Varki, A.; Cummings, R.D.; Esko, J.D.; Freeze, H.H.; Stanley, P.; Marth, J.D.; Bertozzi, C.R.; Hart, G.W.; Etzler, M.E. Symbol nomenclature for glycan representation. *Proteomics* **2009**, *9*, 5398–5399. [CrossRef] [PubMed]

26. Giese, C.; Lubitz, A.; Demmler, C.D.; Reuschel, J.; Bergner, K.; Marx, U. Immunological substance testing on human lymphatic micro-organoids in vitro. *J. Biotechnol.* **2010**, *148*, 38–45. [CrossRef] [PubMed]
27. Seifert, M.; Lubitz, A.; Trommer, J.; Könnig, D.; Korus, G.; Marx, U.; Volk, H.D.; Duda, G.; Kasper, G.; Lehmann, K.; et al. Crosstalk between immune cells and mesenchymal stromal cells in a 3D bioreactor system. *Int. J. Artif. Organs* **2012**, *35*, 986–995. [CrossRef]
28. Geiss, G.K.; Bumgarner, R.E.; Birditt, B.; Dahl, T.; Dowidar, N.; Fell, H.P.; Dunaway, D.L.; Ferree, S.; George, R.D.; Grogan, T.; et al. Direct multiplexed measurement of gene expression with color-coded probe pairs. *Nat. Biotechnol.* **2008**, *26*, 317–325. [CrossRef] [PubMed]
29. Radke, L.; Giese, C.; Lubitz, A.; Hinderlich, S.; Sandig, G.; Hummel, M.; Frohme, M. Reference gene stability in peripheral blood mononuclear cells determined by qPCR and NanoString. *Microchim. Acta* **2014**, *181*, 1733–1742. [CrossRef]
30. Esko, J.D.; Stanley, P. Glycosylation Mutants of Cultured Cells. In *Essentials of Glycobiology*, 2nd ed.; Varki, A., Ed.; Cold Spring Harbor Laboratory Press: Cold Spring Harbor, NY, USA, 2009; Chapter 46.
31. Stanley, P.; Schachter, H.; Taniguchi, N. *N*-Glycans. In *Essentials of Glycobiology*, 2nd ed.; Varki, A., Ed.; Cold Spring Harbor Laboratory Press: Cold Spring Harbor, NY, USA, 2009; Chapter 8.
32. Radke, L.; Lopez-Hemmerling, D.A.; Lubitz, A.; Giese, C.; Frohme, M. Induced cytokine response of human PMBC-cultures: Correlation of gene expression and secretion profiling and the effect of cryopreservation. *Cell Immunol.* **2012**, *272*, 144–153. [CrossRef] [PubMed]
33. Gabr, M.A.; Jung, L.; Helbling, A.R.; Sinclair, S.M.; Allen, K.D.; Shamji, M.F.; Richardson, W.J.; Fitch, R.D.; Setton, L.A.; Chen, L. Interleukin-17 synergizes with IFNγ or TNFα to promote inflammatory mediator release and intercellular adhesion molecule-1 (ICAM-1) expression in human intervertebral disc cells. *J. Orthop. Res.* **2011**, *29*, 1–7. [CrossRef] [PubMed]
34. Brzezicka, K.; Vogel, V.; Serna, S.; Johannssen, T.; Lepenies, B.; Reichardt, N.C. Influence of Core β-1,2-Xylosylation on Glycoprotein Recognition by Murine C-type Lectin Receptors and Its Impact on Dendritic Cell Targeting. *ACS Chem. Biol.* **2016**, *11*, 2347–2356. [CrossRef] [PubMed]
35. Ghaderi, D.; Taylor, R.E.; Padler-Karavani, V.; Diaz, S.; Varki, A. Implications of the presence of *N*-glycolylneuraminic acid in recombinant therapeutic glycoproteins. *Nat. Biotechnol.* **2010**, *28*, 863–867. [CrossRef] [PubMed]

Materials Science Forum
ISSN: 1662-9760, Vol. 879, pp 236-243
doi:10.4028/www.scientific.net/MSF.879.236

Miniaturized Flow-Through Bioreactor for Processing and Testing in Pharmacology

Andrea Böhme[1,3 *], Lars Radke[2,4], Felix Schütze[1,3], Sylvio Schneider[1,3], Thilo Liebscher[1,3], Sabine Sauer[1], Loredana Santo[3], Fabrizio Quadrini[3], Michael Hummel[4], Christoph Giese[5], Marcus Frohme[2], Andreas Foitzik[1]

Technical University of Applied Sciences Wildau, Hochschulring 1, 15745 Wildau, Germany
[1] Institute for Materials, Product Development and Production (iMEP)
[2] Laboratory for Molecular Biotechnology and Functional Genomics

[3] University of Rome 'Tor Vergata', Department of Mechanical Engineering
Via del Politecnico 1, 00133 Roma, Italy

[4] Charité - Universitätsmedizin Berlin (CVK), Institute of Pathology
Augustenburger Platz 1, 13353 Berlin, Germany

[5] ProBioGen AG, Berlin, Goethestrasse 54, 13086 Berlin, Germany

Keywords: Miniaturization, Perfusion, Bioreactor, Tightness Testing, Pharmacology

Abstract Conventional Bioreactor systems for cultivating cells in Life Science have been widely used for decades. An in vitro cell cultivation bioreactor should reliably and reproducibly mimic the in vivo microenvironment of the cultured cells. Normally, mammalian cell cultures are performed in conventional bioreactor devices such as culture flasks and culture-dishes. However, these tools have fundamental limitations due to being inappropriate for high throughput screening and consume a considerable amount of resources and time [1]. Therefore, there is a trend towards miniaturization, disposables and even micro platforms that fulfill increasing demands strongly aiming for production and testing of novel pharmaceutical products. Here we present the development and manufacture of a disposable miniaturized flow-through bioreactor system that can be produced in large numbers at low costs.

Nano-porous hollow fibers are located at the fluidic sources and drains of the miniaturized bioreactors and retain cells. The necessary mixture of oxygen and carbon dioxide is provided via diffusion through a semi-permeable membrane. Fluidic connections allow the continuous feeding of the cells adding nutrient solution at constant rates at the inlet of the micro bioreactor and removing the solution at the same rate at the outlet. This medium can be collected and used for subsequent analysis. Different designs and concepts for such bioreactors were carried out with varying numbers of plates, and integrated or joined miniaturized reactor chambers. First tests show full technical and biological functionality, cells could successfully be cultivated at high viability rates for some days.

Introduction

Conventional cell cultivation is performed in culture flasks or culture dishes. These devices do not provide the required throughput e.g. in pharmacological screening experiments. Thus, downscaling and parallelization of experiments into multiwell plates are standard but only applicable for batch cultivations with limited complexity. However, miniaturized bioreactors allow a relative high throughput and parallelization as well as low power consumption, portability, reduced space requirements and utilize smaller volumes of reagents and samples. Consequently, this makes it cheaper to manage and manipulate small populations of cells and to study their behavior in greater detail [2].

The issue to test immunogenicity is at historical high due to the recent rapid introduction of biopharmaceuticals, vaccines and adjuvants, nanostructured drug delivery, cell therapies, implants or biomaterials [3]. Besides, the phylogenetic distance between laboratory animals and humans is

considerable [4]. How limited the predictive value for substance testing in animals is became obvious by the TGN 1412 disaster in 2006 [5]. Additionally, in order to reduce and to replace animal testing several – mostly two-dimensional – in vitro testing systems are developed (comprehensively reviewed by Giese and Marx [3]). For example Warren et al developed a T- and B-cell co-culture system – a so called artificial immune system - in order to test drugs or vaccines [6]. However, like in every two dimensional approach, tissue organization is lost, cell morphology is altered and complex communication between different cell types is restricted. Three-dimensional, organoid test systems, however, have organ specific functions and are ideal for cell and molecular analysis of pharmaceutical, cosmetic and chemical substances [7, 8]. A prime example is the human artificial lymph node reactor, developed by the ProBioGen AG [9].

To perform immunologic tests in a miniaturized reactor and represent an adequate portion of the human immunologic repertoire at the same time, the concentration of human lymphocytes has to be relatively high. Thus, a frequent to constant medium exchange is necessary leading inevitable to the use of perfusion reactors. This type of reactor allows optimal and largely constant cultivation conditions over the entire term, which can be up to several months.

To predict the immunologic or toxicological effect of substances in preclinical in vitro tests the recreation of the physical and biological environment of the cells or tissues is the major challenge of in vitro cell cultivation nowadays

Next to the high biological requirements on such systems, the technical requirements are challenging as well. Mammalian cell cultures have to be kept safely for weeks ensuring safe production or testing. The polymeric material has to be biocompatible, thermally stable, easy to machine, transparent as well as resistant to sterilization by means of hard gamma-ray radiation. Major efforts will be necessary for joining techniques ensuring fluidic density of the single reactors as well as the whole reactor system.

We here describe the development of a miniaturized perfusion bioreactor as test system with inline analytics. Its core feature is the modular composition of parallel reaction chambers, which function as multi-purpose cultivation system. It is applicable for 2D and matrix-based 3D cell cultivation and can be operated as batch, fed batch or perfusion reactor. Fundamental quantities to be measured like pH or glucose concentration can be monitored. Due to the use of transparent materials cells within the reactor can be examined via microscopy. At the same time it is easy to handle and can be produced simply and at very low costs.

The reaction chamber itself leaves space for modifications and can be structured more complex. We started to incorporate a micro-electromechanical glucose sensor that operates via the competitive binding of glucose and dextran to Concanavalin A [10].

Within the recursive design and fabrication process we developed an innovative method to examine the tightness of the manufactured bioreactors using fluorescence-microscopy and cyanobacteria. Furthermore, each used material or component of the reactor was screened for its biocompatibility and cell viability assays were performed to check the longtime influence on cultured cells. First tests show full technical and biological functionality. Mice fibroblasts could successfully be cultivated at high viability rates for several days. Furthermore, to demonstrate the applicability for pharmaceutical tests within the reactor, human PBMC were cultured in a more complex 3D collagen matrix.

Culturing cells and organoids in such miniaturized bioreactors are a promising technology for applications in the pharmaceutical industry allowing for high through-put screening with very low amount of tissue, reducing the need for animal testing and opening new doors for personalized medicine.

Methods

Design and Production. For the optimization of design, manufacturing, tightness and handling of the miniaturized perfusion reactors a recursive strategy is necessary. The general manufacturing can be outlined as follows:

The miniaturized in vitro bioreactor was drafted using a computer-aided design (CAD) software (Cimatron E12). The designs were subsequently transferred with the help of a CNC-tool of the same software for fabrication of the reactor compartments on a three-axis micro milling machine (Kern Micro, Kern, Eschenlohe, Germany). The fabricated components were assembled using connection technology, in short: cultivation chambers (7 x 9 x 3 mm) were milled into polycarbonate blocks (PC, 25 mm in height and 4 mm thick). Holes for the hollow fibers, ports and channels were drilled into the PC blocks. Hollow fibers (Accurel® PP 50/200, polypropylene, Membrana GmbH, Germany) were placed into the lateral channels and fixed with adhesive (Acrifix 192, Evonik, Essen, Germany) as well as the fittings, connections for tubes, providing the media using Dichloromethane. The inoculation port is closed with a conical plug. The gas-permeable membrane (bioFOLIE, 25 µm, polyethylene, Greiner Thermanox) is mounted to the backside of the polystyrene slide by application of a layer of transfer glue (9474LE, 3M, Hamburg, Germany).

Microreactor slides are sterilized by flushing them with 70% (v/v) 2-propanol. In addition, after dry up of the slides (50 °C, 12 hours) they are exposed to UV light for at least one hour.

Leakage tightness test. For a later use of the microreactors as a perfusion culture system it is crucial that cells are retained in the cultivation chamber. In order to ensure the tightness of the fabricated microreactors a microscopic leakage test with fluorescent cyanobacteria (chlorophyll A, excitation 435/40 nm; emission 515 nm LP) was established:

Hollow fibers and connections were filled with BG-11 media and 200 µl viable cyanobacteria (*Synechocystis sp*. PCC 6803; approx. 5x10^7 cells/ml) were inoculated in the reaction chamber. A computer controlled micropump (Diluter 4x, Gesim, Großerkmannsdorf, Germany) was connected with a flexible tube to one connector. In the first experimental set-up all remaining connectors were sealed to test the overall tightness of the reactor. Media was pumped into the reactor until the gas-permeable membrane was tightly stretched. Resulting leakages were detected by naked eye or by microscopy. In a second experimental set-up the connection of the micropump was varied and all connectors were sealed apart from the diagonally positioned. Thus a crossflow was achieved as intended in the later use. Flow rates were varied within a range of 2 µl/min up to 2 ml/min. Flow-through fluids were collected and examined for any contaminating cyanobacteria. With the same setup cloaking of the connectors could be detected as caused by some of the tested adhesives.

Cytotoxicity test of adhesives and components. As a testing device in immunologic experiments any bias or cytotoxic side effects caused by components of the reactor itself had to be ruled out.

Cytotoxicity test were performed in increasing stringency. In the first step L929 cells were seeded in 12 well cell culture plates with different small amounts of candidate adhesives being placed in the center. Overall growth of cells (time to reach confluence) and the growth in direct contact to the adhesive was compared to control wells. In the next step cell viability was determined by a live/dead staining using 1 µl SYTO® 9 (stock solution 3.34 mM in DMSO) and 2 µl propidium iodide (stock solution: 20 mM in DMSO) (both part of LIVE/DEAD® BacLight Bacterial Viability Kit, Invitrogen).

Heating system. An external heating source has been developed to temper the microreactor, consisting of a power MOSFET, which converts electric power into thermal heat, and an aluminium heat spreader, which distributes the heat energy over the bioreactors surface. A NTC (Negative Temperature Coefficient)-thermistor is placed outside of the bioreactor chamber to measure the temperature. A position outside of the reaction chamber was chosen to reduce the risk of contamination. The control and regulation technology is implemented in LabView (National Instruments, USA) and is able to monitor each cultivation chamber individually and to maintain a certain temperature using a simple PID (proportional–integral–derivative) algorithm.

Glucose sensor. The monitoring of glucose can be realized by a micro-mechanical device which was developed by the Institute for High Performances (Frankfurt/Oder, Germany). In dependency

of the glucose concentration the viscosity of a polymeric matrix (containing dextran and Concanavalin A) changes, damping the yielding of a cantilever into this matrix. The glucose sensor is placed in an especially drilled hole and has contact to the medium via a small window. For more information a related article "Affinity viscosimetry sensor for enzyme free detection of glucose in a micro-bioreaction chamber" by Liebscher et al is published in this issue.

Function test in a cultivation system using L929 fibroblast. We set up an autonomous cultivation system to demonstrate the functionality, the stability as well as the versatile applicability of the modular microreactor. Therefore, two reactor slides (with 3 cultivation chambers each) were connected to the heating system, placed altogether in a gastight housing, which was flooded with 5% CO_2 and connected to a pump (Symax Spetec, Erding, Germany) for exchange of the medium (twice a day, 100 µl/h). Since PBMC of healthy donors are normally in a resting state until activation, L929 cells (mice fibroblast) were cultivated to be able to compare growth rates as a simple viability marker. 10,000 cells were seeded into each chamber and cultivated for 72 h. Cells of the same concentration were cultured in parallel in six bioreactors in conventional incubators (37°C, 5% CO_2). In addition to the growth rate viability was determined using SYTO 9 and propidium iodide as described above.

Cultivation of human PBMC in 3D matrices. In order to show the ability of the reactor to serve as testing device in pharmacological studies with complex matrices we cultivated PBMC (kindly provided by Annika Lubitz, ProBioGen AG) of healthy donors in 3 different matrices: (1) collagen (0.1%, Biochrom, Berlin, Germany) mixed with DMEM (Biochrom) to a final concentration of 0.05%, (2) collagen mixed with 1% agarose (Biozym, Hessisch Oldendorf, Germany) in DMEM to a final concentration of 0.075% collagen and 0.1% agarose and (3) collagen aided with fibronectin (Biozym) to a final concentration of 0.075% collagen and 0,05% fibronectin. PBMC $2.25x10^4$ were directly mixed with the prepared matrices and instantly given into the reaction chambers. Cell viability was determined at day 1, 3, 7 and 9 via live/dead staining as described above. Furthermore cell viability was compared to PBMC cultured in pure medium within miniaturized perfusion reactors and to a HeLa staining control in 24 well plates (Becton Dickinson Falcon Labware, Heidelberg, Germany).

Results

The final design of the miniaturized perfusion reactor compromises a 190 µl cultivation chamber milled within a medically tested gamma sterilization-resistant PC block. The polymeric material is biocompatible, thermally stable and easy to machine. Gassing with O_2 and CO_2 is ensured by a gas-permeable membrane to which adherent cells can stably attach if 2D cell culture is performed. Membrane and PC are both transparent and allow visual examination of the cells with a microscope. Lateral hollow fibers retain cells while connections at the end of the fibers allow continuous supply of growth medium as well as collection of supernatants. A conical plug locks the re-closable port on the top of the cultivation chamber which serves as port for the inoculation of cells or substances (fig. 1). The number of parallel cultivation chambers placed in one block of PC can be varied. Two reactors measure exactly the width of a standard microscope slide (76 mm), while six reactors in parallel can be placed in a holder with the width of a microtiter plate (127 mm). Thus, compatibility with standard laboratory equipment is given.

The prototyping process included several rounds of redesign in order to ensure tightness and biocompatibility and to optimize the handling. Since all components consist of different materials with different surface properties tight joining becomes a major challenge when biocompatibility must be ensured at the same time. Adhesives must combine pressure-resistance and sufficient viscosity to stay at the application site through the whole joining process but inviscid enough to seal tightly and form-locking. Fissures and micro-pores on the one hand or cloaked hollow fibers on the other hand are the consequences. Both phenomena could be detected with the developed tightness test. Convections of cyanobacteria unveiled leakages occuring especially within the adhesive or at the interface between adhesive and PC (fig. 2).

In parallel each component and each material used was tested for biocompatibility in normal multititer plates. Growth rates and cell morphology of L929 cells in wells with test specimen were compared to cells in control wells. Fig.2 shows an example of good biocompatibility properties of a tested adhesive. Biocompatibility was further proved with a Live/Dead stainings (propidium iodide and SYTO9), which also were compared to control cells (data not shown).

Due to these both testing procedures, the final design of the bioreactor is fabricated from biocompatible material and joined pressure-resistant as flow-through tests are negative for cyanobacteria. Due to further standardization approaches the micro-reactors can be produced with high conformity and low failure rate.

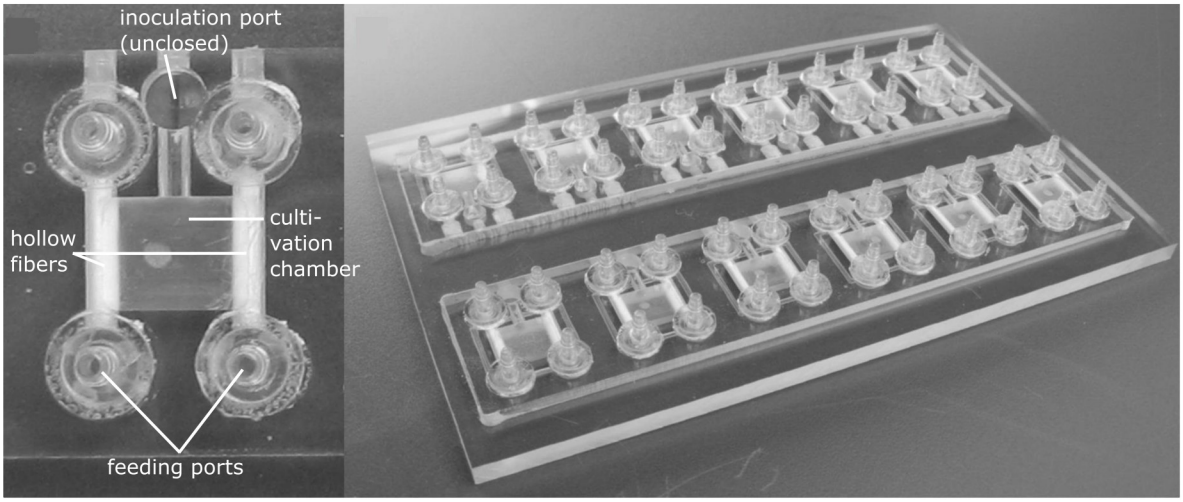

Figure 1: Miniaturized perfusion reactor. Left: Composition of a single reactor (chamber 7x9 mm). Right: Two slides with six reaction chambers in parallel each in a multititerl plate dimensioned holder.

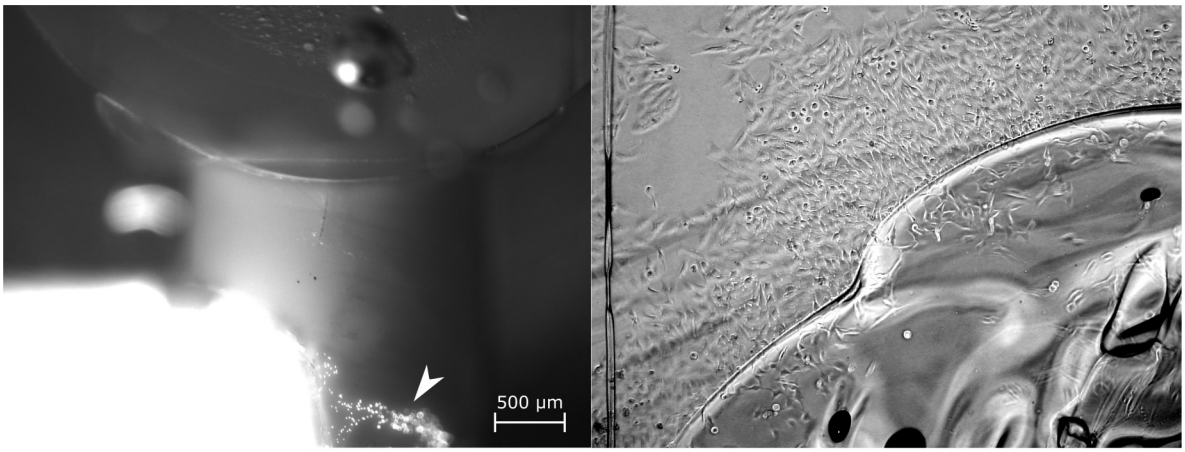

Figure 2: Tightness test with cyanobacteria and viability test.
*Left: The tightness of the reactor was examined using cyanobacteria and a fluorescence microscope (*Ex 435/40 nm; Em 515 nm LP*). The arrow depicts a leakage between the cultivation chamber (white) and the hollow fiber in an image section shown in figure 1a (rectangle).*
Right: Microscopic picture (brightfield) of L929 cells growing after 72 hours in direct contact and on the surface of a tested adhesive (lower right corner, Acrifix 192, Evonik, Germany) showing the biocompatibility of this specimen.

Due to its modular properties, the miniaturized bioreactor can be further modified. Inline analytics can be incorporated to monitor cultivation parameters e.g. a micro-mechanical glucose sensor (fig 3, left) or it can be integrated into more complex experimental setups: The functionality

of the micro reactor was proven in an autonomous cultivation system comprising gassing, temperature control and media exchange (fig 3, right). Details of this setup are discussed in another publication in this issue (Kostova et al.). Viability and growth rates of L929 cells were determined after 72 hours and compared to cells cultured in a standard incubator (fig 4). L929 cells showed higher confluence in the autarkic system (~90% vs 80%) and comparable viability rates (>95%).

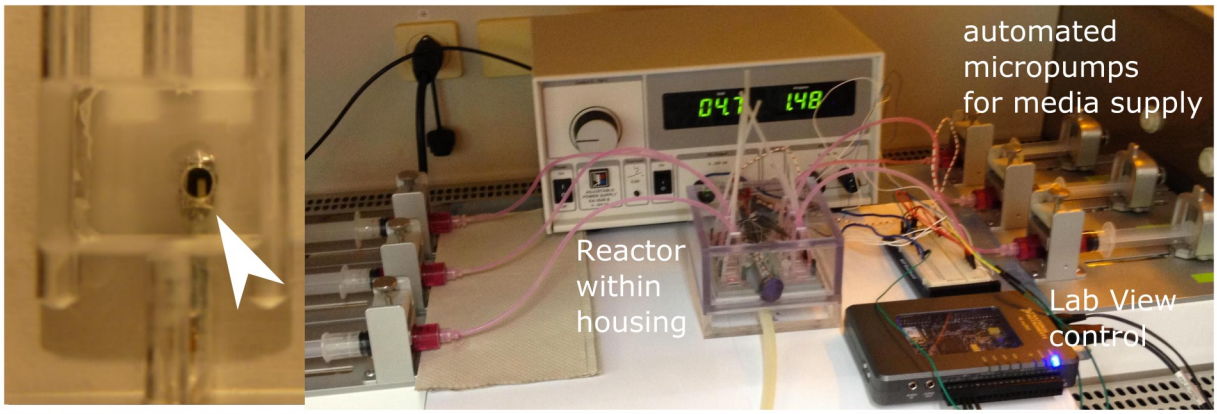

Figure 3: Modular modifications of the miniaturized bioreactor.
Left: Incorporation of an affinity-viscosimetry based sensor for monitoring of glucose (arrow). Right: Six miniaturized bioreactors in an autonomous test system consisting of a housing for gassing, lab view controlled tempering and computer controlled media supply.

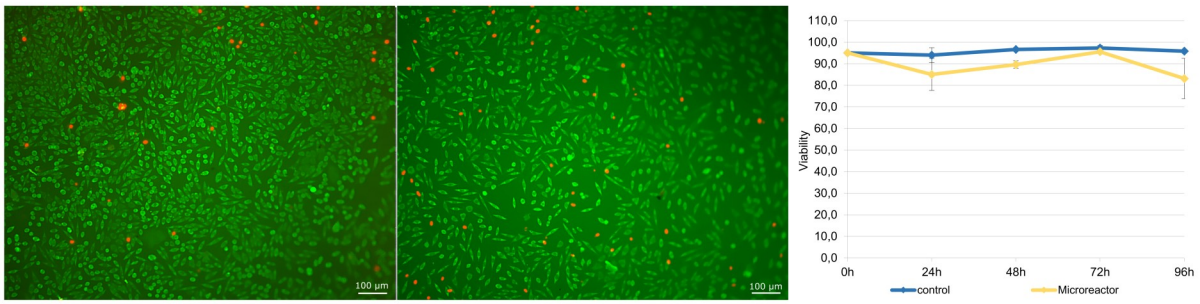

Figure 4: Cell viability of L929 fibroblast after 72 hours of cultivation. Living cells are green (print version grey), dead cells are red (print version white). Comparison of cultures in the autarkic set up with periodic perfusion (left) and without perfusion (mid). The diagram (right) shows the viability over the whole time course.

Since the recreation of the physical and biological environment is crucial to perform close to reality preclinical in vitro tests we cultured human PBMC in different collagen based matrices for nine days. Live/dead staining showed high viability within all three tested matrices up to day 7 (see fig. 5). Viability of PBMC in a 0.5% agarose matrix was also compared with PBMC in liquid medium and a staining control with HeLa cells after 3 days of cultivation. Under both cultivation conditions PBMC started to form small clusters.

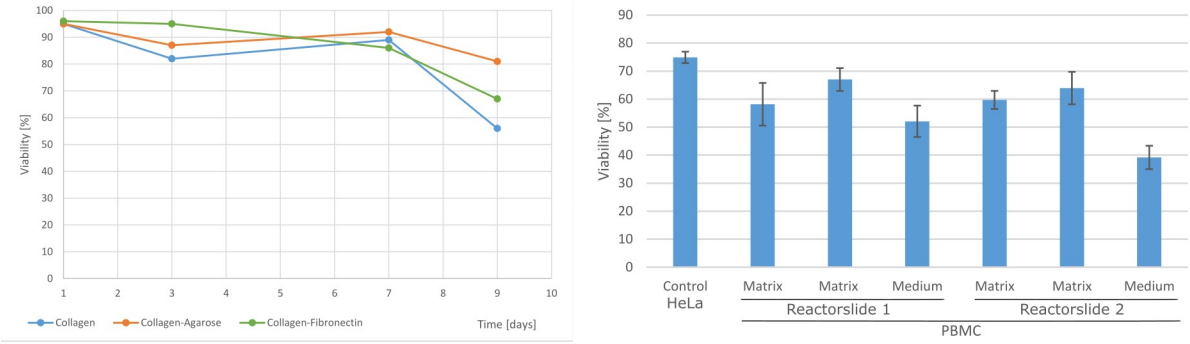

Figure 5: Viability test in 3D matrices.
Left: Cell viability of human PBMC in three different collagen-based matrices. Right: Comparison of viability of PBMC in liquid medium or matrix after 5 days of cultivation in different reactors.

Discussion

Due to the recent development in medicine and pharmacology there is a growing need to test the immunogenicity and toxicity of substances utilized as biopharmaceuticals, vaccines, adjuvants, etc. Developed in vitro testing systems trend to model the in vivo environment more and more precisely. Complex organoid in vitro models have been published for liver [10], skin [11] as well as for immunologic tests [12]. Nevertheless, there is a need for in vitro testing systems that provide a medium throughput and adaptable complexity and can be produced in high numbers at low costs.

Here, we present aspects of the development of a modular multifunctional miniaturized bioreactor which can be equipped with inline analytics. The number of reaction chambers can be modified to fit all kinds of demands of parallelization. The reactor can be simply placed into an incubator and is than operated as batch or fed-batch. However, it can be operated outside incubators to avoid long hoses or the need to place pumps within the incubator. We demonstrated its autarkic operation as a perfusion system with comparable high viability rates. Furthermore, we demonstrated versatile applications by culturing adherent cells in 2D as well as suspension cells in liquid media as well as in different 3D matrices. Viability of cultured PBMC in these matrices were high for up to 7 days. Reduced viability after that period is referred to the absence of stimulants thereby inducing cell death.

The comparison of PBMC viability between different media types showed overall reduced viability after a few days of cultivation. These might be attributed to time delays in sample handling, cell preparation or to donor specific issues. Nevertheless, in most cases substance specific reactions occur within the very first days of cultivation and is often detectable within hours after stimulation.

Within the prototyping process we established an innovative and highly precise tightness test with fluorescent particles. To be rigorous in testing conditions these particles had to be as half as big as typical mammalian cells, i.e. <= 5 µm in diameter. Among the tested particles viable cyanobacteria performed excellent due to their strong autofluorescence, their uniform size distribution, easy keeping and very low costs. In our examination we used the red fluorescent of the cyanobacteria's chlorophyll A (excitation 435/40 nm; emission 515 nm LP). In addition to its measure as optical parameter for the cell viability [13] we here describe for the first time the autofluorescent cyanobacteria as testing objects for leakage investigations.

All applied materials and components have been tested for cytotoxicity to provide a biocompatible environment. In order to measure activation of PBMC in substance testing by means of cytokine gene expression quantification every artificial stimulus has to be avoided. Notably the glucose sensor detects glucose with the help of the lectin Concanavalin A which itself is a predominant immune-stimulant and even is used as positive control in immunologic studies [14].

The miniaturized flow-through reactor will be part of further advancements. The manufacturing process will be transferred to a production via injection molding to be able to produce the reactor

system in higher quantities and at lower cost. In a second step an optical pH sensor was developed and will be integrated within a micro fluidic system (the related article “A new approach for the spectroscopic detection of different pH-values” by Rogge et al is published within this issue).

Our long-term goal is to provide a modular cultivation system for immunologic testing that transfers the organoid testing environment of human artificial lymph nodes (as described in [15]) into a miniaturized reactor system. Thus, the reactor can play a role for example in vaccine development by examining the effectiveness of T- or B-cell activation.

References

[1] A. Abbott, Biology's new dimension, Nature, 424 (6951) (2003), 870-872.
[2] D.B. Weibel, G.M. Whitesides, Applications of microfluidics in chemical biology, Curr. Opin. Chem. Biol. 10 (6) (2006), 584-591.
[3] C. Giese, U. Marx, Human immunity in vitro — Solving immunogenicity and more, Adv Drug Deliv Rev. 69–70 (2014) 103–122, doi:10.1016/j.addr.2013.12.011.
[4] M. Leist, T. Hartung, Inflammatory findings on species extrapolations: humans are definitely no 70-kg mice, Arch. Toxicol. 87 (2013) 563–567.
[5] G. Suntharalingam, M.R. Perry, S. Ward, S.J. Brett, A. Castello-Cortes, M.D. Brunner, N. Panoskaltsis, Cytokine storm in a phase 1 trial of the anti-CD28 monoclonal antibody TGN1412, N Engl J Med 355 (2006) 1018–1028.
[6] W.L. Warren, D.D. Iii, J. Moser, S. Inderpal, H. Song, E. Mishkin; J.G. Tew, Co-culture lymphoid tissue equivalent (LTE) for an artificial immune system (AIS), Pat. WO2007146334 A2, (2007).
[7] L.G. Griffith, M.A. Swartz , Capturing complex 3D tissue physiology in vitro, Nat Rev Mol Cell Biol 7(3) (2006) 211-24.
[8] C. Dieterich, S. Rupp, M. Noll, T. Graeve, In Vitro-Gewebetestsystem - Cartilage replacement, useful particularly for repairing joint defects, comprises differentiated and proliferating chondrocytes in collagen-based biomatrix. Pat. DE10062626 (A1), (2001).
[9] C. Giese, C.D. Demmler, R. Ammer, S. Hartmann, A. Lubitz, L. Miller, R. Müller, U. Marx, A human lymph node in vitro—challenges and progress, Artif. Organs 30 (2006) 803–808.
[10] M. Birkholz, K.-E. Ehwald, T. Basmer, P. Kulse, C. Reich, J. Drews, D. Genschow, U. Haak, S. Marschmeyer, E. Matthus, K. Schulz, D. Wolansky, W. Winkler, T. Guschauski, R. Ehwald, Sensing glucose concentrations at GHz frequencies with a fully embedded Biomicro-electromechanical system (BioMEMS), J Appl Phys 113 (24):244904 (2013).
[10] E.M. Materne, A.G. Tonevitsky, U. Marx, Chip-based liver equivalents for toxicity testing — organotypicalness versus cost-efficient high throughput, Lab Chip 13 (2013) 3481–3495.
[11] M. Noll, T. Graeve, Three-Dimensional Skin Model, Pat. EP 1 290 145 B1, (2001).
[12] M. Seifert, A. Lubitz, J. Trommer, D. Könnig, G. Korus, U. Marx, H. Volk, G. Duda, G. Kasper, K. Lehmann, M. Stolk, C. Giese, Crosstalk between immune cells and mesenchymal stromal cells in a 3D bioreactor system, Int. J. Artif. Organs 35 (2012) 986–995.
[13] K. Schulze, D.A. López, U.M. Tillich, M. Frohme, A simple viability analysis for unicellular cyanobacteria using a new autofluorescence assay, automated microscopy, and ImageJ. BMC Biotechnol. 11:118 (2011), DOI: 10.1186/1472-6750-11-118.
[14] L. Radke, D.A. López, A. Lubitz, C. Giese, M. Frohme, Induced cytokine response of human PMBC-cultures: Correlation of gene expression and secretion profiling and the effect of cryopreservation, Cell. Immunol. 272(2) (2012) 144–153.
[15] C. Giese, A. Lubitz, C.D. Demmler, J. Reuschel, K. Bergner, U. Marx, Immunological substance testing on human lymphatic micro-organoids in vitro, J. Biotechnol. 148 (2010) 38–45.

10.Curriculum Vitae

Der Lebenslauf wird aus datenschutzrechtlichen Gründen in der digitalen Version dieser Arbeit nicht veröffentlicht.

11. Vollständige Publikationsliste

2010 Radke L, López Hemmerling DA, Lubitz A, Giese C, Wildenauer F-X, Frohme M. Etablierung verschiedener Bead-basierter Multiplexmethoden mit einem Suspensions-Array-System für molekulardiagnostische Zwecke. Wissenschaftliche Beiträge der TFH Wildau 14:6-12. https://doi.org/10.15771/0949-8214_2010_1_1

Radke L,López Hemmerling DA, Lubitz A, Giese C, Frohme M. Prediction of cytokine release using gene expression profile analysis. Chimica Oggi / Chemistry Today; 28(5): 2-4.

2011 Radke L,López Hemmerling DA, Lubitz A, Giese C, Frohme M. Induced cytokine response of human PMBC-cultures: Correlation of gene expression and secretion profiling and the effect of cryopreservation. Cellular Immunology; 272(2): 144-53. doi:10.1016/j.cellimm.2011.10.018

2012 Radke L, Lubitz A, Giese C, Frohme M. Einfluss der Kryokonservierung auf die Immunanwort von Leukozyten. Wissenschaftliche Beiträge der TH Wildau 16:9-14. https://doi.org/10.15771/0949-8214_2012_1_1

Wernicke C, Franke P, Radke L, Berge S, Frohme M. Qualitätsmanagement in der RT-qPCR. BIOspektrum 1/2012: 42-5. doi: 10.1007/s12268-012-0142-7

2014 Radke L, Giese C, Lubitz A, Hinderlich S, Sandig G, Hummel M, Frohme M. Reference gene stability in peripheral blood mononuclear cells determined by qPCR and NanoString. Microchimica Acta 2014, 181: 1733-42. https://doi.org/10.1007/s00604-014-1221-x

2015 Keil K, Radke L, Tillich UM, Frohme M. Automatisierung des Bio-Plex Pro™-Analyseverfahrens. Wissenschaftliche Beiträger der TH Wildau 19:15–9. doi: 10.15771/0949-8214_2015_1_2

2016 Gossing W, Radke L, Frohme M, Biering H. ECS-Komplex – ein neuer Biomarker bei Wachstumshormonstörungen? Wissenschaftliche Beiträge der TH Wildau 20:23-9. doi: 10.15771/0949-8214_2016_1_3

2017 Böhme A, Radke L, Schütze F, Schneider S, Liebscher T, Sauer S, Santo L, Quadrini F, Hummel M, Giese C, Frohme M, Foitzik A. Miniaturized Flow-Through Bioreactor for Processing and Testing in Pharmacology. Materials Science Forum, 879: 236-43. doi: 10.4028/www.scientific.net/MSF.879.236

Sandig G, von Horsten HH, Radke L, Blanchard V, Frohme M, Giese C, Sandig V, Hinderlich S. Engineering of CHO Cells for the Production of Recombinant Glycoprotein Vaccines with Xylosylated N-glycans. Bioengineering, 4(2), 38. doi:10.3390/bioengineering4020038

Radke L, Sandig G, Lubitz A, Schließer U, von Horsten HH, Blanchard V, Keil K, Sandig V, Giese C, Hummel M, Hinderlich S, Frohme M. In-vitro evaluation of glycoengineered RSV-F in the Human artifical Lymph Node Reactor. Bioengineering, 4(3), 70. doi:10.3390/bioengineering4030070

Poster

2013 Radke L, Böhme A, Foitzik A, Giese C, Lubitz A, Hinderlich S, Sandig G, Hummel M, Frohme M. Validation of Vaccine Candidates in miniaturized artificial Lymph Nodes. 8. Deutsches BioSensor Symposium, 10.-13.03.2013, TH Wildau

2017 Radke L, Sandig G, Lubitz A, Schließer U, von Horsten HH, Blanchard V, Keil K, Sandig V, Giese C, Hummel M, Hinderlich S, Frohme M. In Vitro Evaluation of Glykoengineere RSV-F in the Human Artifical Lymph Node Reactor. Glyconet BB Konferenz „New and Emerging Technologies“, 11.-13.09.2017, Fraunhofer-Konferenzzentrum Potsdam-Golm.

Präsentationen

2011 Radke L, Böhme A, Frohme M, Foitzik A, Hinderlich S, Giese C. Validation of Vaccine candidates in miniaturized artificial lymph nodes. ZMDB – TH Wildau Workshop “Trends in Bioanalysis”, 26.05.2011, TH Wildau.

Radke L. Validation of Vaccine candidates in miniaturized artificial lymph nodes. Workshop on Biomimetic and Bioanalytical Systems, 12.-13.12.2011, Luckenwalde.

2013 Radke L, Böhme A, Foitzik A, Giese C, Lubitz A, Hinderlich S, Sandig G, Hummel M, Frohme M. Selection and validation of qPCR reference genes examplified for PBMCs in vaccine development. 7th Senftenberger Innovationsforum Multiparameteranalytik, 18.-.19.04.2013, Hochschule Senftenberg.

2014 Radke L, Böhme A, Giese C, Lubitz A, Marx U, Schütze F, Rogge C, Liebscher T, Foitzik A, Frohme M. Miniaturised artifical lymph node reactor – construction and validation of a 3d cell culture device. 3D Cell Culture 2014, 25.-27.06.2014, Konzerthaus Freiburg.

Radke L, Sandig G, Lubitz A, Schließer U, von Horsten HH, Blanchard V, Keil K, Sandig V, Giese C, Hummel M, Hinderlich S, Frohme M. Validation of Vaccine Candidates in Miniaturised Artifical Lymph Nodes. BD Biosciences - NanoString Technologies: Innovative Technologies for Cancer Research Applications, 04.07.2014, Ludwig-Maximilians Universität München.

Reviewertätigkeiten

2013 Full length research article, Microchimica Acta; Thema: chip-based technologies, microfluidics, PCR

2014 Full length research article, Biotechnology Journal; Thema: 3D cell culture, macrotissue, perfusion reactors

2015 Full length research article; New Biotechnology; Thema: gene expression, qPCR NanoString

12. Danksagung

An dieser Stelle möchte ich allen Personen meinen Dank aussprechen, die zur Anfertigung dieser Arbeit erheblich beigetragen haben.

Herrn Prof. Dr. Michael Hummel danke ich für die Bereitschaft die Betreuung zu übernehmen, das Interesse an der Thematik und die gute Zusammenarbeit. Als Doktorvater war er immer erreichbar, machte persönliche Treffen trotz eines vollen Kalenders möglich und lieferte immer schnelle und prägnante Antworten bei Fragen per Email.

Herrn Prof. Dr. Marcus Frohme danke ich als wunderbaren Chef, der immer ansprechbar ist und sich aller Probleme annimmt – egal ob wissenschaftlich-technischen, organisatorischen oder gar persönlichen Dingen. Ich danke für das entgegengebrachte Vertrauen; sei es bei der Anschaffung von Kits (mit Kosten im mittleren vierstelligen Bereich) bei einer Technik, die gerade erst aus den Kinderschuhen entwächst oder der Zuversicht, dass diese Arbeit doch noch einen erfolgreichen Abschluss findet.

Großer Dank gilt allen weiteren Mitarbeitern im Projekt IPoGly. Herrn Prof. Dr. Stephan Hinderlich (Beuth Hochschule für Technik) für die gute Projektkoordination und die gute Zusammenarbeit bei wichtigen Publikationen. Frau Dr. Grit Sandig, die die Herstellung von RSV-F Proteinen mit modifizierten Glykanstrukturen im Projekt erfolgreich meisterte und erst ermöglichte, dass ich etwas zu analysieren hatte.
Von der ProBioGen AG danke ich Herrn Dr. Christoph Giese, der mir immer wieder viele Details im Reich der Immunologie und Zytokine erklärte, so dass sich über die Jahre für mich ein sinniges Bild ergab. Gleiches gilt für Frau Annika Lubitz, die mir außerdem jede Menge zusätzlicher Proben zum Ausprobieren, Optimieren und Etablieren bereitstellte. Frau Dr. Ulrike Schließer danke ich für hilfreiche Beiträge bei der Genexpressionsanalyse aus immunologischer Sicht.
Frau Hedwig Lammert aus der Arbeitsgruppe von Herrn Hummel danke ich für ihre Zeit und die kurzfristige Durchführung von NanoString Experimenten.
Andrea Böhme und Felix Schütze aus der Arbeitsgruppe von Prof. Dr. Andreas Foitzik (TH Wildau) danke ich für die nimmermüde Umsetzung von Kritik in neue Redesigns des miniaturisierten Perfusionsreaktors, mit dem Ziel das Handling und die Dichtheit zu verbessern.
Außerdem danke ich allen in Abschluss- und Projektarbeiten beschäftigten Studentinnen: Ulrike Paul, Karolin Keil und Nicole Gottschalk für die gewissenhafte Durchführung von kleinen und großen Teilprojekten.
Alles in allem war IPoGly ein schönes und vor allem erfolgreiches Projekt, in das alle Beteiligten viel Enthusiasmus gesteckt haben.

Zum Schluss, aber auch im größten Maße, danke ich meiner Familie: meinen Kindern, die selbst in diesem Moment für Ablenkung und Zerstreuung sorgen wollen. Ohne euch hätte ich die schöne Doktorandenzeit nie so lange auskosten können. ☺
Meinen Eltern, die mich zu dem Menschen erzogen haben, der ich heute bin. Erst seitdem ich selbst Vater bin, verstehe und bewundere ich, mit welcher Leichtigkeit die beiden mich ins Erwachsenenalter gebracht haben.
Der wichtigste Dank geht an meine Frau, der Liebe meines Lebens, die mit viel Geduld der Fertigstellung dieser Arbeit harrte und dabei den Überblick im Familienalltag behielt. Ohne Dich hätte ich diese Arbeit nie geschafft und deshalb widme ich diese Dir.